MONTHLY NOTICES

OF THE

ROYAL ASTRONOMICAL SOCIETY

Vol. 99 No. 8

MEETING OF 1939 JUNE 9

Professor H. C. Plummer, President, in the Chair.

The election by the Council of the following Fellows was duly confirmed :—

Terence John Harding, 140 Ravenhurst Road, Harborne, Birmingham ; and

Noel Bryan Slater, Solar Physics Observatory, Cambridge.

Eighty presents were announced as having been received since the last meeting, including :—

Oppolzer, Canon der Finsternisse : Introduction. Translated by Valerie Baker and edited by M. Davidson and D. H. Sadler (presented by the British Astronomical Association).

The President read the following resolution which had been passed by the Council that afternoon :—

"The Council wish to place on record their deep sense of the loss which the Society has sustained by the death of Sir Frank Watson Dyson, who as Astronomer Royal directed the Royal Observatory with distinguished ability for a period of twenty-three years, and who as President, as Secretary, as Treasurer, and at all times, promoted the interests of the Society with unfailing zeal.

"The Council also directs that a copy of this resolution shall be sent to the family with an expression of their sympathy."

The Meeting stood in silence for some minutes in tribute to the memory of Sir Frank Dyson.

UNIVERSITY LIBRARY LEEDS

A STUDY OF THE SOLAR CORONA AND PROMINENCES WITHOUT ECLIPSES

(George Darwin Lecture, delivered by M. Bernard Lyot, Assoc.R.A.S., on 1939 May 12)

The rareness of total eclipses of the Sun, their short duration and the distances one has to travel to observe them, have, for more than half a century, led astronomers and physicists to seek for a method which enables them to study the corona at any time.

The first attempts made to reveal the corona without an eclipse date from 1878. It would take too long to enumerate all those that have since been made. Most of the observers simply photographed that part of the sky where the Sun was, either direct or through coloured filters. An opaque disc, somewhat larger than the image of the Sun, was placed at the focus of the instrument to screen off the direct rays of the Sun and so avoid the photographic halo. At first, only blue, violet and ultra-violet rays were used; but, later on, from 1904, the progress of sensitising allowed the use of red and infra-red radiations, which are not so scattered by our atmosphere. A great number of plates have thus been obtained, generally from high places, sometimes at an altitude of more than 4000 m., and in a very pure atmosphere. They show halos, often irregular, surrounding the Sun, and resembling the corona. Unfortunately, these halos have been obtained with exposures much too short to register the corona itself; they do not show the prominences which are more brilliant than the corona, and, during partial eclipses of the Sun, they even spread on the disc of the Moon without showing the limb of our satellite, which should have been outlined by the light of the corona. These halos were due principally to the light of the Sun scattered by the lens or the mirror of the telescope.

Other observers applied indirect means. In 1893, Deslandres, and after him Hale and Ricco on Mount Etna, tried, but without success, to photograph the corona by isolating the dark K line of the solar spectrum with the spectroheliograph. The inner corona, which has no absorption lines, thus should have appeared relatively more brilliant.

I might mention also: (1) The thermo-electrical procedures tried in 1900 by Hale, then by Deslandres, to detect the infra-red radiations of the corona; (2) the polariscope of Savart used in vain by Wood, to recognise the polarised light of the corona; (3) the spectroscope used by Millochau, in 1906, to look for the green line of the corona close to the limb of the Sun. In consequence of these numerous failures, the problem had long been considered impossible.

In October 1929 I had the pleasure of speaking with the late Professor Henry Osmund Barnard, former Director of the Observatory at Colombo, Ceylon, and giving him the results I had obtained on the planets with my

1

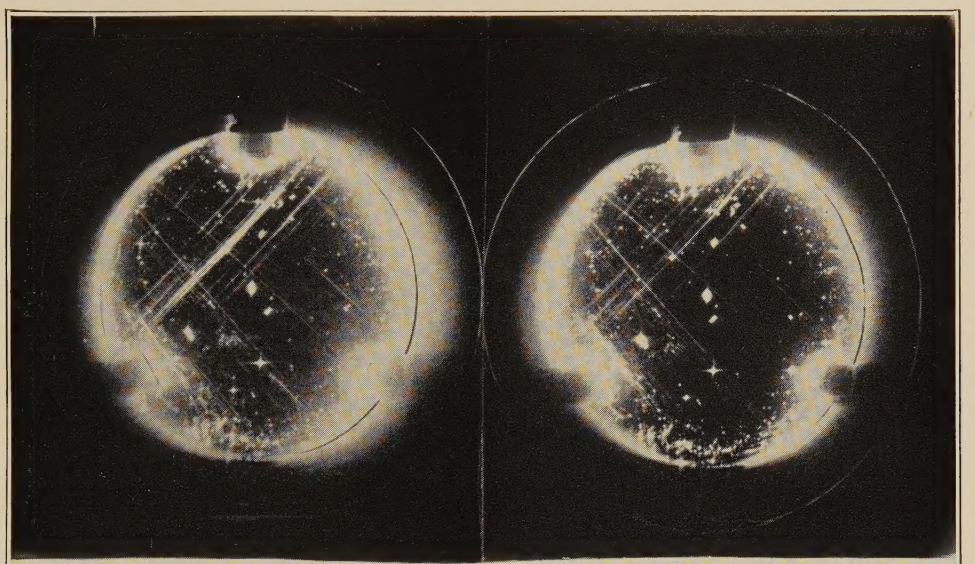

2

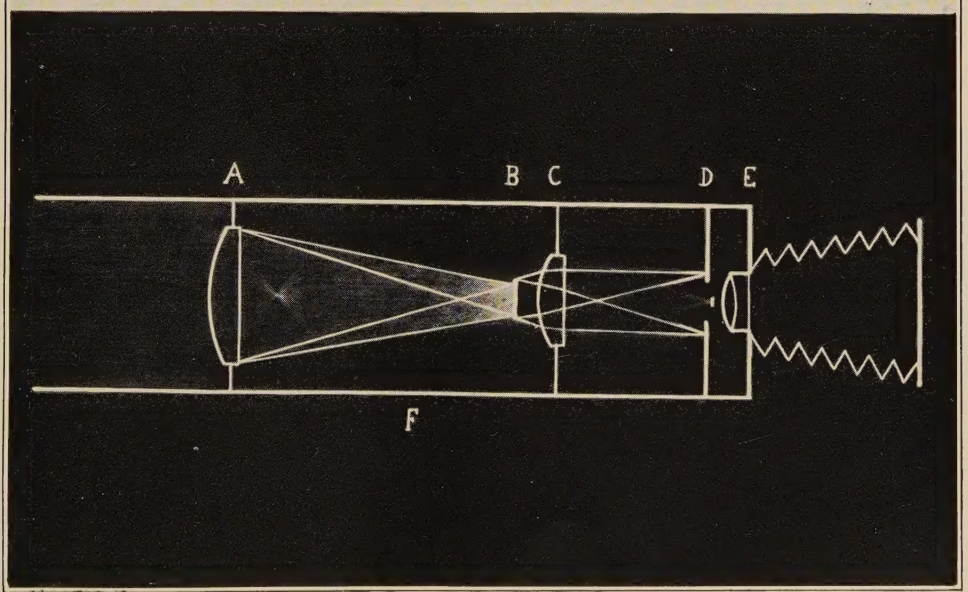

Fig. 1.—Photographs showing diffusion and veins, with 8 cm. lens.
Fig. 2.—Plan of coronagraph.

Bernard Lyot, George Darwin Lecture.

Digitized by the Internet Archive
in 2026

https://archive.org/details/monthly-notices-of-the-royal-astronomical-society_1939-06-09_99_8

polarimeter, sensitive to a proportion of polarised light of one-thousandth. Professor Barnard advised me to renew the attempts of Wood with this polarimeter.

The measurements made during eclipses showed that the brightness of the corona, at 2′ from the Sun's edge, is about a million times less strong than that of the solar disc. To succeed, it therefore appeared necessary, above all, considerably to reduce the diffusion of the light by the telescope. This is clearly shown by the following experiment :—

Diffusion by a Lens.—Let us take, for example, a single lens, 8 cm. in diameter and 2 m. in focal length. At a distance of 10 m. let us place a very intense source of light having the same apparent diameter as the Sun, and, with the lens, form a picture of the source on an opaque disc somewhat larger than this image. If we place the eye behind the edge of the disc we see that the lens is not black.

Two photographs of the lens are seen in fig. 1. Its edge is very brilliant, principally on the side of the source and on the opposite side. This illumination is due to the diffraction of the waves round the edge of the aperture. It fades rapidly when the observer removes his eye from the image of the artificial sun, thus producing around the disc a halo fading towards the exterior. This halo is very strong ; according to a more recent calculation of Nagaoka, at 2′ from the edge of the image, its brightness is 3000 times less strong than the Sun's—that is to say, about 350 times stronger than the corona's. At any distance the halo is more than 200 times stronger than the corona, which renders observations impossible.

A small bright disc is seen in front of the centre of the lens ; it is an image of the artificial sun reflected by the two faces of the lens. The lens appears studded with bright points due to the light diffracted by small bubbles in the glass, small hollows on the surfaces, and particles of dust deposited on them. If the eye follows the circumference of the disc, trails are seen lighting up and fading away twice in every turn. The shortest of these are scratches on the surfaces ; the longest are veins in the glass. Some veins are very faint and not otherwise visible. The background of the lens is generally not black, but covered with a slight mist, due to an imperfect polish. The veins can be stereoscopically localised by using these two photographs taken by inclining the lens in two opposite directions. This lens was cut from plate glass. In another photograph showing a lens 15 cm. in diameter cut from a disc of borosilicate crown glass, the veins have a less regular form. During the last few years the firm Parra-Mantois has succeeded in producing discs in which not a single vein is seen.

This experiment shows the necessity of making a lens as flawless as possible. It is necessary to grind it from a thick disc, choosing the most homogeneous part, and to polish the surfaces for a very long time, without making scratches.

Coronagraph.—The principal defect, that is to say, the light diffracted by the edge of the lens, still had to be overcome. With this object I have made several coronagraphs, of which the plan is seen in fig. 2 (Plate 11).

The single lens, plano-convex, is shown at A ; it forms an image of the

Sun on a blackened brass disc at B projecting beyond the Sun by 15″ to 20″. A field lens C, placed behind the disc, produces an image of the lens A on the diaphragm D in the shadow. The edge of the diaphragm cuts off the light diffracted by the edge of the first lens. A small screen placed in the centre of the diaphragm cuts off the light of the solar image produced by reflection on the surfaces of the lens A. Behind the diaphragm and the screen, protected from the diffused light, a carefully corrected objective E forms an achromatic image of the corona on the plate. The whole apparatus is contained in a tube F, open only during the observations, and coated with thick oil in the interior, to collect the particles of dust. The first lens must be wiped frequently, and with particular care.

Atmospheric Diffusion.—To give good results, the coronagraph must be in a high place, because the dust, which is always present in the lower layers of the atmosphere, produces a whitish aureole of diffracted light around the Sun. This varying aureole is generally more than a hundred times brighter than the corona. The distance to which this aureole spreads varies in inverse ratio to the diameter of the particles producing it ; a few degrees for dust, 5′ to 10′ for the ice crystals of cirrus. When the sky is perfectly clear, the aureole completely disappears, and the brightness of the atmosphere, in red light, diminishes to half a millionth of that of the Sun—that is to say, becomes fainter than that of the corona.

From observations made in the mountains, it appears that the particles of dust are carried by rising currents of air due to the heating of the ground by the Sun's rays ; a layer of air, relatively warmer, suffices to stop them, and they then spread out widely, forming a horizontal sheet of a brownish colour. The height to which the dust rises increases during the period of fine weather and decreases when it rains or snows ; it is greater in summer than in winter, greater towards the equator than towards the pole. In France, during the summer, the highest level of dust is often between 2500 m. and 3000 m. This fact has led me to set up my apparatus in the Observatory of the Pic du Midi, situated in the Pyrenees at an altitude of 2870 m. above sea-level.

The Observatory of the Pic du Midi.—This observatory offers advantages not found anywhere else for studying the corona : on the one hand, a sky, the pureness of which is often perfect, chiefly at the end of spring and the beginning of summer ; and, on the other hand, a dome containing a very firm equatorial, 6 metres in length, on which heavy and cumbersome apparatus can be fixed.

Fig. 3 (Plate 12) shows a view of the observatory taken on 1937 June 29. It is built on a small terrace surrounded with very steep slopes, 15 m. below the summit of the Pic du Midi, separated by 30 km. from the axis of the chain of the Pyrenees. Snowfalls, frequent in spring, purify the air, whilst the sea of clouds remains a long time below the terraces and prevents the dust from rising. The rooms in which we live, seen in the middle of the photograph, are provided with central heating, running water and electricity. The dome opens and revolves electrically. During August and September the observatory is generally free from snow ; in winter and spring, on the

3

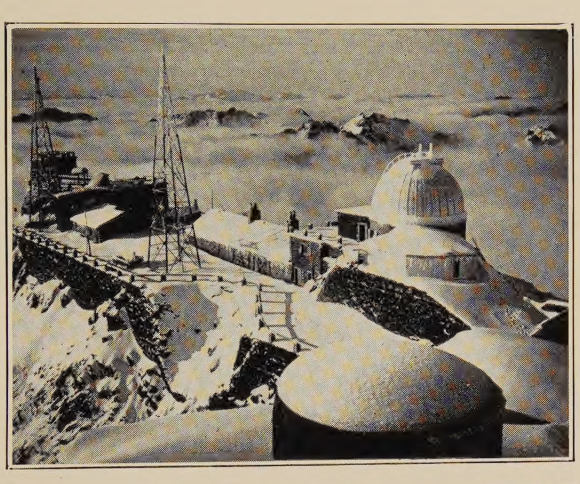

4

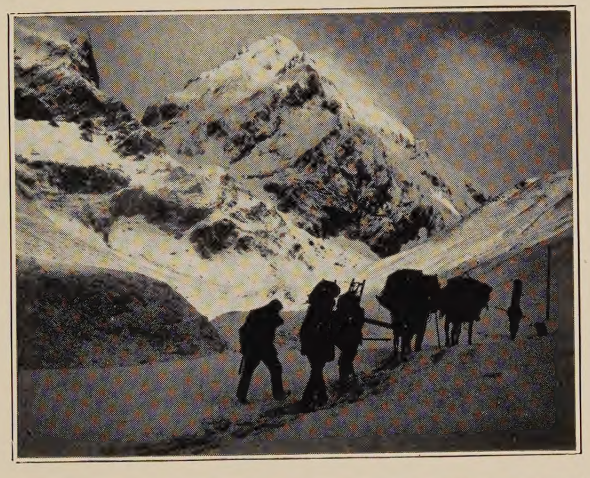

5

Fig. 3.—The Observatory of the Pic du Midi seen from the top, and the Chain of the Pyrénées.
Fig. 4.—The Pic du Midi and the beginning of the ascent (1400 m. elevation).
Fig. 5.—The carriers at 1850 m.

contrary, the buildings disappear under the snow sometimes more than 5 metres deep. The snow on the roof slides, in part, to the outside, by the action of the Sun, forming ice-grottoes which sometimes remain till June. The dome is provided with a special apparatus protecting the rail from snow and allowing it to turn throughout the winter. During August and September the observatory is quickly reached by a road rising to 2600 m. ; it takes a month to clear it of snow. In winter and spring the road completely disappears under the snow and one must go on foot.

Figs. 4 and 5 show some views of the ascent taken on 1936 June 5. One must leave the road at a height of 1100 m. and follow a higher valley, seen in fig. 4, leading to the foot of the Pic du Midi, visible at the end. The carriers leave their mules there, take the apparatus on their backs, and climb towards the left. At a height of 1800 m. (fig. 5) they reach an upper valley, in which they have to take to their skis. In the centre of the picture is the tube of the last coronagraph, closed like a telescope. At 2500 m. the carriers reach a ridge, not exposed to avalanches, by which they climb to the summit, in some places holding on to an iron cable. The observers follow the same route. The ascent takes seven to ten hours, according to the state of the snow.

My work on the corona so far has been made in two stages : the first one from 1930 to 1934, during which I sought to test the new method to obtain the principal results found during eclipses ; the second stage, since 1934, during which I tried to obtain new results.

Observations made in 1930.—The first coronagraph was built in the Observatory of the Pic du Midi, and fixed on the equatorial on 1930 July 25. This very primitive apparatus contained the lens 8 cm. in diameter an 2 m. in focal length, the defects of which have been seen in fig. 1. This lens was placed in a tube built with planks found on the spot. An eye-piece, a polarimeter or a direct vision spectrograph could be fixed at the end of the tube. After reducing the aperture to 3 cm. to hide the principal defects of the lens, prominences with a violet-pink tint were seen. The use of a red glass greatly increased the contrasts and allowed of good observations.

The Sun was surrounded by a slight halo without details. The polarimeter showed that this halo was polarised in a radial plane like the corona, but more faintly. The polarisation appeared at 6′ from the limb ; it increased rapidly towards the Sun and then remained almost constant under 3′. The more transparent the sky, the stronger it was.

Diagrams drawn from the observations * show the proportion of polarised light found in different directions at 80″ from the edge of the Sun, on 1930 July 29 and July 31. The axis of the Sun was inclined 10° to N.E. ; all the diagrams show minima at the poles and maxima above the zones of the sunspots. The proportion of polarised light attained, in some parts, 20- to 25-thousandths, about one-fifth of that of the corona. We can conclude that, in these parts, one-fifth of the light of the halo belonged to the corona, the rest being due to diffusion. On July 30 and the following days the

* *L'Astronomie*, 45, 248, 1931.

spectroscope showed, in the light of the halo, among the solar lines due to diffused light, an emission line, with a wave-length equal to that of the green line of the corona within 1 angstrom.

The first photograph of the spectrum of the corona without an eclipse * was taken on 1930 August 8, with the slit of the spectrograph tangential to the eastern edge of the Sun. When the slit of the spectrograph was moved, the green line underwent great changes in intensity, agreeing with the indications of the polarimeter. By covering the head with a black cloth the red line was seen, but fainter, and with variations of intensity different from those of the green line.

Observations made in 1931.—On 1931 June 12 I again ascended the Pic du Midi with a more elaborate apparatus which had been prepared during the winter in the Meudon Observatory. This apparatus consisted principally of a larger lens, 13 cm. in diameter and 3·15 m. in focal length, ground

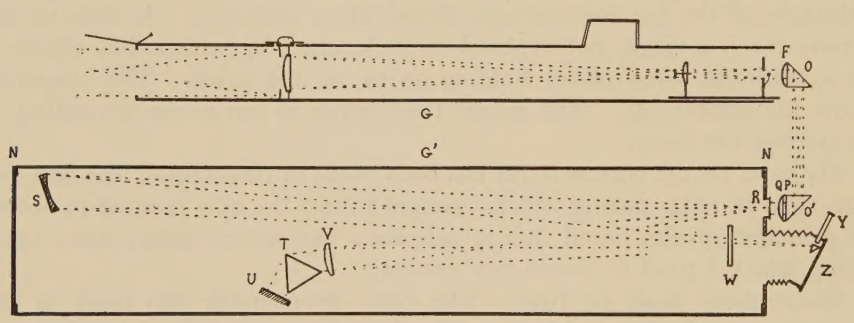

FIG. 6.—*Plan of the coronagraph and the spectrographs used in 1931.*

in the Institut d'Optique de Paris, as well as the chief parts of two large spectrographs and of a spectroheliograph.

Fig. 6 shows the general plan of the installation set up on the Pic du Midi during June and the beginning of July ; G is the coronagraph ; a lens F, followed by two totally reflecting prisms O and O′, casts a picture of the corona on the slit R of the spectrograph. The second prism is followed by a coloured filter P and a field lens Q concentrating the rays on the grating S. This 6-inch grating is concave with a radius of 7 m. ; it forms the spectrum on plate Z. A cylindrical lens W corrects the astigmatism, narrows the spectrum, and increases its brightness. By turning the prism O′ the rays can be thrown on to a prism T with a side of 16 cm., working with a Littrow setting between a plane mirror U and a lens V, 3·60 m. in focus. The pieces of both spectrographs are set up in the tube G′ of the telescope and regulated from the eyepiece by means of seven controlling tubes. Both spectrographs underwent considerable flexures, displacing the lines on the plate more than half a centimetre. To correct these flexures, the plate-holder was furnished with correcting screws and with a microscope Y, in which the observer followed a monochromatic picture of a hole lighted up by an iron arc. The first totally reflecting prism could be turned a little at a time by means of an electro-magnet and a ratchet wheel ; this rotation constituted

* *Loc. cit.*

the first movement of the spectroheliograph. The frame could be moved in its slide little by little by means of a second electro-magnet; this constituted the second movement of the spectroheliograph. Both electro-magnets were fed simultaneously by a contact wheel turned by the driving clock.

The prism spectrograph gave a dispersion of 5 A. per mm. in the green, and 11 A. per mm. in the red. A photograph showed the solar line *Hα* and the red line of the corona 6374 A., visible to a height of 4′·5. The panchromatic plates were not yet sensitive enough; it was necessary to hypersensitise them and make exposures of at least 30 minutes. Another plate was taken on 1931 August 7 by isolating, with the second slit of the spectroheliograph, a portion of the spectrum, 10 A. in width, containing

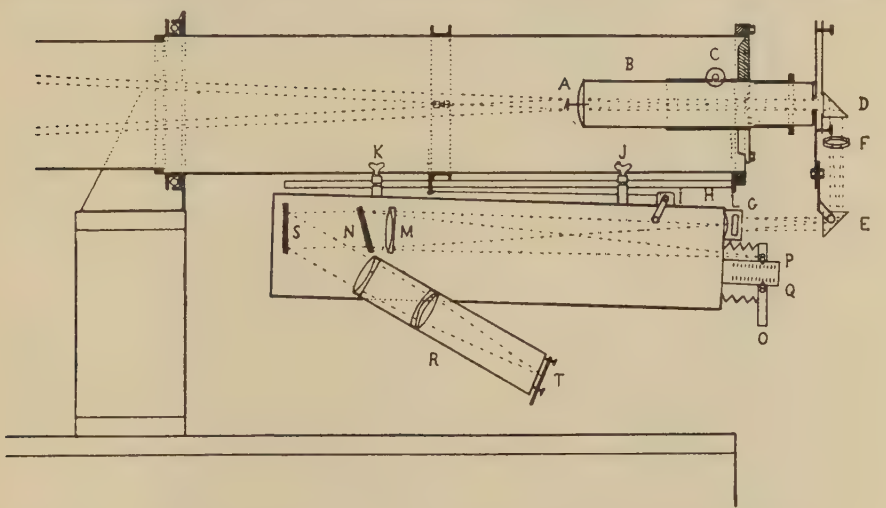

Fig. 7.—*Plan of the final coronagraph and the spectrograph used since 1935.*

the green line λ 5303.* It shows the aspect of this line, section by section, all around the Sun. The length and intensity of the line vary greatly; it has only one maximum in the west, on the equator. A large group of spots and flocculi, the only one then existing on the Sun, passed the limb in this region. An enlargement of the west side of the preceding plate shows the great width of the coronal line as compared with the solar lines. This width can be seen still better on a spectrum taken with the 7-m. concave grating in the second order, with a dispersion of 1·3 A. per mm.* The coronal line has an average width of 0·8 A., and extends to 1·2 A., ten times more than the neighbouring solar lines.

In 1932, the solar activity was approaching its minimum and the coronal lines were faint. I preferred to cease observations for a time and study new apparatus in view of the forthcoming increase in solar activity. This apparatus consisted chiefly of a more powerful coronagraph than the earlier one, connected with a spectrograph easier to manage, very luminous in the infra-red, and with very slight flexure.

The Final Coronagraph.—The chief lens of the coronagraph is plano-

* *Zeitschrift für Astrophysik*, 5, pt. 2, 73, 1932.

convex, with a diameter of 20 cm. and a focal length of 4 m. It was ground at the Paris Observatory, by M. Couder, from a disc of excellent borosilicate crown glass, kindly presented by the firm of Parra-Mantois. The tube is no longer of wood, but of duralumin. It is 6 m. long and weighs only 22 kg. It consists of four parts, which can be put one inside the other to facilitate transport. The eyepiece-holder is provided with a joint allowing the observer to bring any point of the field to the centre of the eyepiece without moving the coronagraph. The latter is carried on two large ball-bearing pedestals and can be turned on its axis. To the coronagraph is joined a single spectrograph (fig. 7) with a plane Rowland grating of 4 inches, reflecting, in the second order, 10 per cent. of the visible and next infra-red rays, and, in the first order, 35 per cent. beyond 9000 A. The grating can be placed at N to reflect the rays back through the objective M of focal length 1 m.; the spectrum is formed in the frame-holder O. The grating can also be placed at N, to form the spectrum in the camera R of 35 cm. focal length. The spectrograph, carried on two steel tubes H, by means of two jaws J and K, can slide in a direction parallel to the axis of the coronagraph to focus the corona on the slit. It is counter-balanced and turns with the coronagraph, permitting the observer to set the slit in any direction.

Fig. 8 (Plate 13) shows the whole of the installation, the tube of the coronagraph A and the ball-bearing pedestals B and C. The chief lens is at D; it is held in its cell by a groove and can be taken out to be cleaned, by means of a handle. Also shown are the spectrograph E, the frame-holder F for the objective and the camera G. This apparatus was set up in 1935 and has been used each year since. It has given the following results :—

Direct Photography of the Corona.—When the sky is very pure, by adapting an orange filter and a weak eyepiece to the coronagraph, the strongest parts of the inner corona are sometimes seen. More often, on the contrary, the coronal forms have slight contrasts and the diffused light makes them disappear in the eyepiece. They can, however, still be well photographed if a red filter and highly contrasting panchromatic plates are used. The photographs you are about to see have been obtained through a filter transmitting wave-lengths of more than 6200 A., on slow panchromatic Guilleminot plates multiplying the contrasts by $3\frac{1}{2}$, for these radiations.

The first direct photograph of the corona without an eclipse was obtained at 16^h on 1931 July 21.* Twelve exposures were taken; after each one, the coronagraph was turned through 30 degrees on its axis. This proceeding enables us to distinguish with certainty the coronal features from the defects due to the instrument, chiefly the spots produced by particles of dust deposited on the second lens of the coronagraph. One positive has been made by printing successively, on the same plate, the six best negatives placed in such a manner as to obtain the coincidence of the images of the prominences; this diminishes the spots which do not coincide, as well as the irregularity of the grain of the negative.

* *L'Astronomie*, **46**, 272, 1932.

Fig. 8.—The final coronagraph with the spectrograph on the equatorial of the Pic du Midi.

This positive shows, but faintly, a wide streamer to the north-east, a narrower one to the south-east and a luminous edge to the west. Only the general shape of the corona appears, because the diameter of the Sun on the negatives is only 12·5 mm., and, on the other hand, for very slightly contrasted details, the photographic plates have a very bad resolving power, equal to several tenths of a millimeter. Therefore the size of the negatives had to be increased.

A series of photographs was obtained in 1936, in the same way *, but with a solar diameter of 30 mm.; they show much more detail, wide streamers, dark gaps and luminous arches surrounding the brightest prominences. This method shows only the inner corona up to 7′ from the Sun's edge; but, in return, it enables us to study its variations.

For example, a picture taken at 8^h on 1936 July 6 shows the south pole very dark; to the south-east, several luminous arches; to the south-west, narrow jets followed by a dark gap; to the west, a dark space above a prominence. On a plate of the next day the dark gap is still seen to the south-west, but the other details have changed very considerably. To the west, the dark space has disappeared; to the south-east, the luminous arches are no longer visible, but another arch has formed towards the equator.

Two other photographs show the corona on 1936 July 19 with two prominences detached from the Sun's edge, and the corona on 1936 August 5.

In 1938, the coronagraph was supplied with a mechanism which turns the second lens and the disc on their common axis during the exposures. The particles of dust, describing circles around the Sun, disappear. This proceeding completely eliminates the spots, and a single negative is sufficient to give a good picture.

Many photographs have been thus taken, each one with a single negative much larger than the preceding ones, on which the Sun measures 65 mm. in diameter. Some parts of the photographs are reproduced in actual size in Plate 14 (figs. 9–17). All the details they show have been confirmed on several negatives taken successively. The north pole of the Sun is at the top. The black disc of the coronagraph appears more regular than that of the Moon on eclipse plates; it is surrounded by a fringe of light due to diffraction which is sometimes increased by bad seeing.

On 1938 July 6, at 9^h (fig. 9), to the north-east, a spot of light surrounded by a luminous ring is seen, and to the south-east, a bright dome. On the same day, at 15^h (fig. 10), to the north-east, the spot and the ring have disappeared; to the south-east, fine arches are substituted for the dome. On the same day, at $17^h\ 55^m$ (fig. 11), one-half of the arches, on the side of the equator, is covered with a new dome. At $10^h\ 30^m$ on July 9 (fig. 12) notice, for example, the entangled arches to the south-west. On the same day, at $15^h\ 2^m$ (fig. 13), these arches are modified and small clouds have formed on the south side. On the same day, at $18^h\ 40^m$ (fig. 14), the clouds are in the same place, but fainter. It would be interesting to study these rapid changes by means of cinema films.

* *L'Astronomie*, **52**, 193, 1938.

On the following day, July 10, at $6^h\ 39^m$ (fig. 15), a bright streamer is seen in place of the arches, throwing a curved jet on the equator and containing a dark arch. On the same day, at $12^h\ 10^m$ (fig. 16), the dark arch has risen. Three days later, July 13, at $9^h\ 50^m$ (fig. 17), the corona has completely changed. It shows numerous fine jets to the east and a dark space connected with a prominence to the west. The north pole is very dark, the south pole is provided with fine jets. The reproductions do not show all the details visible on the negatives.

A photograph on July 18 shows a very bright fan-like streamer, to the west. Another photograph taken on July 19 at $12^h\ 09^m$ shows brilliant trails due to the passing of large particles, which are probably thistle-down, crossing the Sun at an altitude of about 5000 m. These seeds generally precede the particles of dust.

On 1937 May 11, at 9^h, the planet Mercury passed in front of the corona tangentially to the Sun, near the south pole. The sky was completely covered during the first part of the transit across the corona. It became clear at $10^h\ 10^m$, which allowed Mercury to be seen and 16 photographs to be taken.

On the first one, at $10^h\ 22^m$, the planet is $1'\ 10''$ distant from the edge of the Sun ; it passes in front of a prominence. Ten minutes later, Mercury leaves the prominence and is outlined against the corona. The sky was not perfectly clear, as there were very slight cirrus clouds, the ice crystals of which produced streaks. On the last photograph, taken at $11^h\ 14^m$, Mercury is $2'\ 37''$ distant from the Sun, and is still visible due to the coronal light on which it is outlined. Immediately afterwards, the sky became overcast.

On these photographs, neither a line nor a point of light, appears on the edge of the disc of Mercury. We may conclude that the atmosphere of Mercury diffuses light very feebly, and that it produces, on the surface of the planet, a refraction less than one-thirtieth of that of the Earth.

The Spectrum of the Corona.—I have used the spectrograph, last described, to explore the spectrum of the corona, part by part, from 3350 A., the limit of the transparency of the coronagraph, up to 12000 A., the limit of the sensitiveness of the plates. Most of the plates have been taken with the camera of 1 m. focus which gives a dispersion of 5 A. per mm. with the third order of the grating, in the ultra-violet, and a dispersion of 7·5 A. per mm. with the second order, in the visible and the beginning of the infra-red up to 8300 A. Two shorter cameras, of 35 cm. and $8\frac{1}{2}$ cm. in focus, enabled me to continue the registration of the spectrum up to 11300 and 12000 A. It was necessary to use seven different kinds of plates and make exposures from 10 minutes in the visible spectrum up to 4 hours in the infra-red.

Most of the spectra were taken with a slit in the form of an arc of a circle, on the inside of which the image of the disc of the coronagraph was thrown. This image was adjusted in such a way that the slit crossed either the west or the east side of the corona, at about 40″ from the edge of the Sun, between latitudes $\pm\ 70°$.

Fig. 18 (Plate 15) shows the ultra-violet extremity of the spectrum of the west side, from 3330 A. on the left to 3480 A. on the right on 1937 July 19.

10 11

9 12

13 16

17

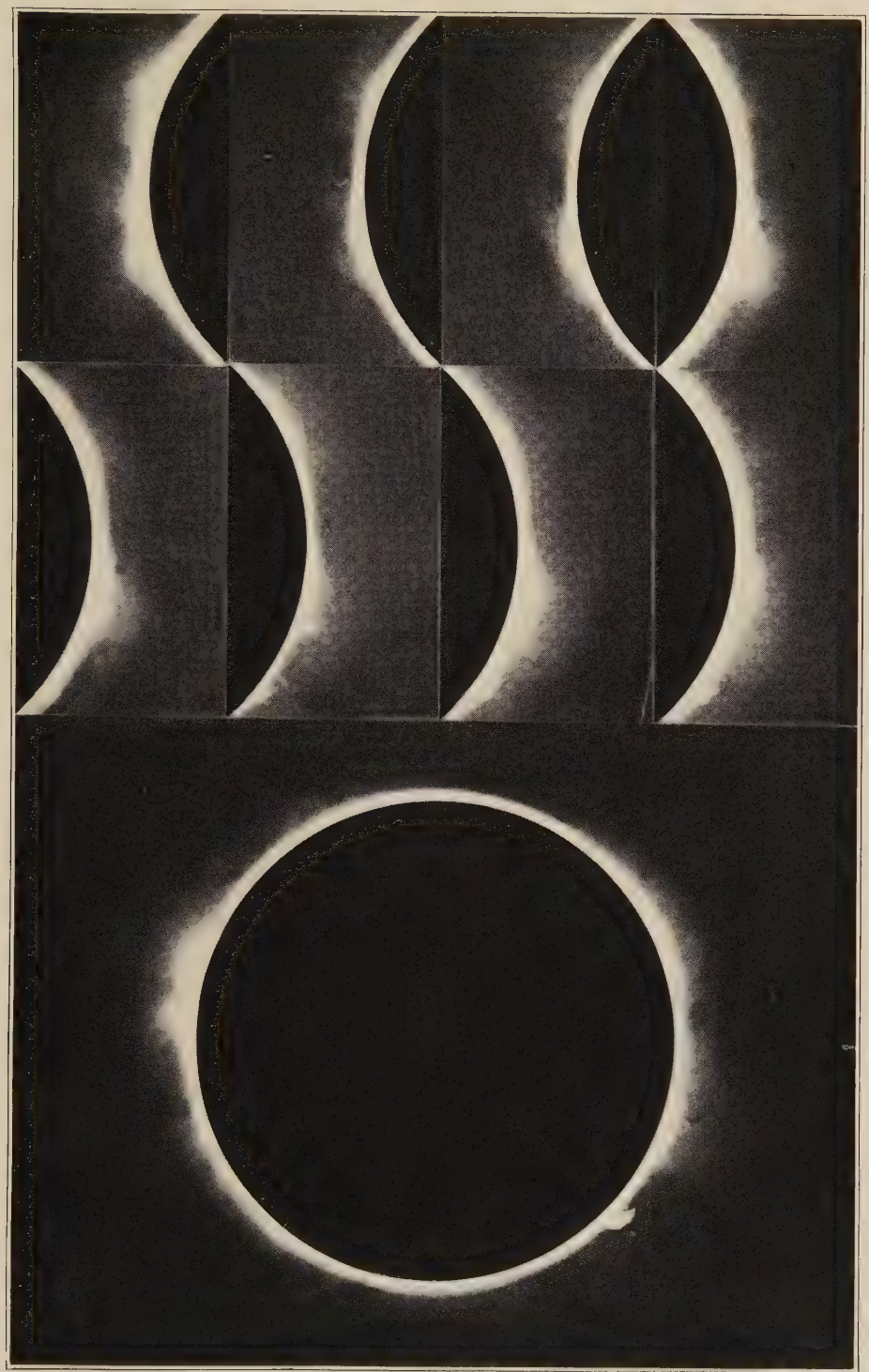

Direct photographs of the corona taken July 1938.

Figs. 9, 10, 11.—East side, July 6 at 9^h, 15^h, 17^h 55^m.
Figs. 12, 13, 14, 15, 16.—West side, July 9 at 10^h 30^m, 15^h 2^m, 18^h 40^m; July 10 at 6^h 39^m, 12^h 10^m.
Fig. 17.—The corona, July 13 at 9^h 50^m.

All the lines are in the form of an arc of a circle which is that of the slit. You see the Fraunhofer lines, due to diffused solar light, and, in the middle, the coronal line 3388 A. having maxima near the equator. The slit crossed a bright equatorial prominence of which you see the emission lines with a faint continuous spectrum.

In the ultra-violet, the violet and the blue, I could not photograph any other line of the corona. The other coronal radiations are fainter and are blotted out by atmospheric diffusion. In the green, the diffusion of the atmosphere is reduced and the conditions are more advantageous. For example, fig. 19 shows a part of the spectrum of the east edge, on 1937 July 18 at $14^h\ 20^m$. We have the *b* group of magnesium and the double E line. The slit crossed 5 prominences, the lowest of which emitted numerous metallic lines and a strong continuous spectrum which produced a bright and narrow horizontal line. Nearer the equator, the slit also crossed a coronal streamer of which the continuous spectrum is visible. On the streamer we see, to the left, the coronal line λ 5116, and, to the right, the strong coronal line λ 5303 between 4 ghosts of the grating. On the continuation of the same plate, the coronal line λ 5536 ought to be seen, but is not visible. It does not appear on any of the plates I have taken in 1936, 1937 and 1938, under favourable conditions and a very strong solar activity. According to the rare observations which have been made of it, its intensity was one-half of that of λ 5116. We can conclude either that it has become much fainter or that it rises to less than 40″, contrary to the other known lines.

Fig. 20 shows the continuation of the same spectrum in the yellow. To the right, we have the bright helium line D_3, then the two solar lines D_1 and D_2 strongly emitted by the lower prominence. The continuous spectrum of the coronal streamer appears very bright. If these plates do not show the line λ 5536, in return they show a new line which has not been observed during eclipses. It appears to the left, on the coronal streamer, while the prominences do not emit it. Its wave-length is 5694·42 A., and its intensity is about half that of λ 5116. A spectrum of the east side taken on 1938 July 6 strongly shows λ 5303 to the left and λ 5694 to the right, but does not show λ 5536 situated between the two. Fig. 21 shows another part of the last spectrum but one, farther away, in the red. We have the coronal line λ 6374 and, in the middle, the line *Hα* so highly exposed that it shows 40 ghosts. After the line *Hα* we have the red helium line emitted by the prominence, and then the coronal line λ 6702.

The spectra do not show any of the new lines found by the Japanese in the eclipse of 1936. These lines were found, indeed, on small-scale spectra on which agglomerations of grains are to be feared.

The beginning of the infra-red is seen on a spectrum of the west side taken on 1937 June 10 from 14^h to 15^h (fig. 23, Plate 16). To the right is the telluric band *a*, and to the left the helium line λ 7065 emitted by the prominences. Slightly to the left of the latter we see a coronal line which had not been known when we found it. It has a wave-length of 7059·62 A. Later, Professor Menzel found this line on a plate taken by him during the

eclipse of 1936. To the right, the two strongest prominences emit a line of oxygen 7254 A. Farther on in the infra-red, fig. 24 shows a spectrum of the west side taken on 1937 May 28 with a three-hours' exposure. In the middle, the coronal line 7892 A.; to the right, a faint coronal line 8024 A., which has not been observed during eclipses. To the left, we see the triplet of oxygen emitted by four prominences. After an extensive tract of the spectrum without coronal radiation are two strong coronal lines, 10747 A. and 10798 A., never yet photographed during eclipses. They appear very bright on a spectrum of the east side, taken on 1936 August 5, from 9^h to 11^h (fig. 25). They are followed by the helium line 10830 A. emitted by a series of prominences, and to the right begins the telluric band Φ. Both coronal lines have an intensity about equal to that of the green line λ 5303. On a spectrum of the east side taken on 1936 July 23 (fig. 26), the helium line is very strong and followed with the line 10938 A. of hydrogen, the sixth term of the Paschen series. Both spectra were taken on Eastman Z plates hypersensitised with ammonia, and by reducing the dispersion to 45 A. per mm. with the camera of 35 cm. focus and the first order of the grating.

Two plates have been taken with the camera of $8\frac{1}{2}$ cm. focus and exposures of 5 minutes and of 3 hours. On the first, the two strong coronal lines are seen; on the second, the spectrum extends to 12000 A. without showing any other emission line.

The spectra, of which these are some examples, are very numerous—about 200. They show eleven coronal lines, five of which are new. These records establish that all the coronal lines are wide.* Taking into account the influence of the spectrograph, their average widths are 0·8 A. in the green, 0·9 to 1 A. in the red and greater in the infra-red.

The wave-lengths have been measured on the best and the most dispersed spectra. The intensities of the strongest lines have been drawn from a series of plates taken on 1936 August 5 with solar comparison spectra. The following list gives for each line: the wave-length, λ, a mean value for the east and west sides, in international angstroms; the probable error, Δλ; the number, *N*, of plates used for the wave-length measurements; the order, *P*, of the spectrum; the dispersion, *D*, in A. per mm.; the mean time, *T*, of

λ	Δλ	*N*	*P*	*D*	*T*	*i*
					h m	
3388·10	± 0·07	2	3	5·2	0 35	...
5116·03	± 0·02	3	2	7·5	0 18	2·6
5302·86	± 0·02	4	2	7·5	0 18	120
5694·42	± 0·05	3	2	7·5	0 10	1·5
6374·51	± 0·03	4	2	7·5	0 27	28
6701·83	± 0·03	4	2	7·5	0 33	3·3
7059·62	± 0·05	2	2	7·5	0 40	4
7891·94	± 0·07	3	2	7·5	1	29
8024·21	± 0·10	1	2	7·5	1	1·3
10746·80	± 0·15	1	1	15	4 10	240
10797·95	± 0·15	1	1	15	4 10	150

* *L'Astronomie*, 51, 211, 1937.

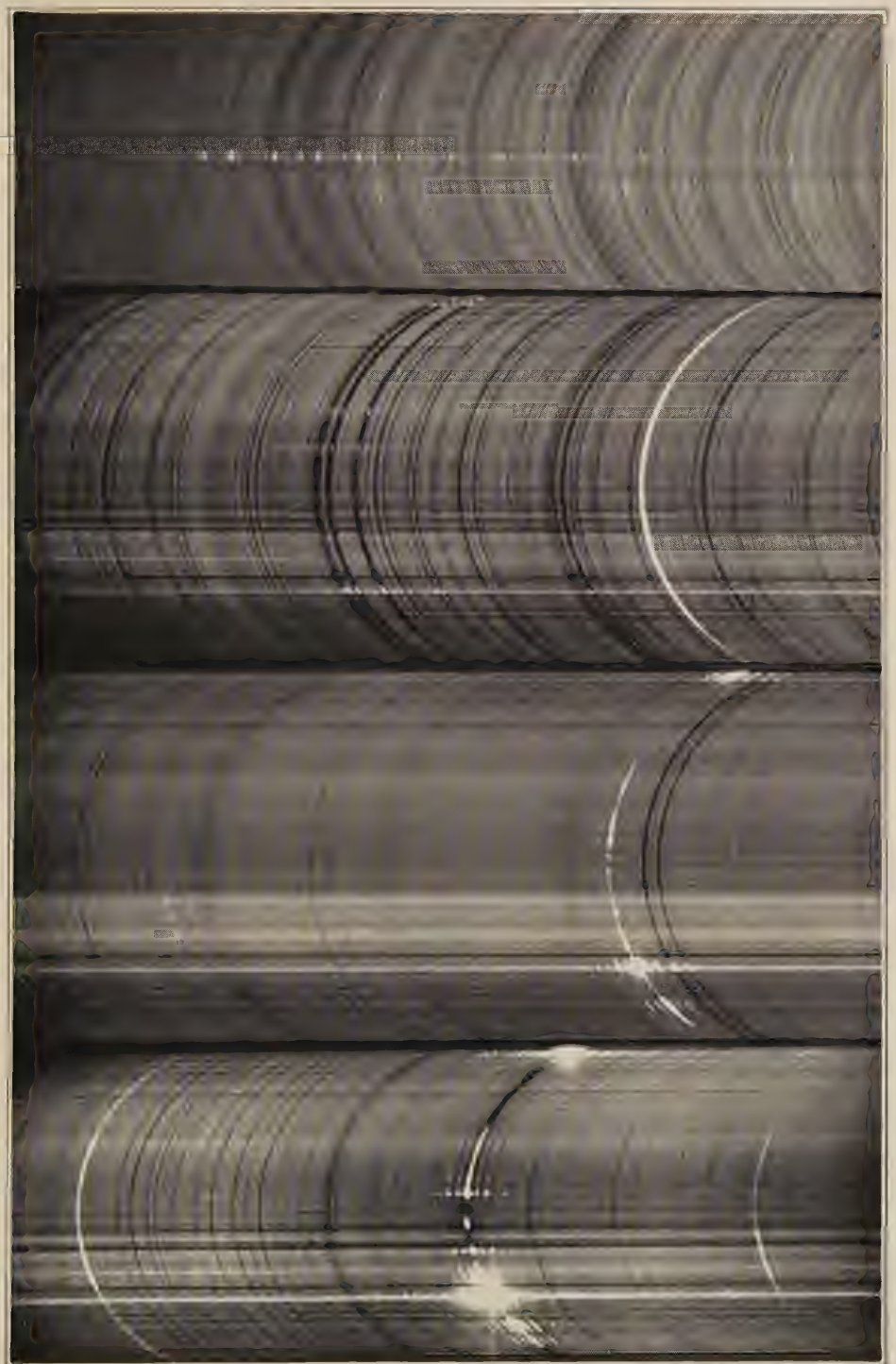

Spectra of the corona and prominences.

Fig. 18.—Line λ3388.
Fig. 19.—Lines $\lambda\lambda$5116 and 5303.
Fig. 20.—Lines λ5694 and D_3.
Fig. 21.—Lines λ6374, Hα, and λ6702.

Bernard Lyot, George Darwin Lecture.

exposure; and the intensity maximum, *i*, of the line compared with the millionth of that of 1 angstrom of the neighbouring continuous solar spectrum.

Measurements of the wave-length of the green line, to the east and west edges, made on spectroheliograms by sections, show that the corona revolves in the same sense as the Sun and at the same rate to within 30 per cent.

The eleven lines of the corona visible on the plates are not all distributed in the same way around the Sun. It is easy to compare the distributions of these monochromatic radiations by placing side by side, on the same plate, the lines which are far away from one another in the spectrum. Fig. 27 (Plate 16) shows, for example, the coronal lines photographed on the west side on 1937 July 18. The north pole of the Sun points to the top. We see, from left to right, lines λλ 8024, 7892, 6702, 6374, 5694, 5303, 5116 and 3388. In the centre, λλ 6374, 5694 and 5303 have different distributions. In fact, (*a*) λ 6374 has, to the north-west, a strong double maximum not existing on the two following lines; (*b*) λ 5694 possesses, slightly above the equator, a maximum corresponding to a minimum of λ 6374; (*c*) on the other hand, under the equator, where λ 5303 is at its maximum, λ 5694 is invisible; (*d*) the line λ 7892 (the second one to the left) agrees with λ 6374 only, whilst the other lines tally with λ 5303.

According to a great number of spectra of this kind, too long to examine here, we can class, in three series, the eleven lines observed. The first series comprises line λ 5303, and lines λλ 3388, 5116, 6702, 7059, 8024, and probably also λ 10747 and λ 10798. The second series comprises only the new line λ 5694, different from all the others. The third series comprises lines λλ 6374 and 7892.

Spectra of the Prominences.—Some of the plates show spectra of prominences particularly rich in lines, the measurements of which are not finished. On the preceding plates you have seen some helium, oxygen and metallic lines of relative intensities very different from those existing in the chromosphere. We are now going to show you the spectrum of hydrogen represented by the series of Paschen and Balmer.

Fig. 28 (Plate 16) shows a spectrum of the north-east side taken on 1938 July 10 with the solar lines of ionised calcium 8498, 8542 and 8662 A. strongly emitted by a prominence, as well as numerous lines of the Paschen series. From right to left: terms 11, 12, 14, 16, 17, 18, . . . up to term 31. The terms 13 and 15 are hidden by lines of calcium. Between terms 17 and 18 we see a line of oxygen, 8446·7 A. From the limit of the series, the continuous spectrum of the prominence (probably due to the solar light diffused by it) is reinforced because a continuous spectrum of hydrogen is added to it. The continuous spectrum of hydrogen is better visible on a spectrum of the south-west side (fig. 29) taken on 1937 June 30 from $11^h\ 30^m$ to $12^h\ 30^m$.

In the same way, in the ultra-violet, figs. 30 and 31 show a spectrum of the north-west side, taken on 1938 July 12 at 8^h. On the right of fig. 30 are term 7 of the Balmer's series close to line H of calcium, then line K of calcium and terms 8, 9 and 10. On fig. 31 are terms 10, 11, . . . up to

term 31 and followed by the continuous spectrum of hydrogen. The lines of Paschen's series are much fainter than Balmer's; but the diffusion, greatly reduced in the infra-red, renders observation of both series equally easy.

Prominences through Coloured Filters.—The continuous spectrum of the prominences had been observed during eclipses, but the plates, generally taken with an objective prism, indicated that this spectrum was emitted only by some particular parts of the most intense prominences.

To check this fact, I have photographed the same prominence through three coloured filters successively. Four photographs were taken on August 27 at $12^h\ 15^m$, on a prominence to the north-west. The first and the last pictures (Plate 17, figs. 32 and 35) were taken through a filter cutting off the chromospheric radiations and allowing only the continuous spectrum between 6100 and 6400 A. to pass. The second picture (fig. 33) was taken with the helium line D_3 and the third one (fig. 34) with the line *Hα* of hydrogen. The pictures obtained with the continuous spectrum are identical with that given by the helium line D_3, both with regard to form and relative intensities. This spectrum comes, therefore, from all parts of the prominence.

Measurements of polarisation made through these filters have given the following results :—

The continuous spectrum of the prominences, in the red and the orange, has about the same polarisation as the corona, in a radial plane.

The radiations *Hα* and D_3 are, on the contrary, about 10 times less polarised, and their plane of polarisation is deviated from the radius, sometimes to more than 20°.

In the visible spectrum, the continuous spectrum of the prominences appears to be due to the diffusion of the solar light by the electrons they contain. It would be interesting to study, as well, the polarisation of the continuous spectrum emitted beyond the limits of the Paschen's and Balmer's series.

Movements of Prominences.—The coronagraph, supplied with a filter isolating line *Hα*, shows the prominences with great brilliancy against a very dark sky, and thus causes their faintest details to appear. Moreover, thanks to the highly favourable situation of the Pic du Midi, the seeing is often very good. Since the summer of 1935, I have taken advantage of these good conditions to register the movements of the prominences on cinema films that we shall presently see on the screen.

The cinematograph possesses a considerable advantage over direct observation; it enables us to vary, at will, the scale of time in order to give the phenomena the speed best adapted to our perception. We have thus been led to accelerate the movements 600 times. The views have been taken on panchromatic 35-mm. films at the rate of two per minute. The exposures were made, sometimes automatically, sometimes choosing, through an eyepiece, the moments of steadiness, which generally gave sharper pictures. The times of exposure were 2 or 3 tenths of a second. The scale of the pictures is such that the total height of the photographs represents

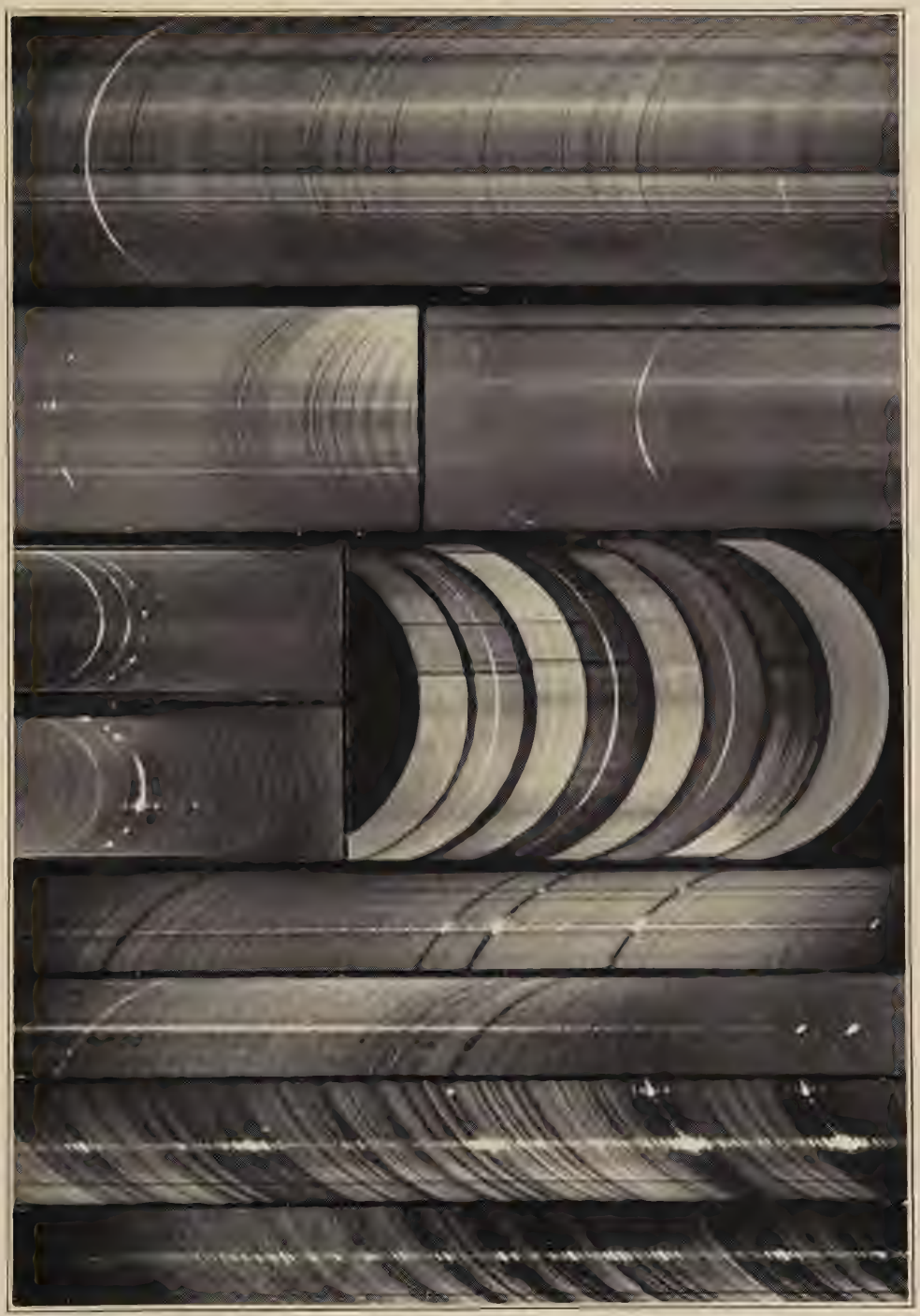

Spectra of the corona and prominences.

Fig. 22.—Lines λλ 5303 and 5694.
Fig. 23.—Lines λλ 7059, 7065 He and 7254 01.
Fig. 24.—Lines λλ 7775 01, 7892 and 8024.
Figs. 25 and 26.—Lines λλ 10747, 10798, 10830 He and 10938 H.
Fig. 27.—Distribution of the coronal lines on the West side, on 1937 July 18.
Figs. 28 and 29.—Infra-red lines of ionized calcium and Paschen's series.
Figs. 30 and 31.—Lines H and K and the Balmer's series.

Bernard Lyot, George Darwin Lecture.

an average of about 380,000 km. ; that is to say, the distance of the Earth from the Moon or 30 times the diameter of the Earth. The films are very short, and, in order to render the movements easier to catch, each one is thrown twice successively on to the screen. Eleven films are projected.

The first one was taken on 1935 September 11.* One branch of the prominence, situated to the north-east, consists of two parts placed one in front of the other. One part is stationary, the other moves upwards.

Another prominence † was filmed to the west, on 1936 August 8 from 8^h to 13^h. A whirling motion is seen in its head. Some filaments, coming from several parts of it, gain impetus in a very active part of the chromosphere surrounded with the most intense coronal dome and in which a bright eruption, 100″ in height, took place after the film was finished. Some filaments fade away in rising and light up again in falling. Near the Sun, they attain a speed of 180 km. per second.

The best film was obtained on 1937 June 12, from $8^h\ 30^m$ to $15^h\ 10^m$, on a prominence situated to the east. At the beginning, it consists of three clouds detached from the Sun's edge (Plate 17, fig. 36). The material flows for 2 hours in the form of very fine filaments, then the right part is blown upwards and falls again to its former level. Towards the fourth hour (of the taking of the film), the cloud on the right becomes very bright. A chromospheric eruption leaves the Sun at the rate of 700 km. per second and cuts the prominence into two parts. The luminous mass, the equilibrium of which is lost, flows on to the Sun ; it seems to make the tour of a rounded invisible obstacle surrounding the place of the eruption.

A film taken on 1938 June 10 shows an arch, to the north, flying up slowly, then more and more rapidly (fig. 37). Unfortunately, the end of the phenomenon is veiled by cirrus.

The last prominence, cinematographed on 1938 July 19, to the west (fig. 38), is similar to those called "coronal" by Pettit. The material moves, on both sides of the arches, in opposite ways ; in some places, it originates in invisible clouds.

In conclusion, it is of interest to compare the results obtained by the two methods—with and without eclipses.

Direct Photographs of the Corona.—The outer parts can be obtained only during eclipses. The method without eclipse shows only the inner corona, but, in return, it alone enables us to follow its variations.

Spectrum of the Corona.—In the ultra-violet, the violet and the blue, the atmospheric diffusion is very strong and the new method is very inferior to the old one. In the green, the diffusion is less strong ; its effects can be diminished by increasing the dispersion and making longer exposures, if necessary. If, moreover, we choose days during which the corona is particularly intense, the faint coronal lines appear then as well as during eclipses. The plates, more numerous and on a larger scale, enable us to distinguish these lines from the agglomerations of grains ; they give their wave-lengths with greater accuracy. In the infra-red, the plates not being

* *L'Astronomie*, **51**, 208, 1937.
† *L'Astronomie*, **52**, 204, 1938.

very sensitive, the method without an eclipse is much superior to the other.

Prominences.—Only the method without an eclipse enables us to wait for the appearance of very bright objects having the richest and most interesting spectra.

We must not conclude that observations without eclipses can replace the expeditions for the study of eclipses. The new and the old methods complete one another on numerous points, and their simultaneous use will increase our knowledge of the outer atmosphere of the Sun much more rapidly.

33 34

32 35

36

37

38

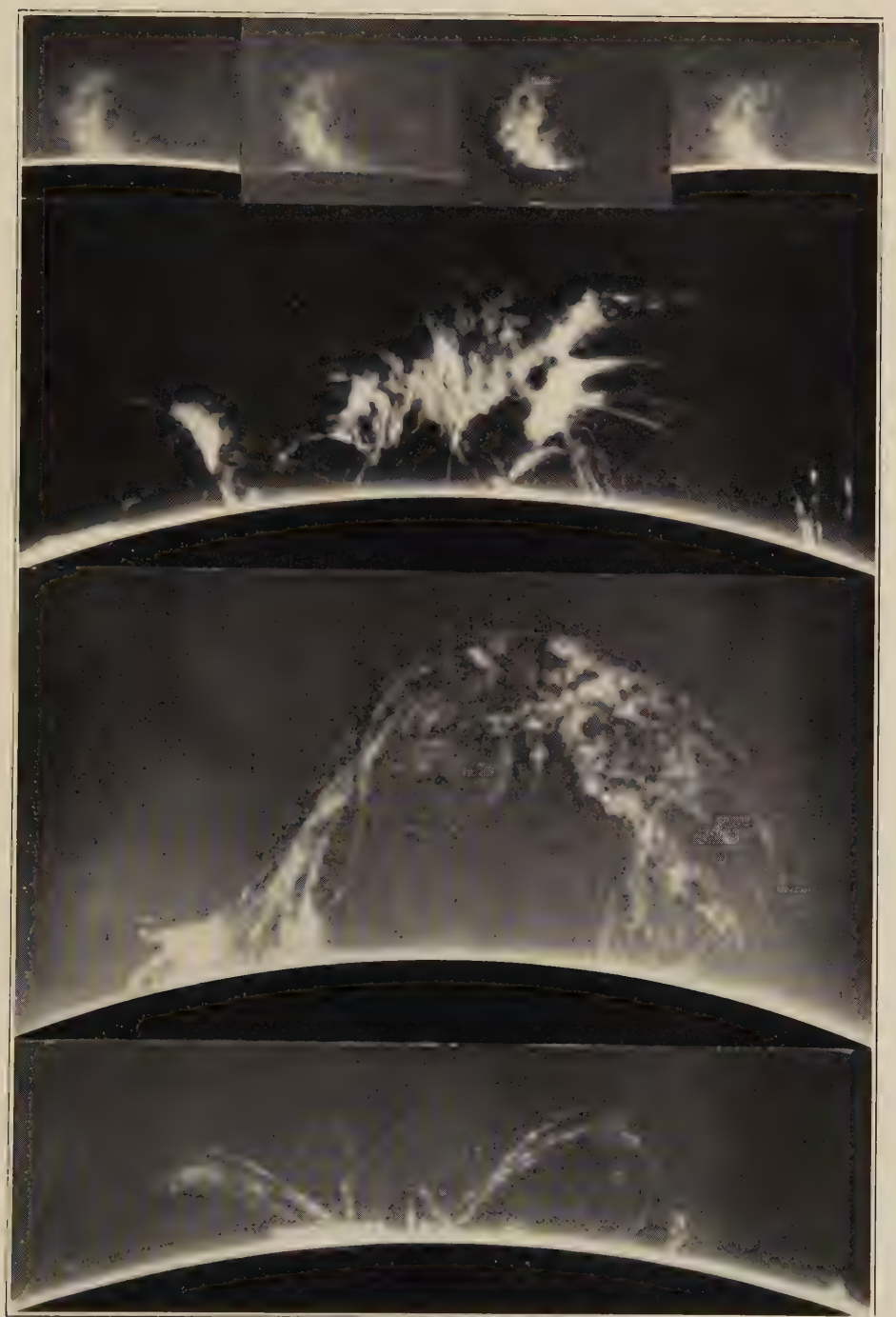

Figs. 32, 33, 34, 35.—Prominence photographed to the North-West, August 27 at $12^h\,15^m$; figs. 32 and 35 with the continuous spectrum, 33 with the line D3, 34 with the line Hα.
Fig. 36.—Prominence to the East, 1937 June 12 at $9^h\,16^m$.
Fig. 37.—Prominence to the North, 1938 June 10 at $12^h\,30^m$.
Fig. 38.—Prominence to the West, 1938 July 19 at $9^h\,32^m$.

Bernard Lyot, George Darwin Lecture.

THE HYDROGEN CONTENT OF WHITE DWARF STARS IN RELATION TO STELLAR EVOLUTION

Sir A. S. Eddington, O.M., F.R.S.

1. *Introduction.*—The physical theory of the state of matter in white dwarf stars was first treated by R. H. Fowler in 1926. His investigation rested on a new departure in wave mechanics which had been made by Fermi and Dirac a few months previously. Fowler obtained the equation of state $P = K\rho^{\frac{5}{3}}$, applying in conditions approximately realised in the interior of a white dwarf. In 1929 E. C. Stoner and W. Anderson independently put forward a modified equation of state supposed to take account of the change of mass with velocity of the electrons, and astronomical discussions have generally been based on their theory. The modification is, however, fallacious; and I think there can be no doubt that the original formula $P = K\rho^{\frac{5}{3}}$ is accurate.

The untenability of the Stoner-Anderson formula has been pointed out in earlier papers.* In reference to a more recent attempt to defend it by Chandrasekhar †, it seems sufficient to say that the wave function treated by him represents a freely dispersing system of electrons moving under no forces, and has no relation to the problem in hand.

Observational data for white dwarfs, although meagre, provide sufficient material for an instructive comparison with theory. There is evidently need for a re-survey of this subject, which had become confused by the distractions of the Stoner-Anderson formula. Almost as important as the elimination of actual error is the restoration of simplicity to a subject which had become highly and, as it now appears, unnecessarily complicated. The formulæ derived from the Fowler equation of state are very simple, and this makes it easy to assess the effect of uncertainties of the observational data.

The most definite line of investigation is a determination of the hydrogen content of these stars. White dwarf conditions are exceptionally favourable for a determination of hydrogen content. The procedure is entirely different from that employed for ordinary stars. It is an impressive illustration of the applicability of physical theory to the stars that the determinations of hydrogen content of Sirius and its companion are in near agreement, that of the companion being perhaps rather the higher; the methods used for the two stars have scarcely anything in common, and diverge through different branches of atomic physics.

Since the theory of maintenance of a star's heat is intimately connected with the supply of hydrogen, we are led on to discuss the special difficulty of including white dwarfs in the evolutionary scheme. In particular, the

* *M.N.*, **95**, 194; **96**, 20, 1935; *Relativity Theory of Protons and Electrons*, § 13.5, etc., 1936.

† *Study of Stellar Structure* (Chicago, 1939), p. 366.

existence of white dwarfs is found to have an important bearing on recent suggestions as to the mechanism of liberation of subatomic energy.

2. *The Principal Formulæ.*—The following formulæ relate to stars at zero temperature (black dwarfs). It is explained in § 6 that the corrections needed to take account of the actual internal temperatures of white dwarfs are likely to be inappreciable.

The physical theory of degenerate matter gives

$$P=\tfrac{1}{5}\left(\frac{3}{8\pi}\right)^{\frac{2}{3}}\frac{h^2}{m}\sigma^{\frac{5}{3}}, \tag{2.1}$$

where σ is the number of free electrons per unit volume, h Planck's constant, and m the mass of an electron. Let μ_1 be the number of units of molecular weight per free electron, so that

$$\rho=\sigma\mu_1 H, \tag{2.2}$$

where H is the mass of a hydrogen atom. By (2.1) and (2.2)

$$P=K\rho^{\frac{5}{3}}, \tag{2.3}$$

where

$$K=\tfrac{1}{5}\left(\frac{3}{8\pi}\right)^{\frac{2}{3}}\frac{h^2}{m}\left(\frac{1}{\mu_1 H}\right)^{\frac{5}{3}}=[12{\cdot}9955]\mu_1{}^{-\frac{5}{3}}, \tag{2.4}$$

the square bracket indicating the decimal logarithm of the coefficient.

The relation (2.3) gives a polytrope with index $n=1{\cdot}5$, and the corresponding relation between the mass and radius is (*Internal Constitution of the Stars*, equation (57·3))

$$\left(\frac{GM}{M'}\right)^{\frac{1}{3}}\left(\frac{R}{R'}\right)^{\frac{3}{2}}=\frac{(\frac{5}{2}K)^{\frac{3}{2}}}{4\pi G},$$

with the values (from Emden's tables) $M'=2{\cdot}718$, $R'=3{\cdot}657$. Hence

$$MR^3=\frac{M'R'^3}{16\pi^2G^3}(\tfrac{5}{2}K)^3=[61{\cdot}6349]\mu_1{}^{-5}. \tag{2.5}$$

For the Sun $MR^3=[65{\cdot}8241]$. We shall henceforth measure M and R in terms of the Sun's mass and radius. In these units (2.5) becomes

$$MR^3=[\bar{5}{\cdot}8108]\mu_1{}^{-5}. \tag{2.6}$$

An important observational datum is the Einstein shift of the spectral lines, which is proportional to M/R. We denote its value (expressed as a Doppler shift in kilometres per second) by α. Since $\alpha=0{\cdot}634$ on the Sun, the general value is

$$\alpha=0{\cdot}634M/R.$$

Eliminating R by (2.6) we have

$$\alpha=15{\cdot}8M^{\frac{4}{3}}\mu_1{}^{\frac{5}{3}}. \tag{2.7}$$

Or, eliminating M,

$$\alpha=[\bar{5}{\cdot}6131]R^{-4}\mu_1{}^{-5}. \tag{2.8}$$

Equations (2.6), (2.7), (2.8) determine μ_1, and hence the hydrogen content, when any two of the three quantities M, R, α are known by observation.

The value of the central density (which in the $n = 1{\cdot}5$ model is just 6 times the mean density) in a white dwarf of given mass or radius or Einstein shift is also of interest. Using (2.6) we find

$$\rho_c = [5{\cdot}1168]M^2\mu_1^5 = [\bar{4}{\cdot}7384]R^{-6}\mu_1^{-5} = [3{\cdot}3191]\alpha^{\frac{3}{2}}\mu_1^{\frac{5}{2}}. \qquad (2.9)$$

3. *The Hydrogen Content.*—The "modified" molecular weight μ_1 differs from the ordinary molecular weight μ, being the weight per free electron instead of the weight per free particle. The difference is important for hydrogen and helium, which give $\mu_1 = 1{\cdot}0$, $2{\cdot}0$ as compared with $\mu = 0{\cdot}5$, $1{\cdot}33$. It is especially noteworthy that the value of μ_1 for helium is precisely the same as for the other common light elements *C*, *N*, *O*, *Mg*, *Si*, *Ca*. Determinations of hydrogen abundance in white dwarfs are therefore entirely independent of the abundance of helium—unlike the determinations for ordinary stars which depend on μ. For *Ti*, *Fe* and elements up to atomic number 40, μ_1 ranges from $2{\cdot}1$ to $2{\cdot}3$; and it increases up to $2{\cdot}5$ for the heaviest elements. We adopt $\mu_1 = 2{\cdot}1$ for the non-hydrogen content; the error is scarcely likely to exceed $\pm\, 0{\cdot}1$. The following table then gives the percentage by weight of hydrogen X corresponding to different values of μ_1:—

μ_1	X	μ_1	X
2·1	0	1·5	36·4
2·0	4·6	1·4	45·5
1·9	9·6	1·3	56·0
1·8	15·2	1·2	68·2
1·7	21·4	1·1	82·7
1·6	28·4	1·0	100

We shall in §§ 4, 5 determine X in three white dwarfs for which more or less satisfactory observational data are available. Apart from the actual value of such determinations, we may notice that it is a striking confirmation of the general validity of the physical theory of degenerate matter that the values of μ_1 which satisfy the observational data lie in the narrow permitted range 1·0 to 2·1.

A determination of X, whether for an ordinary star or a white dwarf, is necessarily a venturesome undertaking; for it assumes that all sources of deviation from the adopted model have been exhaustively studied, so that the hydrogen content remains the only unknown when we come to the fine adjustment of theory and observation. On the whole, the determination for a white dwarf seems less precarious than the determination for an ordinary star; in the latter the highly complicated calculation of the outflow of radiation involves many factors for which we can only give probable estimates. At present, however, the theoretical advantage of the white dwarf determinations is largely counterbalanced by the meagreness of the observational data.

4. *The Companion of Sirius.*—For this star $M = 0{\cdot}95$, so that by (2.7)

$$\alpha = 14{\cdot}8\mu_1^{\frac{5}{3}}.$$

Thus the extreme values of α, corresponding to "all hydrogen" and "no

hydrogen", are 15 and 51 km. per sec. The observed value, found both by Adams and Moore, is 20 km. per sec. This is much nearer to the "all hydrogen" value, and it is unlikely that observational uncertainties can be so large as to upset the conclusion that the companion of Sirius contains a rather large proportion of hydrogen.

The value $\alpha = 20$ gives $\mu_1 = 1{\cdot}20$, $X = 68$. To illustrate the effect of observational uncertainty, the values $M = 0{\cdot}85$, $\alpha = 25$ (which may perhaps be regarded as extreme limits) give $X = 36$.

For Sirius itself B. Strömgren found $X = 40$ on the assumption of no helium content, with larger values if helium is abundant. It would seem therefore that both components have a roughly equal abundance of hydrogen, that of the companion being perhaps rather the greater. This agrees with our usual view of the evolution of a double star. The mass before fission would have rapid rotation, and the material would be fairly well stirred by the convection currents due to rotation. In so far as the mixing was imperfect, hydrogen would preponderate in the outer part—both on account of diffusion and because the elimination of hydrogen by transmutation occurs in the hot central parts. The companion, being formed from the outer material, would therefore start with rather more hydrogen than Sirius; and the excess would slowly increase owing to the more rapid transmutation of hydrogen in the brighter component.

On the other hand our result negatives the view, often suggested, that the reason why a star contracts into a white dwarf is that it has used up its supply of hydrogen.

Instead of using M and α, we might have used M and R, adopting the value of R obtained from the absolute magnitude and the effective temperature corresponding to the observed spectral type. This, however, is much more precarious, because there is great uncertainty in extrapolating the usual temperature-type relation to a white dwarf. Since the temperature corresponding to a given spectral type is considered to be higher in a dwarf than in a giant, we should be tempted to adopt a still higher value in a white dwarf; but actually, to agree with the observed α, the temperature must be lower. From $M = 0{\cdot}95$, $\alpha = 20$, we derive $R = 0{\cdot}030$. From the visual magnitude $8^{m}{\cdot}53$ (Kuiper, 1935) and parallax $0''{\cdot}373$, we obtain the absolute visual magnitude $11^{m}{\cdot}39$. Combining this with R, the effective temperature T_e is 7020°, which is unexpectedly low for a star classed as A5. Presumably therefore we should adopt effective temperatures lower than usual in treating other white dwarfs.

5. *Van Maanen No. 2.*—According to Kuiper, the radius calculated from the absolute magnitude and spectral type is $R = 0{\cdot}0089$. The observed radial velocity is 240 km. per sec., which must be largely Einstein shift. If we assume that α is between 200 and 280 km. per sec., and apply (2.8), we obtain $\mu_1 = 2{\cdot}0$ to $1{\cdot}88$, giving $X = 5$ to 11 per cent. The corresponding mass is 2·8 to 3·9 times that of the Sun.

It would appear that in this star the hydrogen is nearly exhausted. It is difficult to judge whether the accuracy of the observational data is sufficient to render this conclusion trustworthy. If Kuiper in deriving R employed

the ordinary temperature-type relation instead of the specially low temperature scale appropriate to white dwarfs (§ 4), his R would be too small and the resulting μ_1 would be too large.

o^2 *Eridani.*—The combined mass of the double star is 0·65. The mass of the fainter component, which is an ordinary red dwarf, may be estimated from its absolute magnitude as 0·23, giving $M=0{\cdot}42$ for the white dwarf. The absolute visual magnitude is $11^{m}{\cdot}3$.

Using (2.6) to determine R, we can calculate the effective temperature corresponding to any assumed hydrogen content. We have, for example,

X	μ_1	T_e
0	2·1	10,700°
28	1·6	8,300°
45	1·4	7,200°

The star is classed as B9, so that it seems scarcely possible to assign to it an effective temperature much below 10,000°. It would appear therefore that o^2 Eridani, like Van Maanen No. 2, contains comparatively little hydrogen.

A.C. 70° 8247.—This star, discovered by Kuiper, is remarkable as having the smallest radius known. We adopt $R=0{\cdot}005$ as a rough estimate. The point of interest is that even this small radius is consistent with a reasonable value of the mass. For zero hydrogen content (2.6) gives $M=12{\cdot}7$; for 28 per cent. hydrogen $M=49$. For higher hydrogen content M increases to values which we should deem unlikely.

6. *Corrections for Temperature.*—It is believed that the temperature in the interior of the companion of Sirius is not greater than that of a main series star. The argument may be put as follows. Taking the usual opacity law $k \propto \rho/gT^{7/2}$, and assuming first the same temperature in both stars, the luminosity will be proportional to g/ρ. The actual difference of luminosity (7 magnitudes) roughly corresponds to the difference of ρ: more precisely, the guillotine factor g is required to be about 10 times greater in the white dwarf. It is argued that the high proportion of occupation of the energy states in degenerate matter will increase the guillotine factor much more than 10-fold, so that the assumption of equal temperature makes the white dwarf much too bright. The temperature must therefore be lower than on the main series.

The argument is not convincing, because the white dwarf state is far beyond the range to which Kramers' theory of absorption is intended to apply, and the energy-transitions contemplated are of an entirely different nature. At present there is not even a rudimentary theory of absorption in degenerate matter. Rather vague considerations incline me to accept the current view that the opacity in degenerate matter is abnormally low; but there is very little to guide us.

If the temperature is not zero, the usual gas pressure $\mathbf{R}\rho T/\mu$ (as well as the radiation pressure, if appreciable) must be added as a correction to $K\rho^{5/3}$. The condition that this correction does not exceed 10 per cent. is $T < (\mu K/10\mathbf{R})\rho^{2/3}$, or

$$T < [4{\cdot}08]\mu\mu_1^{-5/3}\rho^{2/3}.$$

This is just about satisfied in the companion of Sirius if the temperature does not exceed that of a main series star. The formulæ of § 2 will then give sufficient accuracy.

If the current assumption of low opacity is wrong, so that the internal temperature is higher than we have supposed, R will be thereby increased; and the observed value should be correspondingly reduced before applying the black dwarf formulæ of § 2. By (2.6) μ_1 is increased and the hydrogen content reduced. But this should apply, not only to the companion of Sirius, but also to o^2 Eridani and Van Maanen No. 2, in which μ_1 is so near the limit that no important increase is possible. The latter stars therefore give some support to the view that the opacity in degenerate matter is low enough to avoid temperatures much above those of the main series.

In smaller masses it is necessary to take account of incomplete ionisation of the material, as Kothari has shown. But in white dwarfs the pressure is sufficient to make the ionisation practically complete.

7. *The Transition between a Main Series Star and a White Dwarf.*—It is generally taken for granted that white dwarfs are formed by the contraction of ordinary stars; but serious difficulties confront us when we examine the circumstances of the transition.

For definiteness consider the contraction of the Sun into a white dwarf. The gravitational energy liberated is sufficient to maintain the present rate of radiation for more than 10^9 years, and the time is greatly extended if we allow for the reduced radiation in the later stages. Thus we are threatened with grave difficulty in regard to the time-scale. The amount of energy is incomparably greater than that radiated in a Nova outbreak; hence it seems clear that the passage to white dwarf conditions is not catastrophic.

During the slow contraction the internal temperature rises and then falls. A lower limit to the maximum temperature can be calculated in the following way. During the contraction the model changes from $n > 1{\cdot}5$ to $n = 1{\cdot}5$; but, since the central temperature decreases with n, we shall not exaggerate it if we adopt $n = 1{\cdot}5$ throughout. We have at the centre

$$P = B\rho^{\frac{5}{3}}, \tag{7.1}$$

where, for $n = 1{\cdot}5$ and a mass equal to the Sun, $B = [14{\cdot}702]$. Also (radiation pressure being negligible)

$$P = \frac{\mathbf{R}}{\mu}\rho T + K\rho^{\frac{5}{3}}. \tag{7.2}$$

From (7.1) and (7.2)

$$\mathbf{R}T/\mu = B\rho^{\frac{1}{3}} - K\rho^{\frac{2}{3}}, \tag{7.3}$$

which has a maximum value when $\rho^{\frac{1}{3}} = B/2K$. We then have

$$T_{\max} = \frac{\mu}{\mathbf{R}}\frac{B^2}{4K} = [7{\cdot}891]\mu\mu_1^{\frac{5}{3}}. \tag{7.4}$$

According to the formula, $T_{\max}$ occurs when the ordinary gas pressure and degeneracy pressure are equal and the radius is twice the ultimate radius.

Actually, if we take account of the changing model, it occurs rather earlier. Thus more than half the gravitational energy is liberated after the maximum temperature is passed. It is unfortunately impossible to estimate how much of the contraction occurs during the final stage when the luminosity is decreasing from that of the Sun to that of the observed white dwarfs—a stage greatly prolonged by the slowness of the radiation.

The time occupied by the transition is reduced by the retention of part of the energy in the star, at first as heat energy and later as exclusion energy. In the gaseous stage approximately half the energy is retained ; and, according to the usual derivation of the degeneracy formulæ, this applies also to the degenerate state. But the latter result involves assumptions which may not be warranted ; and I do not think we can exclude the possibility that as zero temperature is approached the whole gravitational energy is being converted into exclusion energy. This would considerably alleviate the time-scale difficulty. The position seems to be that if we strain every doubtful point in favour of rapid transit we can just about fit the evolution of the companion of Sirius into the accepted time-scale. This refers to gravitational energy only, and makes no provision for the disposal of the subatomic energy that may be liberated.

We turn to a still more striking difficulty. The temperature given by (7.4) is some four or five times that of the main series. It is generally agreed that this would enormously increase the rate of liberation of subatomic energy.* The radiation on the other hand increases only moderately. The star would thus be gaining energy thousands of times faster than it radiates. But that means that it cannot be contracting. It appears that there is no way for an ordinary star to reach the white dwarf state, because the intermediate state is incompatible with contraction.

This difficulty is so fundamental that we have to inquire whether there is any conceivable way of meeting it. At present the most plausible theory of liberation of subatomic energy (due to Bethe †) is that carbon and nitrogen act as catalysts for the conversion of hydrogen into helium. It is claimed that most of the steps of the cycle have been observed in the laboratory, and that the calculation that the process occurs in the Sun at a rate sufficient to maintain the radiation is no more than a mild extrapolation of observational data. In solar conditions the rate of production of heat by this process varies as T^{17}. If this is right, the possible conclusions are narrowed down to two alternatives which will be discussed in §§ 8, 9. Serious objections can be found against both alternatives, and it may well be that the ideas now favoured by nuclear physicists require further revision.

8. *First Alternative.*—We have seen that between the ordinary star and the white dwarf there is an intermediate stage of high temperature, and the star will not contract through this stage unless the expected liberation of subatomic energy is in some way inhibited. This can only mean

* A rough calculation with Bethe's formula gives an increase in the ratio 1 to 10^{16}. This is probably an unjustified extrapolation, but it gives an idea of the increase to be expected.

† *Phys. Rev.*, 55, 434, 1939.

that, when the contraction occurs, either there is no hydrogen to be transmuted or the necessary catalysts are absent.

The calculation of hydrogen content of the companion of Sirius shows that the hydrogen has not been eliminated before the contraction. Moreover, the elimination of hydrogen by transmutation is strictly controlled by the rate at which the resulting energy can be got rid of by radiation and cannot have proceeded faster in the small star than in Sirius itself. Since the hydrogen is present, it follows that the catalysts must be absent during the contraction.

We conclude that there is a process (either building up or breaking down) which transmutes carbon and nitrogen into other elements. This must begin at about the temperature of the main series and, like all such processes, increase very rapidly with any further rise of temperature. When the catalysts have been burnt out, the contraction can proceed without opposition.

An objection appears when we try to apply this theory to stars of different masses. The main series temperature has to satisfy two conditions: (1) hydrogen transformation must proceed at the rate required to maintain the radiation; (2) carbon-nitrogen destruction must proceed at a slow but not negligible rate. (If the latter rate were zero the star would remain on the main series until its hydrogen was exhausted.) It is easily seen that the more massive the star the shorter will be the time it remains on the main series. Accordingly, white dwarfs would mostly be massive stars.

A more fundamental objection is that the theory is essentially a "special creation" theory, which supposes the elements (apart from the hydrogen-helium transformation and the breakdown of radio-active elements) to have existed in their present proportions from the beginning; for the conditions at present insisted on by nuclear physicists for transmutation of the elements (with the exceptions above specified) are obviously such as cannot have existed in the universe at any time.

9. *Second Alternative.*—Instead of supposing the catalysts to be destroyed before the contraction occurs, we may suppose that they are not evolved until after it has occurred. If carbon and nitrogen have not then been evolved, it is unlikely that higher elements have been evolved. Pursuing this idea, we arrive at the following theory.

The first stage is a globe of hydrogen (and very little else) contracting without transmutation of energy owing to the absence of catalysts. When the density approaches that of a white dwarf, evolution of the complex elements begins, and continues in spite of the falling temperature, the key process being presumably more dependent on density than on temperature. Carbon and nitrogen are formed along with the other elements; and, as the amount increases, the consequent catalytic transformation of hydrogen gives an increasing liberation of energy which presently exceeds the radiation. The star then expands. With decreasing density, evolution of the complex elements stops, and the carbon-nitrogen content thereafter remains fixed. (There is no burning out of the carbon-nitrogen on this theory.) The star expands very rapidly through the maximum temperature stage; indeed the enormous rate of transmutation of the hydrogen would

probably make the expansion catastrophic. The star then reaches a state of balance on the main series. A white dwarf stage thus precedes the main series stage; but, if the time-scale permits, the star may return a second time to the white dwarf stage after it has exhausted its hydrogen. The two white dwarf stages are distinguished by the large hydrogen content in the first stage and the vanishingly small content in the second stage.

A number of astronomical considerations favour this view. The formation of a first-stage white dwarf does not take unduly long; because the contracting star, being practically pure hydrogen, will be highly transparent and have great luminosity. We see why in the Sirius system the small star is the white dwarf, whilst the massive, and therefore more rapidly evolving, component is a main series star—a paradox very difficult to explain in any other way. Equally the converse condition in o^2 Eridani is explained, if the larger component is a second-stage white dwarf as its low hydrogen content indicates; but unfortunately the time required seems to be prohibitive. One of the most puzzling facts has been the comparative constancy of hydrogen content of stars of the same mass, which is shown (independently of the rather unreliable absolute determinations of hydrogen content) by their remarkably small scatter from a mean mass-luminosity curve. This is explained if the main transmutation occurs in a white dwarf state, which is a constant feature of the history of every star which has reached the main series.

Of special interest is the high temperature intermediate stage, which is passed through three times before the second white dwarf stage is reached. At the first passage we have a star, highly luminous for its mass, with small radius and therefore high effective temperature. It suggests itself that the stars which are the centres of planetary nebulæ may belong to this period. The second passage is probably catastrophic. It is difficult to imagine any other conditions in which development is catastrophic, and we may therefore attempt to associate Novæ with this period. The third passage is presumably made only by very massive stars which have had time to exhaust their hydrogen; it is somewhat similar to the first passage but slower, and the luminosity is not so great. Owing to the rapidity of the second passage and the time-lag of the transmutation processes, the star may at the end of it overshoot the main series and become a giant for a time.

This account does not profess to go further than to show that the theory has a superficial attractiveness, which may well become less favourable on closer examination. It is presented, not on its merits as a speculative explanation, but because the claims at present made as to what has been demonstrated by nuclear experiment and theory seem to leave us no alternative—except the theory of § 7, which has not even a superficial attractiveness. Of the numerous objections which may be urged, we consider two which are of a very general character.

If the main series stars have all passed through a white dwarf stage, their angular momentum is limited by the condition that the star must have been stable with a very small radius. (It is safest to exclude binary stars in which

a subsequent transfer of angular momentum may have occurred.) I think that the observational evidence of rotation of single stars is difficult to reconcile with this limit. But an angular momentum difficulty has appeared in every evolutionary astronomical problem yet investigated, so that we have come to look on it almost as a *pro forma* objection. Presumably the explanation, when it is found, will be a general one covering all the problems in which the difficulty has appeared.

The second objection refers to a general unsuitability of the white dwarfs as a place of evolution of the complex elements.

10. *Where are the Complex Elements Evolved ?*—By complex elements I mean elements other than hydrogen and helium. The considerations which have led nuclear physicists to reject the evolution of complex elements in ordinary stars obviously apply to conditions which are both cooler and more rarefied. We are therefore left with white dwarf stars, or conditions approaching thereto, as the only alternative to assuming that uranium atoms, for example, first come into being fully formed.

Unless we make the very artificial assumption that the complex elements are formed principally from helium in conditions in which there is relatively little transmutation of hydrogen, their evolution must be accompanied by liberation of energy. The most important consideration then is that on the white dwarf side of the stage of maximum temperature the conditions are unstable as regards energy liberation, since expansion gives an increase of temperature ; whereas on the main series side of the maximum temperature stage the conditions are stable (or at the worst have only pulsatory instability), since expansion gives a decrease of temperature. Obviously we shall encounter great difficulties if we place the most important part of the evolution of the elements in the unstable period. On the other hand, if we place it in the stable period it would be (according to the Bethe theory) impossible for the white dwarf stage to be reached—as explained in § 7.

In some respects a white dwarf seems the very worst place to choose for evolution of the elements. Its low luminosity indicates that transmutation of hydrogen is proceeding a thousand times slower than in the Sun. The difficulty of time-scale, always serious, becomes so exaggerated as to seem prohibitive. The maximum temperature phase seems much more favourable, since high temperature and high density ($\frac{1}{8}$ of the white dwarf density) are associated together, and the radiation is great enough to allow a reasonable speed of transmutation. Let us suppose then that evolution of the complex elements first begins when the pure hydrogen star is approaching maximum temperature. It then becomes a critical question whether the evolution proceeds fast enough for the consequent liberation of energy to overtake the rate of radiation before the maximum temperature is reached. If not, the star will pass through the maximum temperature and become a white dwarf. Unfortunately we cannot say that the stars which fail to reach the maximum temperature stage will return to the main series ; the conditions are stable, and the star should remain almost stationary in the state at which the balance is first reached.

11. *Conclusion.*—One thing emerges plainly from this survey of evolu-

tionary possibilities, namely, the decisive importance of an entirely trustworthy determination of the hydrogen content of the companion of Sirius. For theories of transmutation and stellar evolution no other present-day problem is so crucial. Everything turns on whether it is necessary to provide for white dwarfs with considerable hydrogen content or whether the white dwarf state is compatible only with nearly complete elimination of hydrogen. Realising now that a great deal depends on the security of the determination in § 4, we return to consider it. In so doing, we put out of mind the extreme difficulty of conceiving any way in which the companion could have lost its hydrogen whilst the principal star retained it ; this should be balanced against the difficulties which seem to beset every attempt to reach a consistent view of evolution.

The observational side of the question is, Can the Einstein shift really be 50 km. per sec. instead of the value 20 found by two observers? To conform to this we should have to attribute to the star an effective temperature of about 13,000°. Allowing for possible uncertainty of the mass we might perhaps reduce the demand to 44 km. per sec., but not less. We need consider only the values for zero hydrogen content, since 5 per cent. hydrogen would be as decisive as 60 per cent. on the evolutionary questions raised.

If there is no observational error, it remains only to consider whether the radius may have been increased, not by hydrogen content, but by temperature as considered in § 6. To reduce α from 50 (or 44) to 20 the star must have more than double the "cold" radius. By § 7 this places it nearly at the maximum temperature stage. Here the degeneracy is only half complete, the gas-pressure being equal to the degeneracy pressure. Every known consideration indicates that the star will be highly super-luminous at this stage, and we are totally at a loss to account for its having the under-luminosity of a white dwarf.

It may seem suspicious that the companion of Sirius is the only one of three white dwarfs to show considerable hydrogen content. But really the evidence is considerably strengthened by this fact. Any kind of correction to the theory which would reduce its hydrogen content would almost inevitably give the other two white dwarfs (one more massive and the other less massive) a negative hydrogen content.

Though the large hydrogen content may not be established with the ideal security which we should desire in a fact on which far-reaching conclusions are to be based, it must, I think, be admitted that the evidence for it is difficult to shake.

Summary.—Most discussions of our theoretical and observational knowledge of white dwarfs have been based on the Stoner-Anderson degeneracy formula which the author considers to have been disproved in his earlier papers. There is therefore need for a study of these stars based on the earlier formula which appears to be correct. In § 2 the elementary formulæ are put into suitable form for practical use. The chief application is to determine the hydrogen content of three white dwarfs for which data are available.

Special attention is directed to the large hydrogen content found for the companion of Sirius. This is crucial in theories of transmutation and

stellar evolution, since it is often assumed in such theories that stars only pass to the white dwarf state after having exhausted their hydrogen content. The difficulty of reconciling Bethe's transmutation theory with the existence of hydrogen-containing white dwarfs is considered, and alternative ways of meeting the difficulty are discussed ; one alternative in particular (§ 9) has interesting astronomical consequences. But serious difficulties remain outstanding, and in § 11 we re-examine the trustworthiness of the evidence for large hydrogen content. The evidence, however, proves to be very difficult to upset.

A PHOTOELECTRIC RECORDING PHOTOMETER FOR THE SOLAR SPECTRUM

H. A. Brück, D.Phil.

Introduction.—During recent years our empirical knowledge of profiles of Fraunhofer lines has considerably increased largely as a result of refinements in technique. As all such observations of the solar spectrum have been carried out photographically, photographic spectrophotometry has an important part to play in this field. As regards the photographic procedure, there are now generally accepted certain principles which, if followed, will secure consistent spectrophotometric results. Nevertheless, the well-known intricacies inherent in photographic spectrophotometry seem to demand, if only for a check on those results, the development of a photometric method independent of the photographic process.

As has often been pointed out, from the photometric point of view, a most appropriate light receiver is given by the photoelectric cell already widely used in stellar and plate photometry. The practically linear response of the vacuum types of cell, and the fact that the characteristics of a photoelectric photometer does not need to be determined afresh for each individual observation, offer great advantages over the logarithmic characteristics of photographic emulsions which vary from plate to plate. In the case of absorption line photometry, the linear response should result in faint lines being more easily picked up and measured photoelectrically than is possible on photographic plates.

The first photoelectric photometer working directly in the solar spectrum is due to Dunham,* who in 1933 published the main features of his instrument in a note in *Physical Review* and who is now at Oxford doing some more work on these lines. No other investigation in this field is known.

At Cambridge it seemed to be the more desirable to take up photoelectric photometry of Fraunhofer lines because the same high dispersion spectrograph could be used again there which had formerly served Redman for photographic photometrical studies of solar line profiles carried out with special care and precision.† This McClean spectrograph is a 4-prism Littrow instrument with an aperture ratio of $f/84$ and a focal length of 427 cm., yielding a dispersion of 0·52 angstroms per mm. at λ 4227. The spectrograph receives the solar light through a cœlostat and a Cooke lens of 60 feet focal length.

After preliminary tests with this instrument, which showed that the intensity of light per unit wave-length available in this spectroscope would be sufficient to be measured photoelectrically, a suitable photometer was developed during the past year.

* Th. Dunham, jun., *Phys. Rev.*, 44, 329, 1933.

† R. O. Redman, *M.N.*, 95, 742, 1935, and 97, 552, 1937.

The Circuit.—Regarding the problem how to record photoelectric currents as feeble as those we are dealing with in the present case, good use can be made of recent developments in valve technique. In different countries special thermionic valves have appeared on the market which, like an electrometer of low capacity, can be used to measure direct currents down to about 10^{-16} amps., providing thereby a welcome alternative to the delicate electrostatic method of measurement.

In the present case the Osram "Electrometer Triode", one of these "current amplifier valves", is employed * forming the main part of a one-

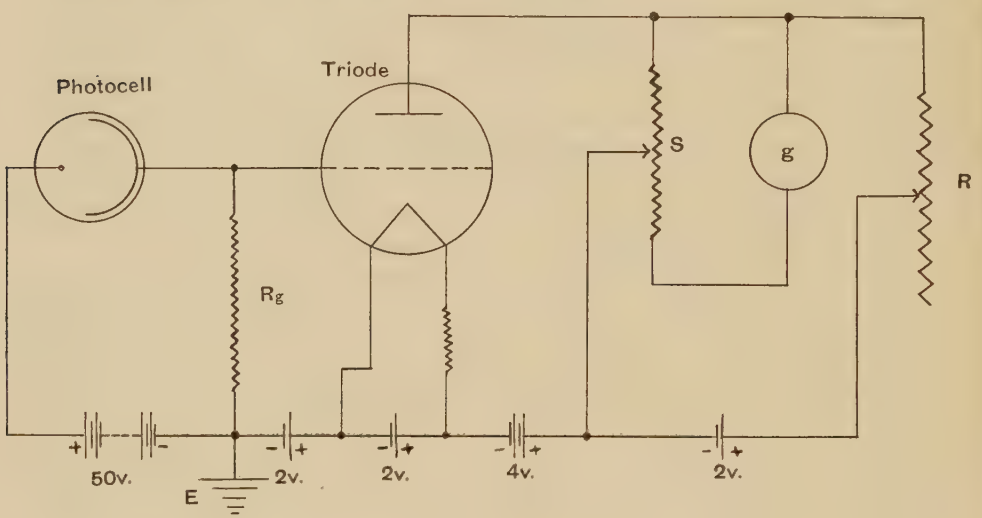

Fig. 1.

stage amplifier. Fig. 1 illustrates the main features of the circuit, which is that normally used for D.C. amplification.

It is one of the peculiarities of the electrometer triode that it has to be worked at a low plate potential. In our case a plate voltage of 4 volts is used, a negative bias of 2 volts being applied to the grid. The rated filament voltage and current are 1 volt and 0·1 amp. respectively. Under these conditions the principle constants of the average electrometer triode are as follows: anode slope resistance (impedance) $R_A = 15{,}000$ ohms, mutual conductance $g_m = 50$ microamp./volt and amplification factor $\mu = 0{\cdot}7$. The capacity between grid and other electrodes is given as 2 micromicrofarads.

In the photometer circuit the grid of this triode is through the grid leak resistance R_g connected to earth and at the same time to the cathode of the photocell for which an Osram potassium on silver oxide vacuum cell, type *KMV* 6, is used. As long as there is no light falling on the cell the grid is kept at its constant bias and a constant current is flowing in the plate circuit. Through the adjustment of the resistance R, consisting of 3 single

* In the work of Dunham (*loc. cit.*), Whitford (*Ap. J.*, **76**, 213, 1932) and others the "Pliotron F.P. 54", a corresponding American valve, plays the same rôle.

rheostats of 10,000, 1000 and 100 ohms respectively, the current in the galvanometer circuit can be balanced out.

As soon as the cell is illuminated a photocurrent flows through the resistance R_g and causes a potential drop across it. As can be readily seen from the diagram, with the actual connections a decrease of the grid bias and thereby an increase of the plate current will be the result. This change in plate current and its variation with varying illumination of the cell are recorded by the galvanometer *g*. The galvanometer actually used was supplied by the Cambridge Instrument Company. It has a period of 1 second, and at 1 metre distance gives a deflection of 610 mm. for 1 micro-amp. Its sensitivity can be reduced by the shunt *S*.

To produce a sufficiently large potential drop by the feeble photo-electric currents available a high grid leak resistance has to be employed. After preliminary tests, as standard a grid leak of 5×10^{10} ohms = 50,000 megohms is being used in the present set. As is sometimes desirable, it can be replaced by another one of 10^{11} ohms. The resistances have been supplied by the Dubilier Condenser Company.

The grid cathode impedance rarely exceeds 10^8 to 10^9 ohms in standard types of triodes used normally in connection with grid leaks between 1 and 10 megohms. The use of a resistance of 50,000 megohms necessary for the present work has only become possible through the design of the special type of valves like the electrometer triode, whose main characteristic is their high grid cathode impedance of the order of 10^{16} ohms.

In the present amplifier with a grid leak of 5×10^{10} ohms a current amplification of 2,500,000 is obtained. With the above galvanometer this corresponds to a voltage sensitivity of 30,000 mm. per volt or to a current sensitivity of $6{\cdot}6 \times 10^{-16}$ amps. per mm. By using the grid leak of 10^{11} ohms these sensitivities can be doubled.

The galvanometer deflection produced with this arrangement (grid leak of 5×10^{10} ohms) with a slit 0·05 mm. wide (corresponding to 0·03 angstroms near λ 4227) and 3 mm. long, by the intensity of the continuous solar spectrum near the line λ 4227 is 250 to 300 mm. The corresponding photocurrent is therefore about 2×10^{-13} amps. producing a change in grid bias of 1 hundredth of a volt.

With the exception of the voltage on the photocell, all the potentials necessary for working the amplifier are supplied by a 12-volt accumulator battery of 48 amp. hours for each cell, two cells connected in parallel providing the current for the triode filament. The battery is kept well charged, and recharging is normally done at the same rate at which the current is taken out to reduce possible drifts and fluctuations from this source.

The Photometer.—Fig. 2 gives a schematic drawing of the whole instrument, while fig. 3 shows a photograph of it without the recording system.

The light coming from the spectrograph, and normally falling on the photographic plate, has to pass through a slit S_P in the focal plane of the camera lens and within the space otherwise reserved for the plate holder. This slit is of the same width as the spectrograph slit S_S (visible on the left of fig. 3), both being used ordinarily at 0·05 mm., corresponding to 0·03

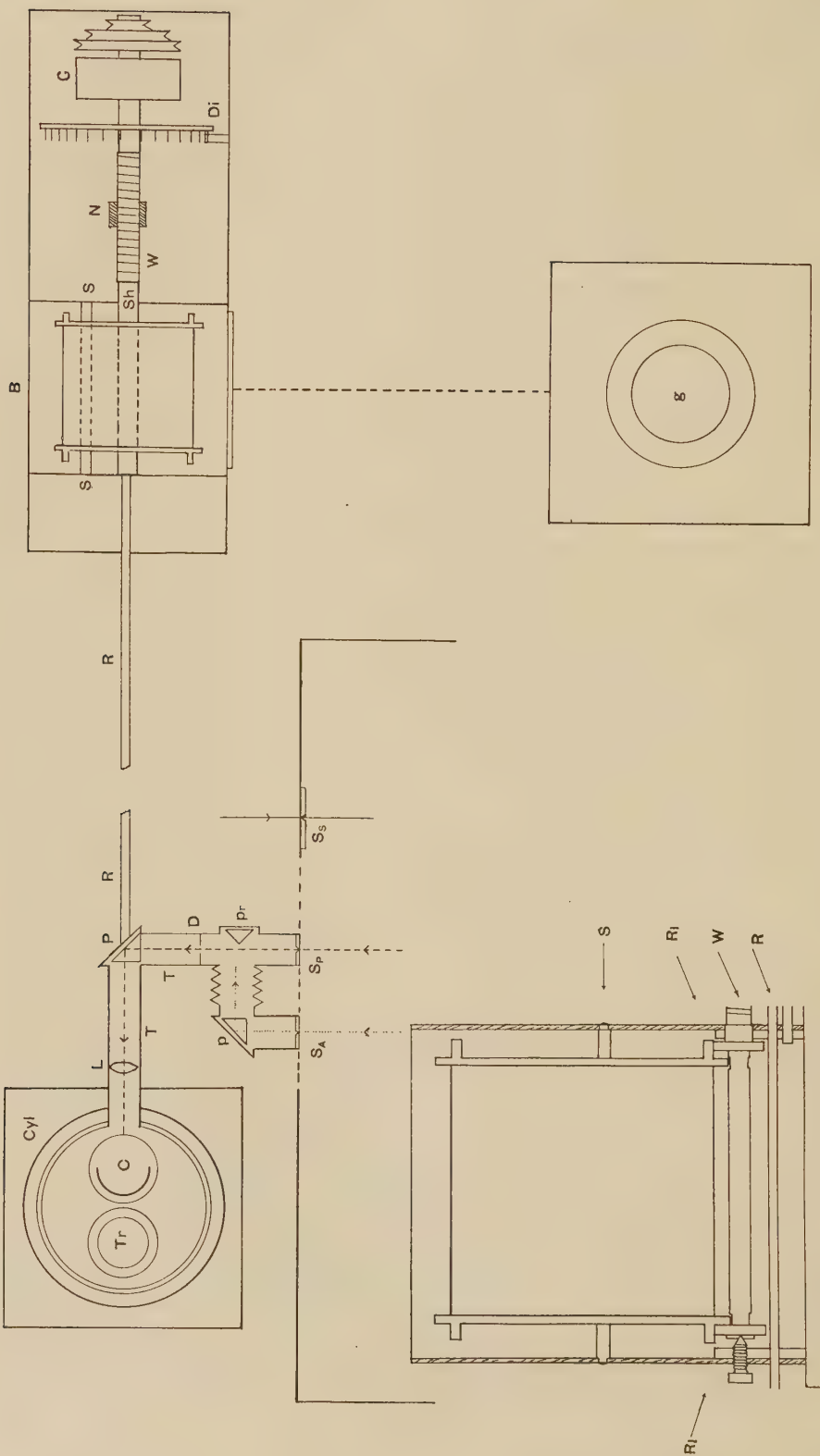

FIG. 2.

FIG. 2 (A).

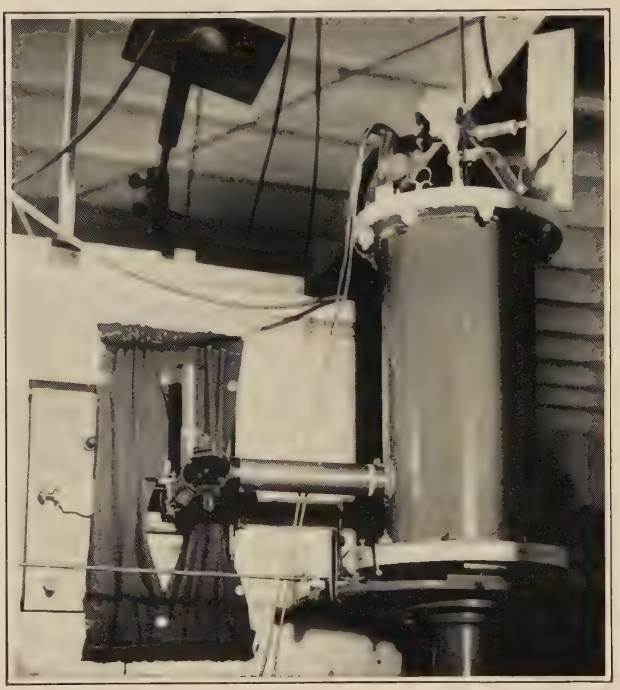

Fig. 3.

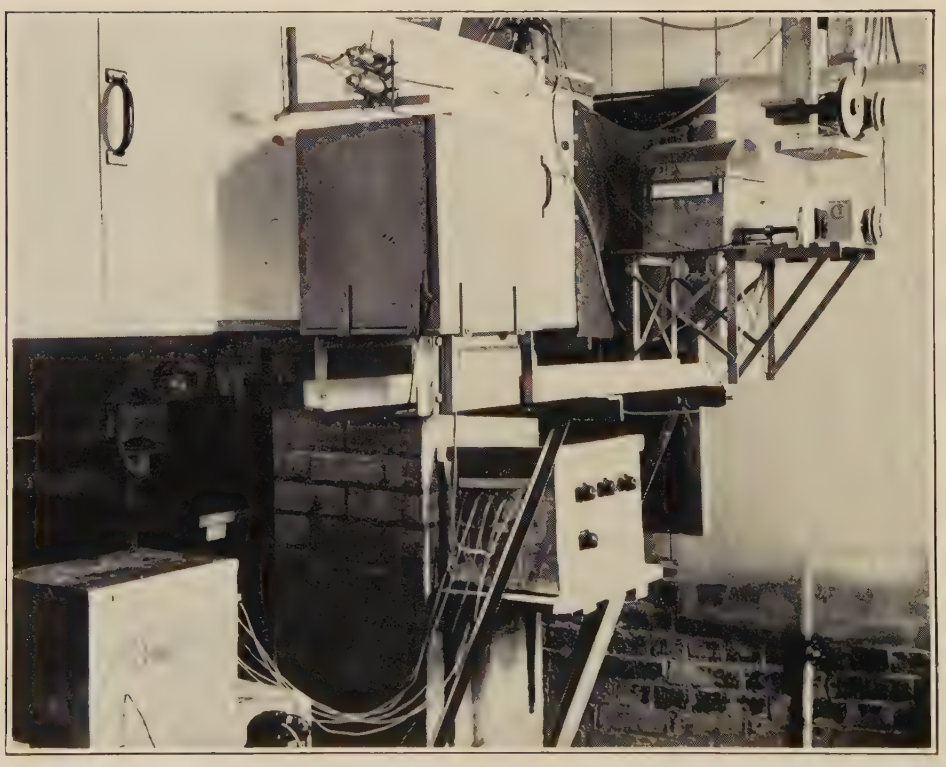

Fig. 4.

H. A. Brück, A Photoelectric Recording Photometer for the Solar Spectrum.

angstroms near the line λ 4227. To reduce the effect of light scattered in the spectrograph* the slit is kept as short as possible. One mm. is adopted as standard length and only in exceptional cases is it made longer than 3 mm.

A viewing telescope (visible only on the photograph of fig. 3) can be moved into the beam and used to look at the photometer slit. Having passed through the diaphragm D the beam is reflected by the prism P and, after having been spread out by the lens L ($f=2$ cm.), directed on to the photocell C. The cell is 45 cm. away from the slit S_P. For convenience of alignment the back plate carrying the prism P can be taken off while the tubes T are rigidly connected with each other.

Cell C, triode Tr and grid leak resistance are contained in a heavy cast-iron cylinder Cyl into which on one side a short piece of pipe with a glass window on its other end is inserted. Over this pipe the tubes T can be fitted so that cylinder and tubes form one unit. The cylinder is closed by two end plates and sealed with a cellulose lacquer. Following the example of Dunham (*loc. cit.*), Whitford (*loc. cit.*) and others, for the sake of greater electrical stability, this cylinder is evacuated to a vacuum of about 1 mm. The pressure can be measured by a small mercury manometer, attached with a tube containing phosphorus-pentoxide to the top plate of the cylinder.

The effect of evacuation may be seen from fig. 5, showing the way in which initial fluctuations die down when the pressure in the cylinder is diminished from 1 atm. to 10 mm. The tracing is taken with full sensitivity of the galvanometer. In this case the eventual maximum fluctuations giving a kind of "plate grain effect" are $\pm$ 1 mm. Normally a reduced sensitivity of the galvanometer can be used and the corresponding fluctuations remain well within the mm. Hand in hand with the decrease of fluctuations goes an increase of the total sensitivity, which varies between 30 and 50 per cent. of the sensitivity at atmospheric pressure, a result pointing apparently to the influence of a film of moisture on the leads and especially on the grid leak resistance.

This part of the photometer consisting of cylinder and tubes must be moved along the solar spectrum. For this reason the cylinder rests on 3 steel balls (see fig. 3) which are allowed to travel between straight channels 3 inches in length. These are fixed to an iron base, which can be easily levelled and adjusted for height, so that the centre of the photometer slit can be brought on to the middle of the solar spectrum, and the motion of the photometer can be made parallel to the direction of dispersion. With strong iron brackets the whole arrangement is fixed to one side of one of the concrete piers which carry the McClean spectrograph.

The Recording Parts.—In the same way to the other side of the pier is bracketed the equally heavy support for the driving and recording parts of the instrument. Tests with 2 synchronous motors driving photometer and recording drum separately proved unsuccessful.

* Regarding the effect of scattered light in the McClean spectrograph compare the investigations of Redman (*loc. cit.*).

In the arrangement finally adopted (see fig. 2 and fig. 4) a synchronous motor with 1500 revolutions per minute is coupled through a belt over change-over pulleys to a reduction gearbox (3000 : 1) *G*, the shaft of which is fixed to one end of a worm *W* with a pitch of 2 mm. and a length of 14 cm. Through a steel rod *R* which is about 1 metre long, fixed to the nut *N* and clamped to the Cylinder *Cyl*, this worm is driving the photometer along the spectrum while a weight is taking up slack.

The revolving of the recording drum carrying the bromide paper has been arranged in the same way as in the Cambridge microphotometer designed by Carroll and Moss * which has proved to work very satisfactorily. As seen best from fig. 2A the continuation of the worm is a shaft *Sh* on which a pair of rollers R_e has been fixed.† The recording drum is either resting on these rollers, or with two flanges on the shaft itself, and is at the same time supported by an adjustable shaft *S* mounted in the drum-box *B*. The drum is a brass cylinder of $6\frac{1}{2}$-inch diameter with flanges $\frac{3}{4}$ of an inch larger. It is driven by friction, and, by displacing it sideways and bringing it into contact with rollers or shaft, magnifications near 1 : 20 or 1 : 50 can be obtained—comparing distances in the tracings with those in the original spectrum. The measured ratios are 1 : 18·5 and 1 : 49·2.

Light falls on the bromide paper through a cylindrical lens. For convenience of measurement this lens has an engraved millimetre scale, which is made visible on the tracings by a general illumination fogging the paper slightly. On this background the galvanometer deflections are recorded as a black line. Besides this millimetre scale black reference marks perpendicular to it are seen as well on the tracings. These are due to flashes coming from a third lamp mounted on top of the galvanometer case, underneath the light source for general illumination (see fig. 4 in which the galvanometer box with these two lamps is in the foreground, while the light source for the galvanometer beam can be seen underneath the drum-box). That lamp is turned on every time a spring contact is closed by one of the 20 pins fixed to the disc *Di*. While this disc is revolving together with the worm, the pins are distributed so that the distances between two vertical marks correspond to a travel of $\frac{1}{10}$ of a mm. in the spectrum.

The switchboard (near the pier on fig. 4) containing in a shielded box the different resistances for adjustment, is mounted separately. All the wires leading from here to the shielded battery box and to the cylinder with cell and triode run in a shielded conduit.

Speed of the Instrument.—With the normal speed of the instrument the photometer is travelling along the spectrum at the rate of about 1 mm. in 1 minute. This speed can be varied by means of change-over pulleys, but must not be much faster if the record is not to be distorted by the inertia of the instrument. Near the line λ 4227 the recording of 4 angstroms will take about 10 minutes.

During this time the transparency of the sky might change to a certain extent. In order to check such an effect at any time during the run a

* J. A. Carroll and E. B. Moss, *M.N.*, **91**, 191, 1931.

† The rod *R* as seen from fig. 2A runs underneath the worm and shaft.

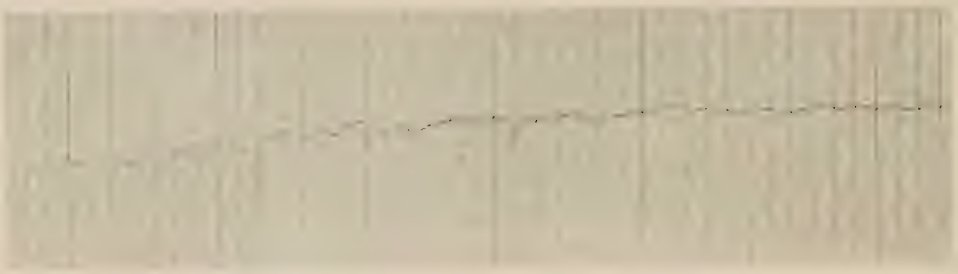

Fig. 5.

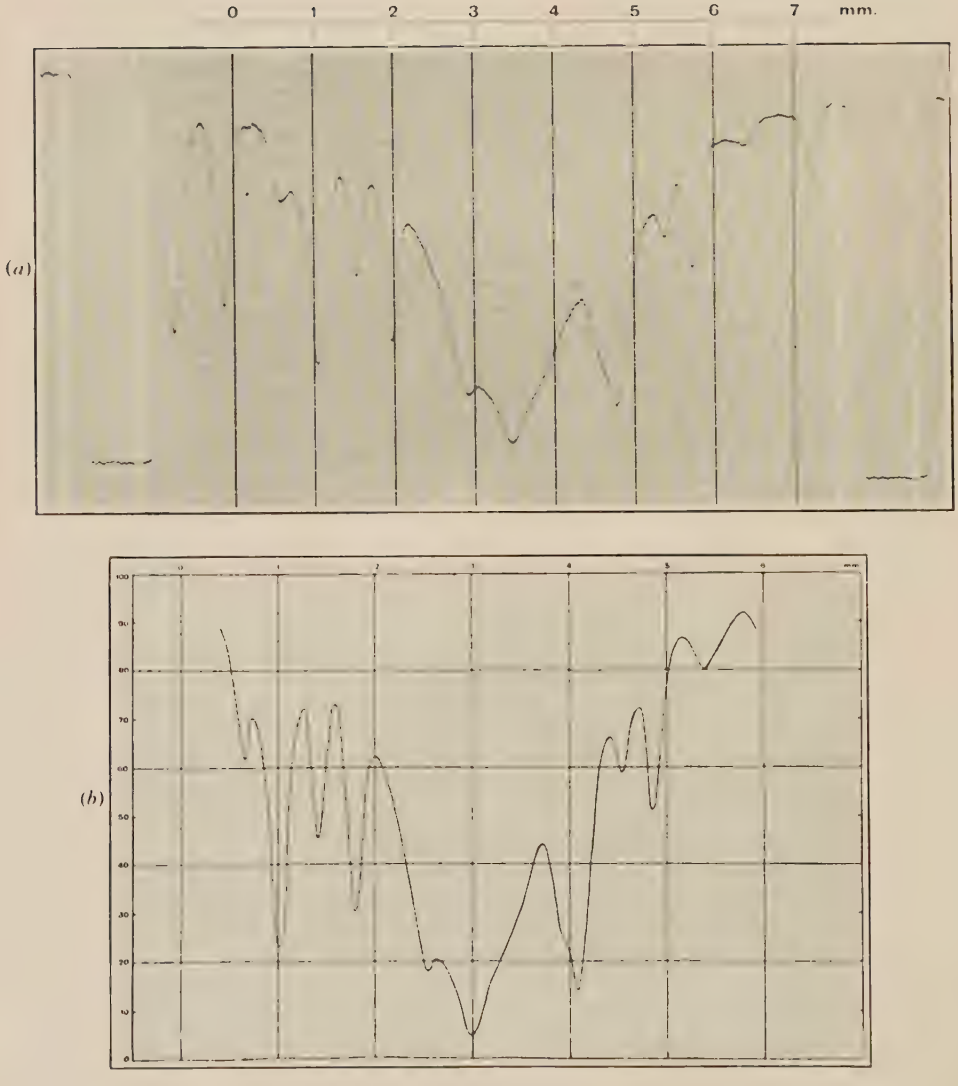

Fig. 6.

H. A. Brück, A Photoelectric Recording Photometer for the Solar Spectrum.

simple device has been introduced. As fig. 2 shows, there is mounted at one end of the plate-holder frame, beside the photometer slit S_P and in the same plane, an auxiliary slit S_A. While the photometer slit is travelling along the spectrum, slit S_A remains at its fixed position. Light coming from a certain part of the spectrum and passing through slit S_A is reflected by the prism p on to the prism p_r. This is normally moved to the side so that the beam from the photometer slit may pass unobstructed. But it can be turned round, cutting off then this beam and reflecting instead the light from the auxiliary slit on to the photocell. The tubes carrying the two slits are connected by bellows.

With this arrangement any gradual changes of transparency can be detected and accounted for. As a normal run does not take more than a few minutes, under fair conditions of sky, records of the transparency are only made before and after the run, but frequently they are also taken a number of times in between. The device has proved very useful, if only for rejecting unsatisfactory material. Naturally, irregular changes will only be checked by repeating a certain tracing several times.

The Performance of the Instrument.—The tests of the mechanical and electrical properties of the instrument and their results will be discussed in a later paper together with the observations of Fraunhofer line profiles. However, it seems worth while mentioning the result of preliminary tests of the characteristics of the instrument. For testing the relation between light intensity and galvanometer deflection there was placed in front of the spectrograph slit a Zeiss step wedge whose transmission had been kindly determined by Mr. J. R. F. Jeffreys and Dr. R. v. d. R. Woolley. The intensity transmitted by the 5 steps of this wedge varies between 100 and 2 per cent. Within this range no deviation from linearity could be found exceeding the errors of measurement of the wedge calibration (1 per cent.).

Figs. 6 (*a*), 7 (*a*), 7 (*b*) and 8 show some records taken with the instrument of the region near the neutral Calcium line λ 4227, visible in the centre. The tracings have been taken with the magnification of 1 : 18·5 and reference marks have been recorded for each mm. of spectrum only.* On fig. 6 (*a*) on both sides of the spectrum a short record may be seen of the galvanometer reading for full darkness showing a certain drift, and a little of the record for sky transparency. For comparison, an intensity curve 6 (*b*) is given which has been derived by Redman from photographic measurements.

While special results obtained will be published later, fig. 7, representing a copy of two records, may give some idea how the device for checking the transparency of sky works on a fine (fig. 7 (*a*)) and on a hazy day (fig. 7 (*b*)). In the first case the transparency has only been tested before and after the run and the corresponding records are seen at each end of the tracing. In the second case, in addition to similar records the run itself has been interrupted several times to observe the changes in transparency taking place.

* There is a small difference of dispersion between the present setting of the spectrograph with 0·52 angstroms per mm., and the setting as Redman used it with 0·64 angstroms per mm. It can be seen from the different position of the mm. marks on 6 (*a*) and 6 (*b*).

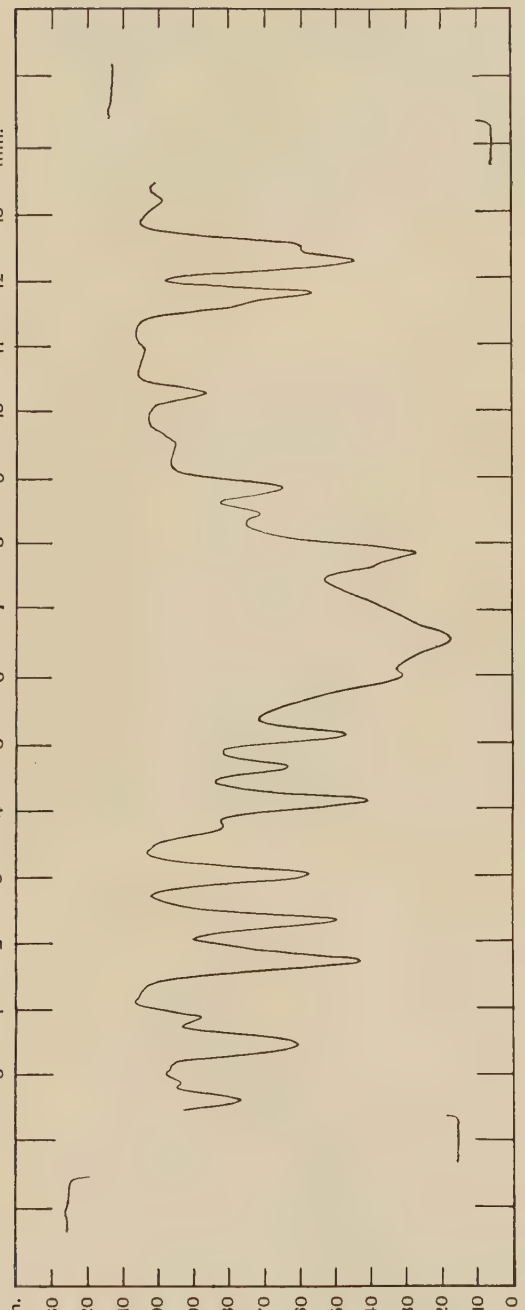
mm.
0
10
20
30
40
50
60
70
80
90
100
110
120
130
0 1 2 3 4 5 6 7 8 9 10 11 12 13 mm.
(a)
mm.
0
10
20
30
40
50
60
70
80
90
100
110
0 1 2 3 4 5 6 7 8 9 mm.
(b)

FIG. 7.

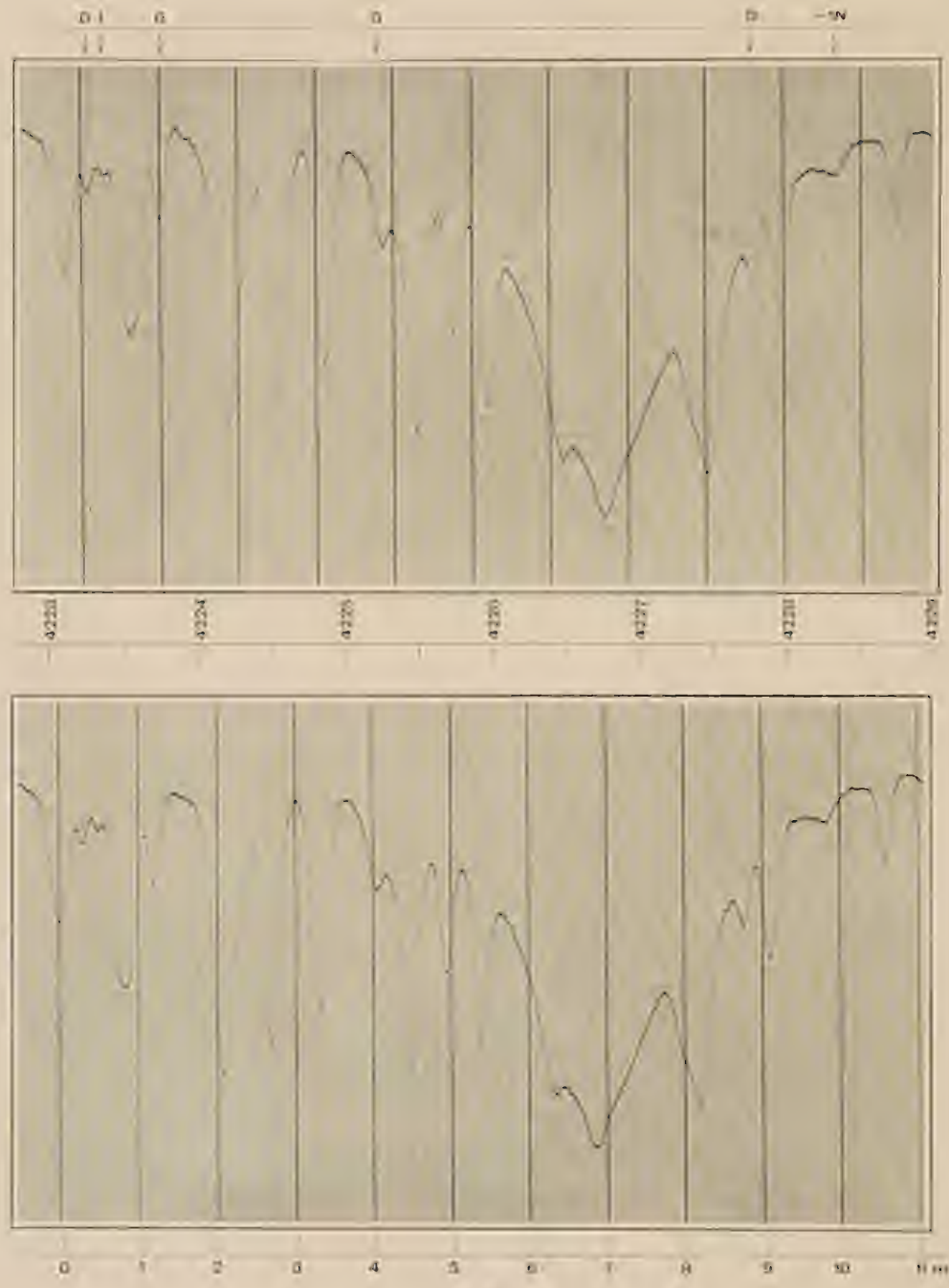

Fig. 8.

H. A. Brück, A Photoelectric Recording Photometer for the Solar Spectrum.

The two records of fig. 8, taken of a somewhat wider region of spectrum, have been run through by the photometer in opposite directions to show how details reproduce themselves. The arrows on top of this figure point to lines of Rowland intensity 0 and −1 respectively.

Further details about these tracings will be discussed after the conclusion of the work on line profiles which has only just been started.

Summary.—A recording photoelectric photometer attached to the Cambridge McClean solar spectroscope is described which can be used for investigations of Fraunhofer line profiles without photographic procedure.

In conclusion it is my pleasant duty to express my sincere thanks to Professor F. J. M. Stratton for the great interest he has taken in this work. I would like to thank also Dr. R. O. Redman and Mr. W. Moss for helpful discussions. Mr. W. H. Manning has helped greatly with the illustrations. The mechanical parts of the instrument were made with great care by Mr. L. J. Stanley in the workshop of the Solar Physics Observatory.

Solar Physics Observatory,
Cambridge :
1939 *June* 4.

ON THE CHEMICAL NATURE OF THE COLOURATION IN JUPITER'S CLOUD FORMS

Rupert Wildt

(Communicated by H. N. Russell)

The visual study of the delicate and transitory hues on Jupiter's cloud forms has been pursued for decades mainly by a group of British astronomers under the guidance of the Reverend T. E. R. Phillips, who as Director of the Section for the Observation of Jupiter of the British Astronomical Association has been mainly responsible for the co-ordination and publication in the society's *Memoirs* of a series of observations now extending over more than forty years. Of his collaborators there must be mentioned particularly the late A. Stanley Williams, who found evidence of periodicities in approximately twelve years in the colour changes of the two equatorial belts and the equatorial zone, and Mr. Bertrand M. Peek, who has now succeeded Mr. Phillips as Director of the Section. Considering the elusive character of all detail in planetary discs, it is very gratifying to realize that photographic studies have substantiated this valuable body of visual observations. The most extensive series of photographs of the planets is that secured by E. C. Slipher at the Flagstaff Observatory. Important contributions to this field of research have been made, among others, by W. H. Wright at the Lick Observatory, who, during the 1928 opposition of Jupiter, duplicated by a series of photographs taken through colour filters the findings of the British astronomers. As the latest advance in the photographic documentation of Jupiter's colours must be mentioned the direct colour photographs made by Th. Dunham, Jr., on Kodachrome film at the Coudé focus of the 100-inch telescope on Mount Wilson. These show marked differences in colour between the belts and other parts of the surface, though there may be some lack of accuracy in the reproduction of various shades.

It appears to be taken for granted generally that the vivid and varied colouration of Jupiter's surface results from incrustation of the clouds by various pigments, and is not of the nature of the iridescent colours arising from the diffusion of light in colloidal systems. Though it would be difficult to disprove the second alternative conclusively, we shall here follow the general trend and proceed on the first one. Yet it may be borne in mind that perhaps differences in the state of dispersion of a certain pigment will give origin to conspicuous variations of shade. There exist of course an enormous variety of highly coloured inorganic compounds, but our choice among these is rather restricted if due regard be given to the cosmic abundance of the elements and to the physical and chemical conditions likely to be realized at Jupiter's surface. As a further lead may serve the fact that

the display of colours on Saturn is rather poor compared to the brilliant Jovian phenomena. Considering the great similarity of the two planets in most respects, this difference may have some significance and preferably should be included in a tentative explanation of the colours. The intrinsic probability that any particular identification of the tingeing matter be correct would seem to be greatly enhanced if it could be shown how the whole range of colours observed, or at least most of them, might be derived from a single chemical principle on suitable changes of certain chemical or physical parameters. The only well understood difference between the surface conditions of Jupiter and Saturn is the lower temperature of the latter and the concomitant decrease of the vapour tension of ammonia, manifesting itself in the weakening of the absorption spectrum of this gas. There is good reason to assume that the clouds visible on Jupiter and Saturn consist solely of ammonia. Hydrogen, nitrogen, carbon monoxide and the three lightest noble gases cannot contribute to the clouds on account of their low critical temperatures, and neither can methane, because the gaseous CH_4 coexistent with the hypothetical condensed phase would produce a far stronger band absorption than the observed one. There is no spectroscopic evidence of the presence of higher hydrocarbons. Three other common substances with somewhat higher critical temperatures, namely, H_2O, H_2S and CO_2, are liable to react with ammonia. The compounds thus formed have vapour tensions so much lower than that of pure ammonia that the surface of Jupiter would have to be about at room temperature in order to maintain the spectroscopically determined amount of ammonia in equilibrium with the solid products of reaction. Such a high temperature is incompatible with the radiometrically measured total radiation emitted by the planet. The presence of halogen hydrides is ruled out on the same grounds. The atmospheres of all the giant planets are thought to be rich in hydrogen and free of oxygen and oxides. Hence, chemically they constitute a reducing medium, distinctly different from the terrestrial atmosphere.

There remains to be mentioned one more suggestive difference between Jupiter and Saturn, whose surfaces can be characterized summarily as turbulently active and predominantly quiescent, respectively. In a report on the Jovian phenomena of the 1938 opposition E. C. Slipher * has advocated the thesis that the energy responsible for the recent extraordinary activity, which was accompanied by colour effects far exceeding in intensity anything observed during more than thirty years, is released from some source in the planet's interior. He also seems to imply some causal relation between the appearance of the colours and the eruptive transport of matter from greater depths to the surface. This suggestion is at variance with the assumption that the occasional "outbursts" mainly serve to churn the visible cloud formations and to heat them above their average temperature, in certain areas at least. In speculating on the chemical nature of the colours we will obviously lose ground by admitting that they are genetically related to the supply of certain substances from the interior, of whose composition we are entirely ignorant as far as the finer traits are concerned.

* *Publ. of the Amer. Astr. Soc.*, 9, 167, 1939.

Though we may have to resign ourselves to such an admission eventually, it will be of interest to examine an idea which suggested itself in consequence of the identification of the D-lines of sodium in the spectrum of the night sky. It was this discovery which led the writer to consider the implications of the possible presence of metallic sodium in Jupiter's atmosphere. The

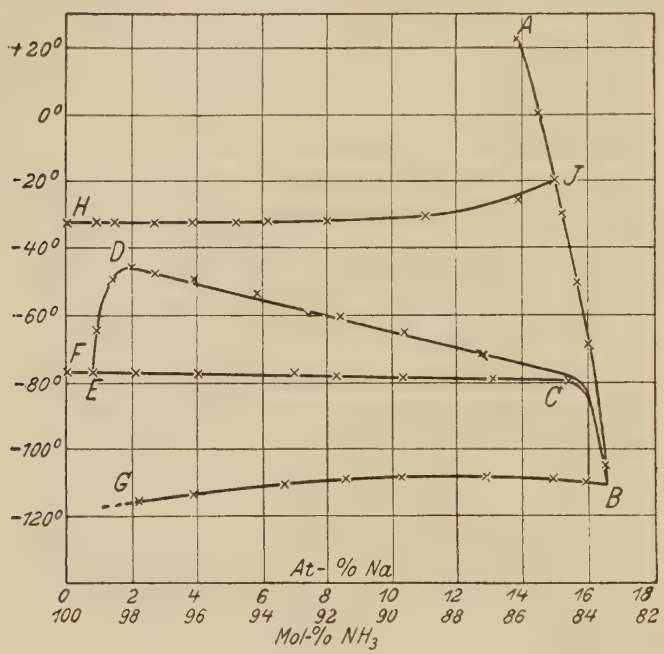

FIG. 1.—*Phase Diagram of the System Na-NH_3.*

argument to be presented is, however, quite independent of the origin of the free sodium, and the discussion of this point may conveniently be deferred to the end of this paper.

The action of metallic sodium on both gaseous and condensed ammonia offers attractive possibilities of producing manifold coloured systems, liquid as well as solid. All the other alkali metals and calcium, strontium and barium too are known to exhibit very similar, though less well investigated phenomena on being brought in contact with ammonia. A description of the features of the system sodium-ammonia will be greatly facilitated by the use of the phase diagram *, fig. 1, taken from a paper by O. Ruff and J. Zedner.† The ordinates are temperatures on the Celsius scale, and the abscissæ give the composition of the system, the units x of the lower scale being the mol per cent. of ammonia in the mixture, and the complemental

* The reader not familiar with the thermodynamical theory of binary and ternary mixtures is advised to consult for further details *The Phase Rule and Phase Reactions*, by S. T. Bowen (Macmillan & Co., London, 1938), especially Chapter V, "Solutions of Liquids in Liquids," and Chapter IX, "Aqueous Solutions."

† *Berichte der Deutschen Chemischen Gesellschaft*, **41**, 1948, 1908.

y of the upper scale the atom per cent. of sodium. The percentage by weight—x' and y', respectively—is easily found by the formulæ :

$$x' = 17x/(17x+23y), \qquad y' = 23y/(17x+23y).$$

The curve AB, bounding the diagram towards the right, marks the maximum solubility of sodium in liquid ammonia. H is the boiling-point of pure ammonia under atmospheric pressure, which rises along the line HJ with increasing amounts of the solute. Along the same line the density of the solution decreases from 0·68 g. cm.$^{-3}$ at H to 0·58 g. cm.$^{-3}$ at J. In fact the solutions of the alkali metals in liquid ammonia are the specifically lightest solutions known so far, and less dense than both solid and liquid NH_3. Their colour changes with increasing concentration of the metal from light blue to a deeper shade of blue, finally becoming opaque and assuming a strong metallic luster of bronze colour. The upper region of the phase diagram, above the boiling curve HJ, can be reached only by maintaining an ammonia pressure higher than the normal atmospheric pressure. Cooling of a solution of any specified composition corresponds to a movement of the image-point representing the system vertically downwards, *i.e.* parallel to the temperature axis, and on transgressing the line EDB the homogeneous solution becomes unstable. At any point inside the closed area EDBCE of instability the virtual system will split into two solutions of different composition and density, the lighter bronze one floating on top of the denser blue one. The compositions of the two liquid phases correspond to the intersections of a horizontal straight line through the chosen point with the curves DE and DB, respectively, the relative mass of the two phases being inversely proportional to the distance of the points of intersection from the chosen point. The exact location of the critical point D has later been determined to be at $-41°{\cdot}6$ C. and 4·15 atoms per cent. sodium. On further cooling of the more dilute blue solution, the precipitation of solid ammonia begins when the solution FE is reached and then proceeds along the line ECB, while the solution being in equilibrium with the solid ammonia assumes the bronze colour and becomes more and more concentrated following the curve DB. The cusp DBJ is the field of stability of the brown solution, which solidifies in the point B at $-112°$ C. The eutectic B is described as lead-coloured crystals showing metallic luster. The nature of the solutions of metals in ammonia has not yet been unanimously agreed upon. There are still a few investigators who accord to them a colloidal constitution, though the majority appear to regard them as true solutions, analogous to the aqueous solutions of ionizing salts. The decision of this problem has some pertinency to our intended interpretation of Jovian phenomena. If the brown liquid phase were a true solution, it should be formed from sodium in contact with solid ammonia at temperatures higher than the melting-point of the eutectic B, in the same way as the addition of salts to snow makes the latter melt (formation of a cryohydrate), but such could scarcely be expected if the system NH_3-Na were colloidal. H. Moissan * remarked briefly that none

* *Comptes Rendus*, **127**, 685, 1898.

of the alkali metals reacted with solid ammonia at $-80°$ C., but that the reaction started if the temperature was raised ever so slightly above the melting-point of ammonia ($-78°$ C.). It should be of interest to verify this statement and to test the possibility that *Na* is still reacting with solid NH_3, though at a greatly reduced rate. The solution of sodium in ammonia is not entirely stable even in the dark, but decomposes slowly by forming sodium amide $NaNH_2$ and freeing hydrogen. Sodium amide is very little soluble in liquid ammonia and therefore is precipitated as a white solid with faint yellow tinge. On cooling to $-60°$ C. the rate of thermal decomposition becomes practically negligible. The photochemical decomposition of the dilute blue solution by ultra-violet light has been studied by R. A. Ogg, P. A. Leighton and F. W. Bergstrom.* Sodium amide and hydrogen are formed by the same range of wave-lengths as absorbed by gaseous ammonia, which in Jupiter's atmosphere would act as a screen partially protecting the incrustation of the clouds from photochemical decomposition.

The solutions of other light metals in ammonia are far less well explored. Magnesium is very little soluble with blue colour. The binary systems $Li\text{-}NH_3$ and $K\text{-}NH_3$ are entirely homogeneous down to $-70°$ C., but the ternary systems $Na\text{-}Li\text{-}NH_3$ and $Na\text{-}K\text{-}NH_3$ split into two liquid phases at $-55°$ C. The colouration of the solutions of different alkali metals is identical. Incidentally, a colour-sketch of both the blue and the brown solution of sodium is reproduced in a paper by W. C. Johnson and W. C. Fernelius.† The colour of the concentrated brown solution is said to change from a dull coppery tone to a more yellowish, brass-like shade if viewed very obliquely. From the solutions of calcium in liquid ammonia there can be isolated a well-defined compound $Ca(NH_3)_6$, the colour of which is described by various authorities as fiery red, reddish gold and the like.

On the basis of the data related in the last paragraphs, the colouration of Jupiter's belts may tentatively be identified with the brown concentrated solution of sodium formed on the ammonia clouds at temperatures above $-112°$ C. Since Saturn must have a temperature lower than that of Jupiter, as is indeed indicated by the total radiation, the absence of conspicuous belts on this planet is readily understood. Of course our hypothesis does not explain in itself the preferentially zonal distribution of the brown shades on Jupiter. Here it would be necessary to introduce rather specialized assumptions of meteorological character. Since the equatorial plane of the planet very closely coincides with the orbital one, the general atmospheric circulation between the equatorial and polar regions of Jupiter must lack the strong seasonal variations observed on the Earth. In particular, the polar caps are doubtless maintained at temperatures considerably lower than that of the zones of low latitude, and actually may never reach the eutectic temperature of $-112°$ C. below which the brown solution solidifies into grey crystals. It should be noted that Jupiter is generally credited with an average surface temperature of only $-140°$ C., but the conventional

* *Journal of the American Chemical Society*, **55**, 1754, 1933.
† *Journal of Chemical Education*, **7**, 981, 1930.

method of computing planetary temperatures from the observed total radiation involves so many delicate assumptions, that the supposedly 40° or even 50° higher temperature of the cloud surface is by no means incompatible with the observational data. The dilute blue solutions can exist only at temperatures higher than $-78°$ C. This will account for the comparatively rare appearance of rather small strictly blue areas, almost exclusively during periods of great eruptive activity which may result directly from an anomalous release of internal energy. Judging solely from the descriptions of the belts as observed with reflecting telescopes and even making some allowance for the different impressibility of various observers, there still is good evidence of an enormous range of brownish and reddish hues. Part of this variation might be ascribed to secondary physical factors, like the average size of the crystals or droplets constituting the clouds, or the varying thickness of the coloured incrustation. Moreover, the presence of metallic calcium may be responsible for the more vividly reddish tones. Calcium, like sodium, is a common metal of great cosmic abundance, and the resonance line λ 4227 of *Ca*I has been suspected to occur in the spectrum of the night sky.* Consequently there appears to be no difficulty in providing for the whole scale of shades derived from yellow, orange and red. As for the cyclical changes of the conspicuousness of Jupiter's two equatorial belts, the northern and southern belts alternatingly fade out more or less and grow prominent again at intervals which in the long run agree with the planet's sidereal period of revolution according to Williams's investigations.† Apparently here we meet with a weak manifestation of seasonal differences. It is worth noting that the maximum and minimum colouration of either belt coincides rather closely on the average with midsummer and midwinter of the respective hemisphere. This implies a strong positive correlation between higher temperatures and stronger colouration. In the light of our hypothesis, such correlation would seem to indicate that the average summer temperature cannot be far above the eutectic point ($-112°$ C.), and that during winter the temperature may fall enough to make most of the brown liquid phase freeze into the grey eutectic. Jupiter's famous Red Spot also undergoes remarkable changes, bleaching at times almost completely. It has not yet been ascertained whether this is a material change or the whole area is temporarily being covered by an opaque white haze.

In conclusion it must be admitted that it would be difficult to design a test which could serve either to verify or to reject this hypothesis concerning Jupiter's colouration. The chief merit of it should be seen in the way it permits one to co-ordinate and interpret the observed colours as reducible to a single chemical principle without unduly straining one's imagination. Evidently, the still rather obscure chemistry of Jupiter's and Saturn's outer layers would warrant a good deal more of experimental work on the solutions of metals in liquid ammonia. The problem of Jupiter's colouration has held the writer's attention for many years, but all the previous tentative solutions

* J. Cabannes, J. Dufay and J. Gauzit, *Ap. J.*, **88**, 172, 1938.

† *M.N.*, **97**, 105, 1936.

proved unsatisfactory in the end. For a while it was suspected the brown pigment might be iron pentacarbonyle $Fe(CO)_5$, which could be formed by the reaction of metallic iron with carbon monoxide at higher temperatures (meteorites in *CO* atmosphere); furthermore, the reaction product would undergo photochemical decomposition into other highly coloured iron carbonyles. However, it was realized later on that Jupiter's atmosphere cannot contain *CO*, because this molecule is liable to be completely destroyed by a photochemical reaction with NH_3.* All the other brownish iron compounds are derived from the trivalent ion Fe^{+++}, which scarcely could be formed in a reducing medium like Jupiter's atmosphere. With iron as the most common metal ruled out, one would only reluctantly resort to the other heavy metals, many of which give vividly coloured compounds, if mainly in the higher stages of oxidation. Inasmuch as the light metals sodium, calcium and magnesium are very abundant cosmically, they may readily be invoked as agents contributing to the pigmentation of Jupiter's clouds, in distinct preference to the by far rarer heavy metals. In order to consummate our argument, a way ought to be shown by which elementary sodium becomes available in the atmosphere of Jupiter. This is a difficult task.

Sodium and the other light metals are highly reactive substances, which never are found in elementary form near the Earth's surface by reason of their great affinity to oxygen. The origin of the sodium atoms observed in the spectrum of the night sky is not yet definitely known. There appears to be a widespread feeling of hesitation to admit that the sodium could be imported from extra-terrestrial sources. In particular, J. Franck and C. A. Rieke † have pointed out that oceanic salt spray, carried by the vertical atmospheric circulation beyond the ozone layer, is apt to be dissociated by ultra-violet sunlight. It would seem more difficult to explain the terrestrial origin of molecules like *CN* and *CH*, which also contribute to the luminosity of the night sky and are characteristic features of the cometary spectra. J. Dufay and J. Gauzit ‡ have stressed the general similarity of the spectra of the comets and of the night sky. The possibility that metallic sodium is carried into the planetary atmospheres by meteoric dust should not be dismissed categorically. The appearance of the D-lines in emission, as soon as a comet has approached the Sun to about 0·7 astronomical units, is in itself an indication that there exists free sodium on the surface of the solid cometary particles. Although the vapour tension of sodium metal becomes appreciable at temperatures of 350° to 450° K., as attained by a small black particle at about the distance of Venus, such temperatures would be insufficient to free sodium from the sodium silicates found in meteorites through reduction by metallic iron. The necessary temperatures may be reached if the comet approaches the Sun to Mercury's distance or closer.§ The meteorites gathered at the Earth's surface do not constitute a fair sample of the cometary and meteoric bodies,

* R. Wildt, *Ap. J.*, **86**, 321, 1937. † *Ap. J.*, **89**, 463, 1939.

‡ *Journal de Physique et Le Radium*, **5**, 523–527–601, 1934.

§ The writer is much obliged to Prof. V. M. Goldschmidt, Oslo, for having brought this process to his attention.

because all those consisting of easily oxidable substances would be completely burned during their flight through the atmosphere. W. A. Wahl * has observed that the meteorites of Hvittis and Bustee contain just enough oxygen and sulphur to keep all the light metals in combination with these elements. He goes on to remark that these meteorites are obvious limiting cases; for if the meteoric magma had been less rich in electro-negative elements, there would have condensed stony meteorites consisting in part of light metals or silicon in native form, and such bodies could never reach the Earth's surface unimpaired. Jupiter's atmosphere appears to be free from all oxidising agents. Therefore cosmically supplied sodium could accumulate, and it would show little tendency to sink to deeper levels since its solutions are considerably lighter than liquid ammonia. The hypothetical cosmic origin of the sodium required has only been discussed at such length, because, at present, the writer is unable to suggest any mechanism by which metallic sodium could be set free from the sodium compounds that must have formed during the condensation of Jupiter, and now probably are stored in the interior. Notwithstanding that, it is believed that the hypothesis proposed here concerning Jupiter's colouration involves a minimum of assumptions.

Summary

The reaction between ammonia and metallic sodium produces highly coloured systems, both liquid and solid. With due regard to conceivable differences in temperature, it appears possible to render account of the whole range of colours observed on Jupiter and of the absence of vivid colouration from Saturn's surface. The origin of the elementary sodium involved must be left undecided at present.

Princeton University Observatory,
Princeton, New Jersey:
April 1939.

* *Zeitschrift für anorganische und allgemeine Chemie*, 69, 92, 1911.

ON SOME OBSERVATIONS MADE WITH A MODIFIED PICKERING POLARIGRAPH

Yngve Öhman

(Communicated by R. d'E. Atkinson)

Introduction.—The analysis of light with respect to polarization is an important though not very often employed method in the study of celestial bodies. As a matter of fact this line of attack may give valuable information in addition to ordinary photometry and spectrum analysis. But in applying it, the astronomer has to overcome many difficulties. Most polarization effects appearing in celestial sources of light are faint, and a high accuracy in the measurements is therefore needed. On the other hand, the light itself is often very faint in celestial objects, and the most sensitive methods of observation can therefore only be used in the case of the more luminous ones. The present paper deals with a sensitive instrument which can be employed even when studying very faint objects such as nebulæ, comets, etc.

Before entering upon a description of this instrument and on some observations made recently by the writer, it may be worth while to give a brief survey of the different kinds of polarization effects which may be present in celestial objects. Let us consider first the different types of radiation in which polarization effects may be present.

1. *Emission.*—A real self-luminous body can only give rise to polarization effects if electric and magnetic fields are present (Stark and Zeeman effects in line spectra). It is true that the thermal emission, and notably the infra-red radiation from oblique surfaces of hot solids or liquids, may be partly polarized, but in this case there has been a refraction in the surface layers before the radiation escaped from the body.*

2. *Secondary Radiation.*—Secondary radiation is often more or less polarized. This is the case with reflected light. We have no example of ordinary reflection from optical surfaces in celestial bodies, not even from liquid surfaces. Diffuse reflection is often observed, however. The diffuse reflection gives rise to interesting polarization effects depending principally on the phase angle, but showing marked differences for different materials. A careful study of the detailed relationship between polarization and phase angle can give very valuable information about the Moon and the planets, as has been shown by Lyot in his remarkable pioneer work in this field.

Among the effects of polarization in connection with secondary radiation those resulting from the scattering of light play an important rôle in astronomy. We have here to consider the scattering by small particles, molecules and free electrons.

* This effect could perhaps be present on certain parts of the Moon, notably during a lunar eclipse. But the surface is probably too rough to show the effect, though the conditions are more favourable in infra-red radiation than in visible light.

Finally, the polarization effects in connection with resonance radiation and fluorescence are of astronomical interest too.

3. *Absorption.*—Polarization effects in connection with absorption lines can only appear in the presence of magnetic or electric fields. They are of a particular interest in the study of sunspots, as was shown for the first time by Hale in his brilliant discovery of 1908. The explanation of this effect, known as the inverse Zeeman effect, is that a certain component corresponds to an absorption of a certain kind of vibration. If by some polarizing apparatus we take out, say, left-handed circular vibrations, certain dark components will appear. But taking out only right-handed circular polarization the same lines will not be present in the spectrum, as no such vibrations are absorbed for the wave-lengths in question.

Instead of grouping the different polarization effects according to the above scheme, it may sometimes be better to take together all effects appearing in *continuous spectra* in one group and those appearing in *line and band spectra* in another group. This has been done in Tables I and II, where the celestial bodies showing the different kinds of effects are listed as well. The most important references are given in the last column. The question mark (?) means that an effect of the kind in question probably contributes to the phenomenon shown by the object though no clear evidence has yet been found.

The Modified Pickering Polarigraph.—In an interesting paper of 1885 Edward C. Pickering* gave a description of a new form of polarimeter. He combined a series of metallic bars separated by intervals equal to their width, with a double-image prism placed at such a distance that the separation of the ordinary and extraordinary images was equal to the width of the bars. By combining this instrument with a Nicol prism he could, by turning the prism, give all the bands the same intensity and in this way measure the polarization of light. This polarimeter was used by Pickering in the study of atmospheric polarization, but though very good results were obtained, it seems to have been almost forgotten and no astronomical applications have so far been made with it.

Without knowing anything about Pickering's paper, which came to my notice quite recently, I have constructed a polarigraph on very much the same principle.† As is shown in fig. 1 (p. 628), my instrument is composed of a grating of metallic bars G, a plane-parallel plate of Iceland spar I and a lens L giving an image of the grating on the photographic plate P. The instrument has been used in conjunction with the 20-cm. Zeiss astrographic telescope of the Upsala Observatory. The focal length of this telescope is 100 cm. The objective L has a diameter of 21 mm. and focal ratio 1 : 2. It is placed in such a position that it gives an image of the grating on a scale reduced to 0·70. By this arrangement the intensity is doubled, which compensates for the dividing into halves by the double refraction. The aperture is full until a distance from the centre of the plate of 1 mm. (This corresponds to the width of two strips.)

* *American Academy of Arts and Sciences, Proceedings*, New Series, **13**, 294, 1886.

† Compare a somewhat similar instrument made of polaroid film and described by the writer in *Annales d'Astrophysique*, **1**, 141, 1938.

TABLE

Scheme of Polarization

(Intensity of secondary radiation $=\mathcal{J}$,

Matter	Secondary Radiation by	Theory	$\mathcal{J}(\lambda)$
Natural surfaces (even powdered) of bodies $>> \lambda$	Diffuse reflection	Reflection from elementary mirrors + repeated reflection and scattering from deep layers (Umow, Woronkoff, Pokrowski, Jentzsch)	The albedo is as a rule a function of λ
Particles, crystals and droplets of a size comparable with λ	Diffraction	The diffraction and scattering of light by spherical particles (Mie, Debye, Schirmann, Shoulejkin, Blumer)	$\mathcal{J}$ is a function of θ, λ, size of particles and of the optical constants
Particles of a size $<< \lambda$	Scattering	The same theory as above. Partial waves of 1st order. The same formula as for a dipole	$\mathcal{J} \sim \frac{1}{\lambda^4}$
Molecules and atoms	Scattering	Theory of molecular scattering (Lord Rayleigh, Gans, Born, Cabannes and Raman)	$\mathcal{J} \sim \frac{1}{\lambda^4}$
Free electrons (and ionized atoms)	Thomson scattering	Vibrations of free electrical charges	$\mathcal{J}$ is independent of λ

The width of the bars in the grating is 0·71 mm. and the space between the bars is 0·67 mm. The Iceland-spar plate has a thickness of 6 mm. and is covered on each side with a $\frac{1}{2}$-mm. glass plate. The principal section is perpendicular to the bars of the grating.

The polarigraph is attached to the astrographic telescope in such a way that the grating is situated in the focal plane of the 20-cm. object-glass. When photographing a celestial object with this arrangement, we obtain a striped image in which two adjacent strips belong to the same strip of the object but are polarized at right angles. If the object is polarized the adjacent strips will differ in intensity.

The advantage of this instrument compared with an ordinary double-image prism is that the regions to be compared are very close to each other

I

Effects in Continuous Spectra

degree of polarization $=p$, phase angle $=\theta$)

$p(\lambda)$	Object and References
p increases if the albedo decreases (Umow). p is a function of θ. As a rule maximum if $\theta =$ twice Brewster's angle. p sometimes faintly *negative* for θ close to 0°	Moon (Arago, Lyot, F. E. Wright, etc.) Mercury (Lyot) Mars (Lyot) The asteroids (Lyot) The innermost ring of Saturn (Lyot)
p is a function of θ, λ, size of particles and the optical constants. p can sometimes assume strong *negative* values	Venus (Lyot) Clouds on Mars (Lyot) Jupiter (Lyot) Zodiacal light (A. W. Wright, Dufay) Reflection nebulæ (Struve, Henyey, etc.) Obscuring clouds in the Andromeda nebula (Öhman) Solar corona? Comets? (Campbell, Duncan, Öhman, etc.) The outer ring of Saturn? (Lyot)
p is independent of λ. Polarization is complete for $\theta = 90°$	Solar corona? Atmospheres of planets? Comets?
p is independent of λ. When $\theta = 90°$ polarization is complete for isotropic molecules and slightly less for anisotropic ones	Venus? Jupiter? Saturn? (Lyot)
p is independent of λ. Complete polarization for $\theta = 90°$	Solar corona (Secchi, Young, Fessenkoff, Dufay, Cohn, Baumbach, etc.) Prominences. Continuous spectrum (Lyot)

on the plate, whereby a higher accuracy can be obtained in the measurements. Moreover, the dispersion in double refraction will be very small, and consequently the definition is not spoiled, as is often the case if we use a powerful double-image prism without grating. The slight difference in focus for the ordinary and extraordinary rays does not influence the definition in my instrument.*

The degree of polarization can easily be obtained from photometric

* In order to avoid this fault completely it might be better to replace the Iceland-spar plate by a double-image prism giving a small angle between the ordinary and extraordinary rays. In this case the instrument will resemble a spectrograph with collimator and camera, where the slit is replaced by the grating and the ordinary prism by the double-image prism.

TABLE II

Scheme of Polarization Effects in Line- and Band-spectra

Condition	Phenomenon	Polarization	Object and References
Magnetic fields	Zeeman effect	Plane and circular polarization	Sunspots (Hale)
Electric fields	Stark effect	Plane polarization	Not observed
Resonance and fluorescence	Polarization of resonance radiation and fluorescence	Plane polarization	Prominences? Comets? (Öhman) β Lyrae? (Öhman)
Canal rays	Stark-Lunelund effect	Plane polarization	Not observed

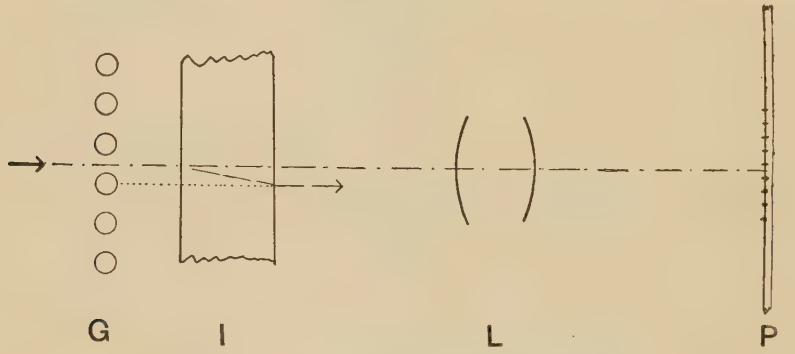

FIG. 1.—*Schematic plan of the polarimeter.*

measurements if some sort of intensity scale has been recorded on the plate. Suppose that the stronger strip has the intensity $\mathcal{J}_1$ and the fainter one the intensity $\mathcal{J}_2$. Then the degree of polarization is given by

$$p = \frac{\mathcal{J}_1 - \mathcal{J}_2}{\mathcal{J}_1 + \mathcal{J}_2} = \frac{\mathcal{J}_1/\mathcal{J}_2 - 1}{\mathcal{J}_1/\mathcal{J}_2 + 1}. \tag{1}$$

$\mathcal{J}_1/\mathcal{J}_2$ is directly found from the photometric measurements and thus p can be found.

An estimate of the accuracy of the method can be made in the following way. If p is only a few per cent., as in most astronomical applications, we have with sufficient accuracy

$$dp = 1{\cdot}15 d(\log \mathcal{J}_1/\mathcal{J}_2). \tag{2}$$

Now $\log \mathcal{J}_1/\mathcal{J}_2$ can be determined from photographic photometry with a mean error of about 0·01 corresponding to 0·025 stellar magnitudes. This would correspond to slightly more than 0·01 in dp. We can thus expect to measure effects of polarization with a mean error of 0·01, or if the polarization

is expressed in per cent. we can expect a mean error of 1 per cent. Though this accuracy is not so high as in the case of Lyot's and F. E. Wright's polarimeters, it is as good as we can expect for faint objects.

The measurements are not difficult to perform if the plane of vibration is known in advance. But if we have to determine the degree of polarization and the position of the plane of vibration as well, we must at least make two independent determinations. A theoretically very elegant method, which has several times been employed in such investigations *, is to turn the instrument through 45° in position angle between the two measurements. Let p_1 and p_2 be the observed polarization in the two positions. (Here polarization is considered positive if the ordinary image is the stronger one.) Then the true polarization p and the angle v between the plane of vibration and the direction of the strips (vibration of ordinary image) are obtained from the following formulæ :—

$$\left.\begin{aligned} p &= \sqrt{p_1^2+p_2^2}\,; \\ \tan 2v &= \frac{p_2}{p_1}. \end{aligned}\right\} \qquad (3)$$

In the present work no use has been made of formulæ (3) because the plane of vibration could be considered a known quantity for the objects which have been tested.

In order to get the amount of polarization the plates have been standardized with a wedge copied on every plate. The wedge has proved to be very nearly linear, and a displacement of 10 mm. along the wedge has been found to correspond to a difference of 0·94 in log intensity of the transmitted light.

Some Tests on the Moon.—In order to test the instrument I secured some photographs on high-contrast plates of the Moon. Figs. 2 and 3 show the Moon on February 28 and March 5, 1939. (Reproductions are positives.) The position angles of the strips were 357° and 90° respectively.† As is very apparent, the first plate, taken one day after first quarter, shows marked effects of polarization notably on the maria, some of which are considerably darker in one strip than in the other one. This result is in good agreement with earlier observations ; for instance, Lyot's and Wright's extensive study. Fig. 3, on the other hand, which is taken close to Full Moon, does not show any clear effects of polarization on any part of the surface. Even the maria show up with the same density in the two strips. This is also in good agreement with earlier well-known results.

From two plates taken on February 27·875, with the strips parallel and perpendicular to the terminator, I have from a great number of settings derived a mean polarization of 6·3 per cent. This agrees well with Lyot's value 6·7 per cent. for the Moon in first quarter obtained from visual measurements.

* E. C. Pickering, *American Academy of Arts and Sciences, Proceedings*, **9**, 1, 1873, and B. Lyot, *Annales de l'Observatoire de Meudon*, **8**, fasc. 1, 1929.

† By a remaining small fault of adjustment the strips are not quite perpendicular to the line of junction between the ordinary and extraordinary images. But this small error has been neglected in order not to cause confusion.

The two plates show a difference indicating a (real or apparent) instrumental polarization of about one per cent. This effect is eliminated by taking the mean of two plates obtained for perpendicular directions.

A centre correction as to instrumental polarization is to be expected at least for distances from the centre of more than four strips. The definition is not very good when exceeding this limit. It seemed advisable therefore to use only the centre of the field.

Observations of Comet Jurlof-Achmarof-Hassel.—The instrument was constructed mainly for the purpose of studying faint objects such as nebulæ, comets, etc. It has been in use from the beginning of 1939, particularly in a study of the Andromeda nebula. When comet Hassel appeared, however, the instrument was tried on this object, and as the plates obtained are very instructive I will give a description of them before dealing with the nebula.

In all, 10 plates were obtained of the comet from April 18 to April 24. Fig. 4 shows plate 27 obtained on April 18 (see Table III) and fig. 5 shows the plates 28 (left) and 29 (right) obtained on April 19. The plates 27 and 28 were taken with the strips in position angles 98° and 101°; plate 29 was taken in position angle 281°—that is, the instrument had been turned 180° compared with plate 28. This was done in order to eliminate possible Eberhard effects or other influence from the luminous head of the comet.

As is apparent from the photographs, the tail as well as the head of the comet is definitely faintly polarized. In fig. 4 the upper strip in each pair is somewhat stronger than the lower one. The same effect can be seen in the left image of fig. 5, whereas the right one shows the opposite effect, which is to be expected as the instrument has been turned through 180°. The polarization effects can be traced in the first pair as well as the second pair above the head. But the effects seem to have disappeared in the third pair as far as can be judged from the original negatives.

The same strip of the tail sometimes shows variations in the polarization. The fainter parts of the tail seem to be somewhat stronger polarized than the stronger parts for the same distance from the head.

Six of the plates have been measured in the Schilt photometer. I confined myself to the first pair of strips at the side of the head corresponding to an angular distance from the head of 4′·7. Table III gives the mean

Table III

Date: April	Plates No.	Exp.	Position Angle	Polarization in per cent.	Phase Angle
		m	°		°
18·872	26	10	0	6·7	105
	27	21	98		
19·933	28	15	101	6·3	102
	29	26	281		
21·893	30	20	292	6·0	98
	31	22	112		

polarization obtained from about 6 different settings in each strip of this pair. Plate 26, which has the strips nearly parallel to the tail, was measured on corresponding points.

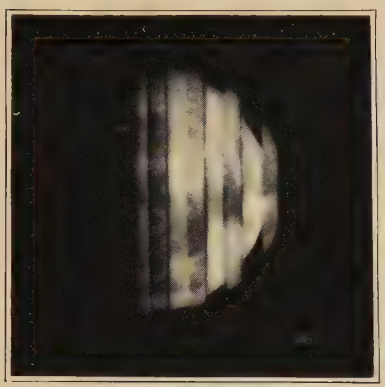

Fig. 2.—Polarization of the Moon shortly after first quarter. Note the strong effects on the maria. (Enlarged 4·7 times.)

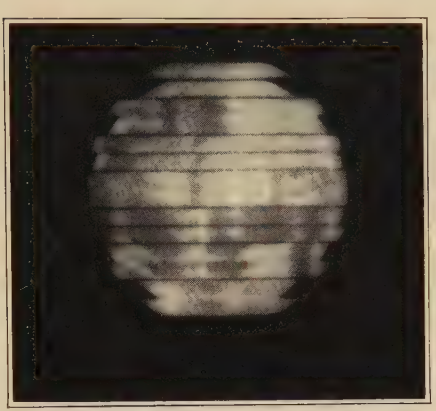

Fig. 3.—Absence of polarization at Full Moon.

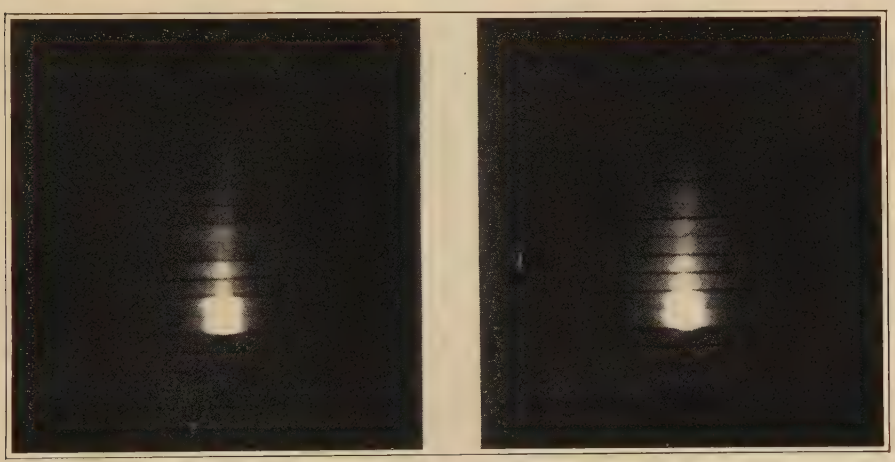

Fig. 5.—The comet on April 19. The photograph to the left shows the upper strips stronger than the lower ones. The photograph to the right shows the opposite effect because the instrument has been turned 180°.

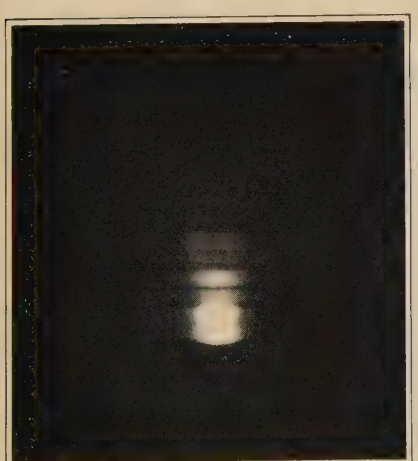

Fig. 4.—Comet Jurlof-Achmarof-Hassel on April 18. Polarization is present in the coma and tail because the upper strip of each pair is stronger than the lower one.

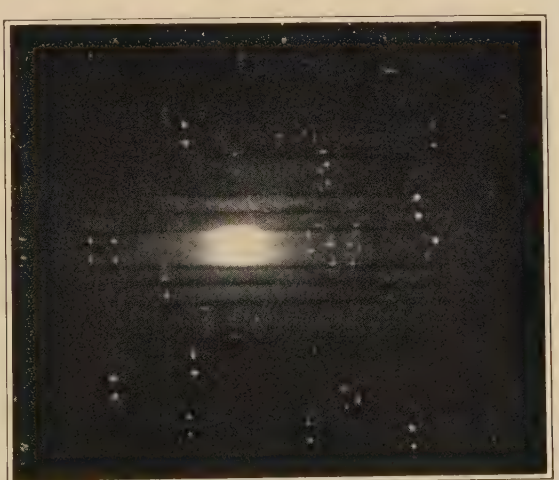

Fig. 6.—The Andromeda Nebula photographed with an exposure time of 1 hour. The strips are nearly parallel to the major axis of the nebula. Polarization is indicated in the first pair above (north-west of) the centre in the region of strong obscuring clouds.

As can be seen from the table, the mean polarization of the tail at a distance from the head of 4′·7 has been found to be about 6·5 per cent. In the last column the phase angle has been given. It has been calculated from Möller's ephemeris, given in *Copenhagen Circular*, 762, using the formula

$$\sin\frac{\alpha}{2}=\frac{1}{2}\sqrt{\frac{(R+\Delta-r)(R+r-\Delta)}{r\Delta}}. \qquad (4)$$

The plane of vibration is perpendicular to the tail—that is, the polarization is positive.

A small decrease in polarization is indicated during the days of observation. As an increase instead of a decrease might have been expected from the run in phase angle, the observed effect indicates a physical change in the tail between the different days. But the observations are not accurate enough to settle this question. In fact, observations of April 19 and 21 might have been slightly influenced by a small instrumental polarization found from the plates of the Moon and of the comet on April 18. Applying this correction would increase the polarization for April 19 and 24 by about one per cent.

The observations of this comet are in good agreement with earlier polariscopic observations made on comets; for instance, Campbell's and Duncan's observations in 1907 of comet *Daniel*.* But no measurements have so far as I know been made before.

In order to discuss the nature of the polarization effects spectrographic data of the coma and tail are very important. Unfortunately, only a few observations of the spectrum of the comet have yet been published. Vsessviatsky and Shulman report in *I.A.U. Circular*, 764, that the continuous spectrum is not intense compared with the band spectrum. The same result has been found by Hinderer in Babelsberg (*Zirkular der Astr. Nachrichten*) for the head of the comet. If the continuous spectrum was very faint in the tail of this comet, the polarization effects are probably due, not to a scattering from small particles, but to fluorescence. We must wait for more spectroscopic data before settling this question.

Obscuring Clouds in the Andromeda Nebula.—Many attempts have been made to detect polarization in extragalactic nebulæ, but no clear effects have yet been found.† In order to test the polarigraph I photographed the great Andromeda nebula on January 19 this year with an exposure time of one hour. I had expected to get an image without any trace of polarization, and was therefore very much astonished in obtaining the plate reproduced in fig. 6, which shows a faint effect of polarization in the first pair above the nucleus. As can be seen, the lower one of the two strips is fainter than the upper one. The strips have a position angle of 50°, so they have very nearly the same direction as the major axis of the nebula.

The strips showing the effect contain the *dark lanes* on the north-west part of the nebula running parallel to the major axis in a distance from the nucleus of about 5′. If the effect is real and not a photographic one the

* *Lick Observatory Bulletin*, 126 and 135, 1907.

† J. H. Reynolds, *M.N.*, 72, 553, 1911; W. K. Green, *Pub. A.S.P.*, 29, 108, 1917; W. F. Meyer, *ibid.*, 31, 194, 1919; and Sinclair Smith, *Mount Wilson Contr.*, 524, 1935.

plate indicates faint polarization in the region containing the obscuring clouds.

In order to try to settle this question, I took five more plates of the Andromeda nebula. A list of the plates is given in Table IV.

TABLE IV

Plate No.	Date	Exp. Time	Position Angle of the Strips
		h m	°
2	Jan. 19	1 0	50
5	Feb. 8	1 15	320
8	„ 15	0 52	135
9	„ 16	1 0	135
10	„ 20	1 14	135
21	Mar. 12	1 0	315

The other five plates were taken with the strips nearly perpendicular to the direction of the first plate in order to eliminate eventual errors. Moreover, for two of the plates the instrument was turned through 180° relative to the position for the three other ones.

Fig. 7 shows microphotometric tracings along the strips for the five new plates. The slit of the photometer had a length of half the width of the strips. The tracings are grouped in the figure according to vibrational direction. The position of the dark lane is marked by an arrow in the left tracings and by a dotted line in the right tracings. The plate numbers and position angles of the strips are given at the side of the figure. It is to be remarked that the lowest tracings, corresponding to plate No. 5, do not record exactly the same direction as the other plates, but one differing 5 degrees. This may be the reason why the dark lane does not show up in the same way for plate No. 5.

It is evident from the figure that the dark lane is deeper and more apparent when the vibration is perpendicular to the direction of the strips than when it is parallel with this direction. If this polarization effect, in the "dark" lanes, is due to a scattering of the light from the luminous nucleus this would mean a *negative* polarization.

It is difficult to get a measure of the polarization from the faint images, but from microphotometric measures it seems to be about -7 per cent. The negative polarization indicates that the scattering is produced by particles of a size somewhat smaller than the wave-length of light.* The polarization is in favour of Lindblad's conception †, that the dark lanes are situated in that half of the Andromeda nebula which is most distant from us because otherwise the phase angle would probably be not very far from 180°, which would be unfavourable for polarization effects.

It may seem strange that polarization can appear in obscuring clouds. But if these clouds send us faint radiation, this radiation is probably of the same kind as that from reflection nebulæ. In the obscuring clouds the reflected and scattered light is not mixed with much starlight, and consequently polarization should be expected to be strongest in such parts of the nebula.

* See Marie Anna Schirmann, *Ann. Physik*, 59, 493, 1919; *Meteorologische Zeitschrift*, 37, 12, 1920.

† *Annales d'Astrophysique*, 1, 173, 1938.

It is planned to undertake an extensive study of these effects and with a greater instrument, because the present scale is rather small for measuring

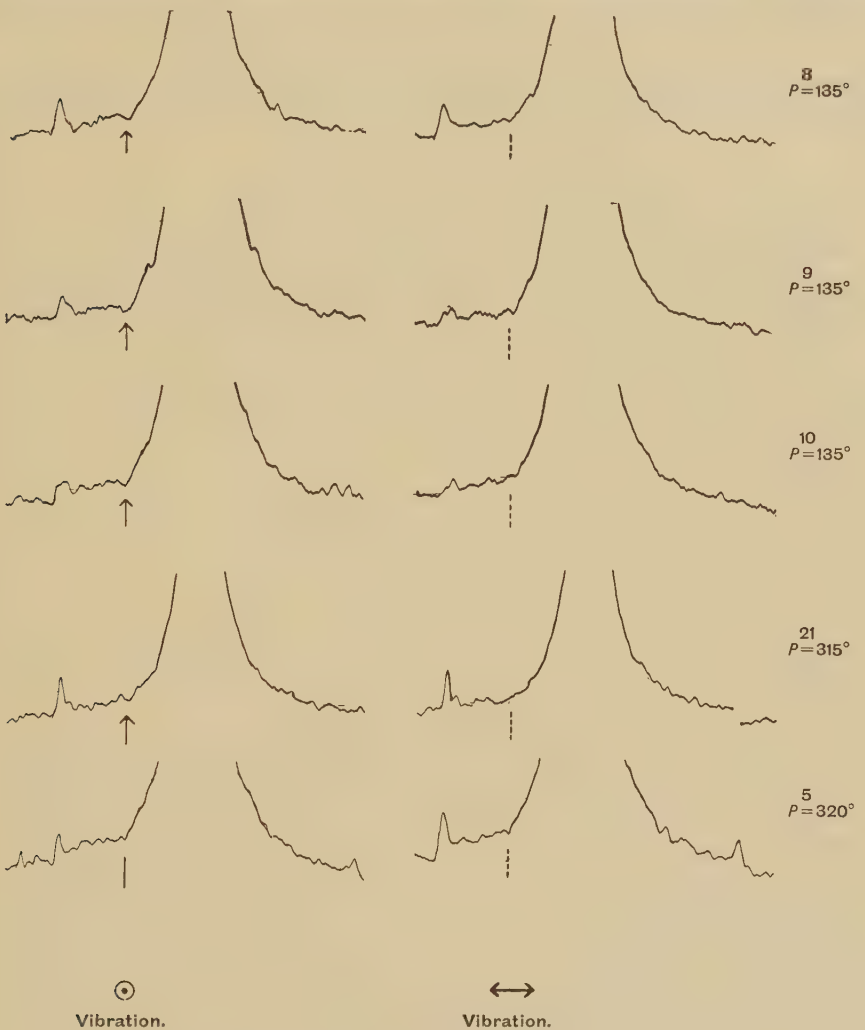

FIG. 7.—*Microphotometric tracings along the strips of five plates taken with the instrument turned through 90° compared with the position of fig. 6. The obscuring clouds show up most when the plane of vibration is perpendicular to the line of junction between the clouds and the nucleus.*

the effects. It would be of much interest to measure the polarization in red light too, as this might give valuable information about the size of the particles. Indeed, we may very well expect polarization to be positive in red light according to Miss Schirmann's calculations on Mie's theory.

Summary.—A brief survey is given of polarization effects in celestial objects. A description is made of a new polarigraph constructed on a principle similar to that of Pickering's polarimeter of 1885. The instrument is tested on the Moon and applied to a study of Hassel's comet and of obscuring clouds in the Great Andromeda nebula.

ON THE MOTION OF SOLAR PROMINENCES AND STREAMERS

H. R. Hulme, M.A., Ph.D.

(Communicated by the Astronomer Royal)

Introduction.—The motion of solar prominences has been studied extensively by E. Pettit *, who has photographed them at the various stages of their development. Later, a very successful technique was developed by McMath and Pettit †, whereby motion pictures of the prominences have been taken at the McMath-Hulbert Observatory. On the basis of pictures of a large number of prominences, Pettit has formulated the following two laws for the upward motion :—

Law I. The motion of a portion of a prominence or of the prominence as a whole measured along its trajectory is uniform, increasing suddenly at intervals as if by an impulse.

Law II. When a change of velocity takes place the new velocity is a small whole multiple of the old. Occasionally the *last* velocity is a whole multiple of the second previous.

Pettit and McMath also state that, in the matter descending, the knots and streamer ends observed also obey the first law, though not in general the second. Of these two laws McMath ‡ remarks :

"To say that these curious laws of prominence motion are mysterious is very definitely an understatement. They contradict every known law of the motion of particles under the action of a gravitational attracting centre ; it is as though acceleration in prominences functioned only in definite 'acceleration-quanta.' The very large amount of measurement that has now been made upon the motions of knots and other formations in prominence streamers of all types corroborates Pettit's Laws of Prominence Motion beyond the shadow of a doubt. But an acceptable theory of these apparently almost instantaneous integral changes in velocity will doubtless be far more difficult than has been the collection of the observational data bearing thereon."

It therefore seems worth while to examine the data of Pettit and McMath, on which these laws are based. These are given in the form of diagrams in which the height (of prominences) or the distance travelled (by streamers) is plotted against the time. For prominences and streamers obeying the first law, these plots will consist of a series of straight lines, end to end, representing the uniform speeds. We shall endeavour to show in this note

* *Ap. J.*, **50**, 206, 1919 ; *Publ. Yerkes Obs.*, vol. iii, p. 205, 1925 ; *Ap. J.*, **76**, 9, 1932 ; *Ap. J.*, **84**, 319, 1936 ; *Nat. Acad. of Sciences*, **22**, No. 5, p. 249, 1936.

† *Ap. J.*, **85**, 279, 1937 (referred to as M.P. I) ; *Ap. J.*, **88**, 244, 1938 (referred to as M.P. II).

‡ *Proc. Amer. Phil. Soc.*, **79**, 493, 1938.

that, *for the descending matter*, most of the distance-time plots may be equally well represented by smooth curves, although this is not true for the ascending matter.

Explanation of Diagrams and Discussion of Pettit's First Law.—We shall be mainly occupied with the descending streamers, etc., and unless expressly stated to the contrary, the remarks following apply only to descending matter.

If we examine the diagrams of streamer motion given in the papers quoted, it will be seen at once that the deviation of the measured points from the straight lines is not a random one. In the table below we give the distribution of residuals for streamers numbered 1, 4, 7, 10, etc. in two diagrams, one taken from M.P. I, p. 287, and the other from M.P. II, p. 268. Plus and minus denote positive and negative residuals, and no sign indicates that the point is centred on the line as far as the eye can distinguish. Thus +3, 1, −4 indicate 3 points above the line followed by 1 on and 4 below.

1, +3, −2, +1, 1, +1, −3, +1, −1, +9 −2, +2, −4, +5, −5, 2, +1, 1, −1, 1, +1 +2, −8, 1, +4, −2, +2	M.P. I
1, +1, −1, 1, +1, 1, −1, +1, −1, +2, −3, +1, − 1, +1 −3, +1, −1, +1, 1, +1, −1, +3, −4, 1, −1, 1, −4, +1 +3, 1, −2, +1, −1, 1, −3, +3, −2, +2, −2, +2, −5, +3, 1, −4 −1, +2, −1, +3, −2, +2, −4, 1, +4, −3 +4 −4 +3, 1, −1, +5 −1, 1, +1, 1, −1 −3, +2, −3, 1, +2, −2, +1, 1, +1, −1, +1, −3, +1, −1, 1, +1, −2, 1, −2	M.P. II

It will be seen that in some of the streamers groups of 3, 4 and 5 occur much more often than they would in a random distribution of errors. The phenomenon is more marked in the streamer diagrams shown on pages 252, 253 and 254 of M.P. II.

It seems clear, therefore, that the deviation of the points from the straight lines fitted to them is not entirely due to random error of identification and measurement of the object, and we must assume that the wavyness represents a real phenomenon. This may be a real motion of the knot or streamer end under investigation, or an apparent motion, caused, for example, by one part becoming brighter for a short time and causing an apparent displacement. *In many cases, therefore, the measurements are not adequately represented by either straight lines or a single smooth curve, but by an irregular wave-like line.* Pettit's first law must therefore be regarded as applying to the underlying general motion, disregarding the superimposed "waves." The question now to be answered is whether this (general) motion is better represented by a series of straight lines or by a smooth curve.

In the attempt to decide this point we have constructed diagrams 1 and 2 as follows: The corresponding diagrams (M.P. I, p. 287, and M.P. II, p. 268) were photographed, and an enlarged image ($\times 2\frac{1}{2}$) of each was thrown on to a piece of paper in an enlarging camera. The centres of the dots representing observations were then pricked through on to the paper

and surrounded by circles again $2\frac{1}{2}$ times as large as the dots in the original diagram. Smooth curves were then drawn to represent the observations as well as possible. The numbering of the streamers is the same as in the original figures, but in fig. 1 the "broken" prominence No. 5 has been

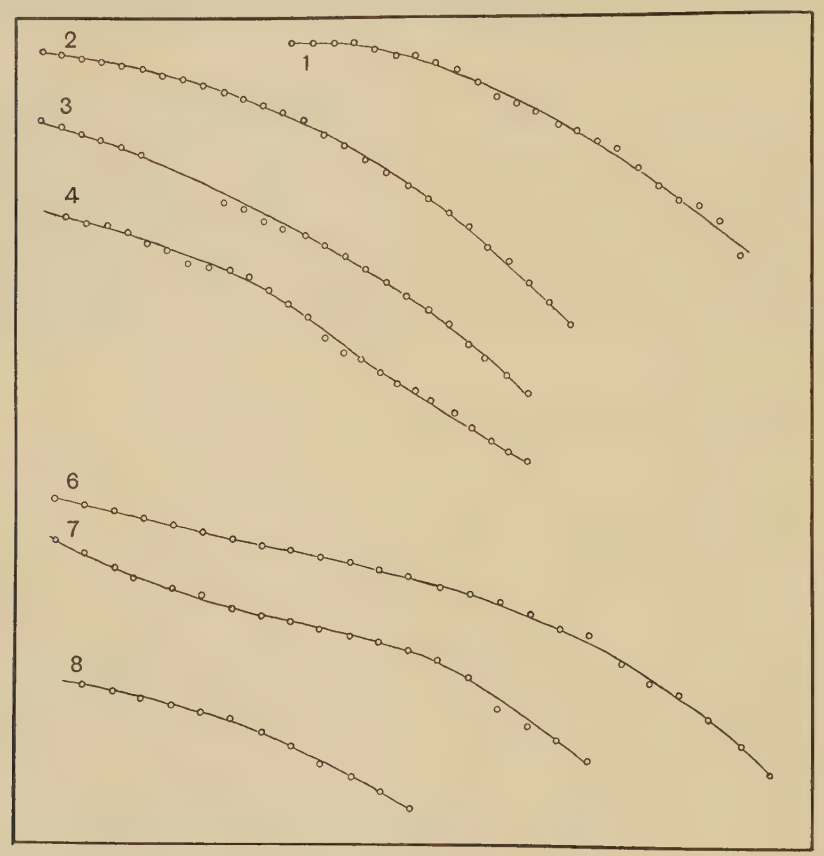

Fig. 1 (M.P. I, p. 287).

omitted, and in fig. 2 several prominences have been omitted to avoid congesting the diagram.

The natural procedure now is to measure the vertical distances of the observed points from the straight lines and the curves in the two diagrams respectively. This was done with a small microscope to the nearest $\frac{1}{10}$ of a mm.* The results are given below: c denotes the sum of the distances from the curve and s the same sum for the straight lines. The quantity $\frac{200(s-c)}{(s+c)}$ gives a convenient measure of the superiority of the curves in representing the observations. The unit is 0·1 mm.

* The author's thanks are due to Dr. G. A. Archenhold for his assistance in measuring the diagrams.

Prominence		c	s	$200(s-c)/(s+c)$
M.P. I	1	97	95	− 2
	2	55	43	−24
	3	65	39	−50
	4	89	98	+12
	6	48	92	+63
	7	58	100	+53
	8	15	15	0
M.P. II	3	90	82	− 9
	6	102	79	−25
	8	101	100	− 1
	9	116	153	+27
	10	225	159	−34
	11	216	309	+35
	12	152	208	+31
	13	72	85	+17
	14	160	190	+17
	15	153	153	0

In columns 2 and 3 we give the sum of the distances, rather than the sum of the squares of the distances, because the deviations are not random, and sometimes contain very large residuals which would influence the mean

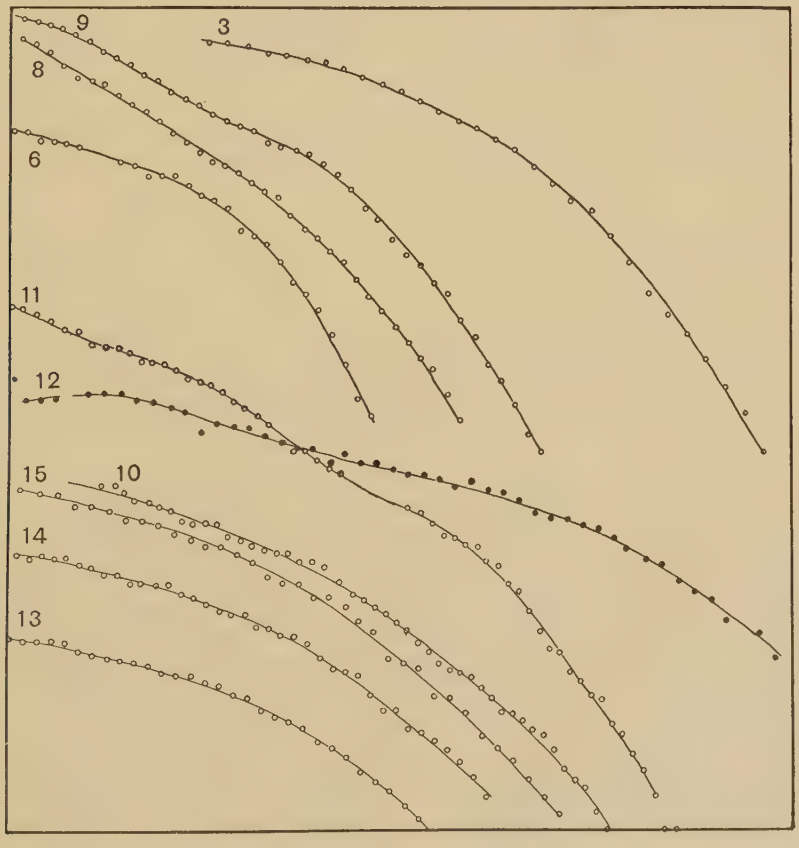

Fig. 2 (M.P. II, p. 268).

square too much if included. It will be seen that of the sets of observations chosen, 8 are better represented by curves and 5 are better represented by straight lines, whilst in 4 cases there is little difference.

On the basis of these examples we do not think that Pettit's first law can be regarded as established for descending matter.

It might, however, be argued that since some of the observations are better represented by sets of straight lines, the existence of sudden changes of velocity is definitely established, and all descending matter should be regarded as obeying Pettit's first law. On this view the circumstance that the observations sometimes fit smooth curves is to be explained by assuming that observational error has smoothed out the sharp changes of velocity. This is a possible but, in our opinion, a very dangerous conclusion. Firstly, because it would be a generalisation that is difficult to justify; and, secondly, for a reason which is best illustrated by the following experiment.

A number of smooth curves were drawn with a collection of wooden curves. Vertical displacements were then given to points on these curves by drawing numbers at random from a collection representing approximately the error law. The displaced points were then considered, and straight lines were drawn to give as good a fit as possible (this was done by eye). As the displaced points were pricked through the paper, it was possible to draw on the other side of the paper the corresponding curves giving the best fit. The fit was then tested as before by taking for each streamer the sum of the displacements from the curve and from the straight lines. Denoting these two quantities again by c and s, the values of $200\frac{(s-c)}{(s+c)}$ were found to be as follows :—

Curve No.	1	2	3	4	5	6	7	8	9	10
$200\frac{(s-c)}{(s+c)}$	+2	−44	+1	−29	−50	−29	−9	−20	+18	−4

These figures show that in the majority of cases the examined straight lines give the better fit—even though no physical reality can be attached to them. The displaced points and the fit by straight lines is shown in fig. 3.

It will be seen that the density of the points is not as great as that in most of the diagrams of McMath and Pettit. We must remember, however, that the displacements considered in fig. 3 are random ones, whilst the points of McMath and Pettit tend to deviate in small groups from the general curve (or straight lines) of motion. It is probably better to regard the points in fig. 3 as corresponding to the small groups of points in figs. 1 and 2. Strictly speaking, the two sets of data are *not* comparable, and it is not possible to say what density of points and what probable error should be chosen in fig. 3. This figure must therefore only be regarded as illustrating the fact that if the points on a curve are displaced owing to experimental error, the result is often better represented (in the sense discussed) by a set of straight lines, which, however, have no physical significance.

To sum up, we may say that it is very difficult to decide if any physical reality is to be attached to a representation by straight lines of the motion of all the descending streamers, etc. By this we do not mean that there

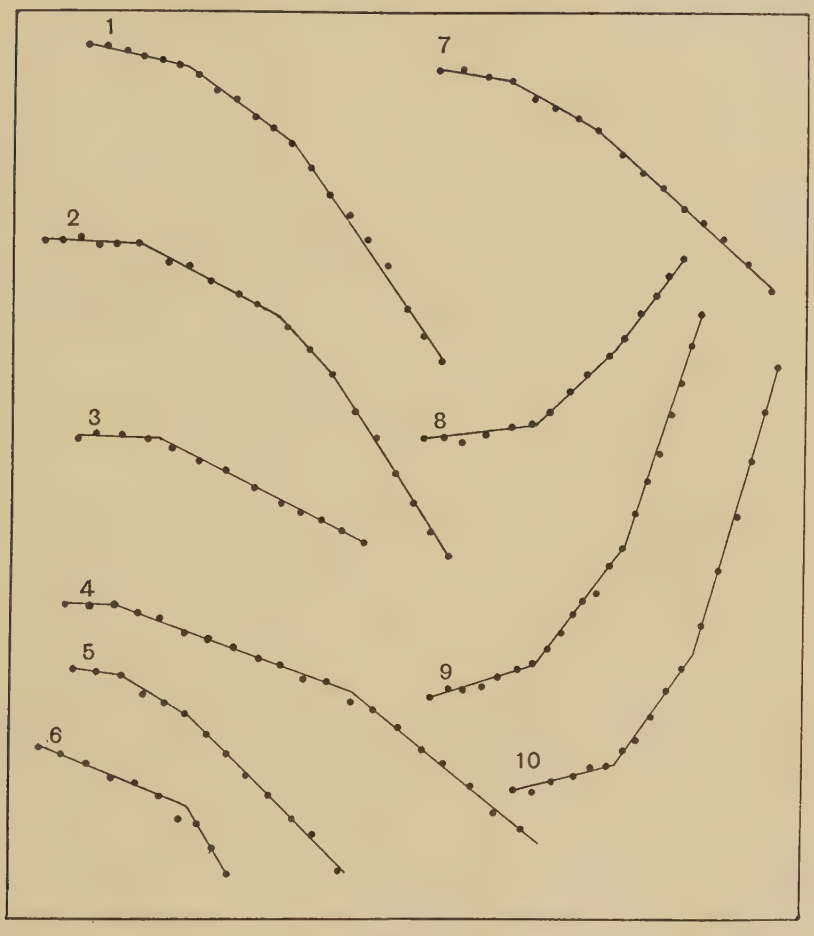

Fig. 3.

are no sudden changes of velocity of the type contemplated by McMath and Pettit, but they are the exception rather than the rule.

Turning now to the ascending prominences, we must include 8 more examples observed by Waldmeier *, which show very sharp bends, indicating rapid changes of speed. One or two of these could be represented by curves (*d*III, *g*II, *f* I), as could some of the diagrams of McMath and Pettit. On the whole, however, the evidence favours the existence, in many cases, of sudden changes from one uniform speed to another in accordance with Pettit's first law.

It seems probable that the upward motion of prominences is mainly, though not always, due to sudden bursts of ultra-violet light †, of varying

* *Zeit. f. Astroph.*, Bd. 15, p. 299, 1938.

† Unsöld, *Physik der Sternatmosphären*, pp. 424–425.

Number of Changes of Speed

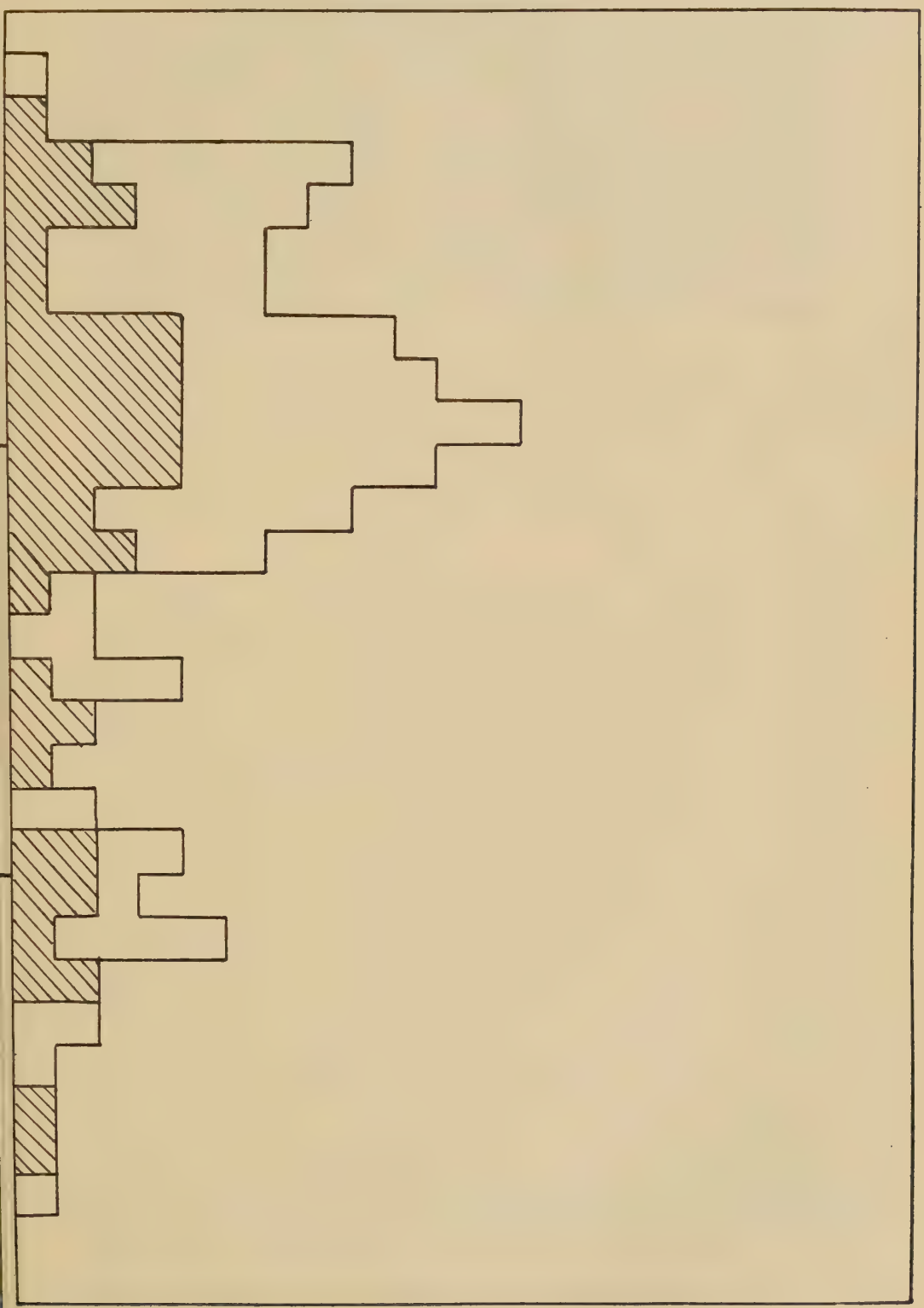

strength and duration (see the next paragraph), whilst the downward motion of the streamers is more akin to a fall under the influence of gravity and a much more (though not always entirely) uniform light pressure. McMath and Pettit have also given evidence of centres of attraction, not necessarily sunspots, to which the streamers flow.

This state of affairs is more easily reconciled with our knowledge of the Sun than one in which *all* motions obey Pettit's first law. As such we feel it is to be preferred until Pettit's first law is more firmly established in the case of descending matter.

Pettit's Second Law.—This law has already been criticised by Waldmeier (*loc. cit.*) in its application to prominences. He has pointed out that if we take only those prominences where the uniform velocities are determined by at least two observations, the following ratios are found for the velocities after and before an increase :—

Number of Changes of Speed with Ratios	Integer ± ·25	Other Values
Observed by P. and M.	12·5	13·5
Observed by W.	7	7

This includes Pettit's prominences as far as No. 40. Of the later ones we feel that the straight lines, if they are there, are not always determined with sufficient accuracy to justify inclusion. No. 47H (M.P. II, p. 248), for example, is represented as 5 straight lines which cannot, in our view, be determined with sufficient accuracy. It is clear from these figures that the second law is not obeyed by prominences.

In the case of streamer ends and knots in streamers we have suggested that they should in the main be regarded as following smooth distance-time curves. Should this prove to be untrue, it is of interest to examine Pettit's second law in its application to descending matter. Accepting McMath and Pettit's figures for the velocities, we have analysed the ratios at each change of speed for the streamers given in M.P. I and M.P. II.

In fig. 4 we give the distribution for streamers of class I (shaded) and class III (unshaded). We have drawn the figure so that the upper outline represents the distribution for all streamers. It is clear that the second law is not well founded.

In conclusion, I should like to thank Mr. P. J. Melotte, Mr. H. W. Newton and Mr. F. Jeffries for their assistance and advice.

Summary.—Pettit's two laws for the motion of prominences and streamers are discussed. The conclusion reached is that the second law is unfounded, and that the application of the first law to the case of descending streamers is not yet justified.

Royal Observatory,
Greenwich.

THE LAW OF ERROR AND THE COMBINATION OF OBSERVATIONS

H. R. Hulme and L. S. T. Symms

(Communicated by the Astronomer Royal)

1. *Introduction*

The normal or Gaussian law of error is commonly used by astronomers and others interested in the combination of observations, primarily on the grounds of its simplicity. It leads at once to the arithmetic mean of a series of observations as the best value for the quantity observed, and it has a plausible theoretical foundation. In addition, series of observations have occasionally been adduced to show that observed errors do actually follow this law. On closer analysis, however, it is not so satisfactory, and may be criticised on various grounds, which we indicate below.

(1) If we compare experimental results for the distribution of errors with a Gaussian curve of the same probable error, we find in many cases that the large errors are far more numerous than the normal law indicates. This point has been treated at length by Simon Newcomb*, to whose article we shall be referring frequently. In fact, a series of errors obeying the normal law seems to be the exception rather than the rule.

(2) The normal law is also defective from the theoretical point of view. According to Jeffreys †, "It involves a number of approximations, and when these are examined it is found that the law should hold only up to a moderate multiple of the standard error." Newcomb has also pointed out (*loc. cit.*) that a series of observations, ordinarily considered as homogeneous, need not in reality be so. A typical example of this is afforded by the observations recorded by the Cookson ‡ floating photographic telescope, which is used for the determination of the variation of latitude at Greenwich. The plates are exposed by a number of different observers under widely differing atmospheric conditions, and it therefore seems reasonable to suppose that the probability of an error x is better represented by the function

$$p(x) = \Sigma_r p_r h_r e^{-h_r^2 x^2} \qquad (1)$$

than by a simple error curve. As is well known, any function of the above type will lead to a distribution which has a preponderance of large and small residuals as compared with the normal law §, and a corresponding deficiency of medium ones.

(3) A further difficulty of the normal law is that it affords no really

* *American Journal of Mathematics*, vol. viii, No. 4, 343, 1886.

† *Phil. Trans. Roy. Soc.*, **237**, 231, 1938.

‡ See Greenwich publications on the "Variation of Latitude."

§ Eddington, *Proc. Phys. Soc.*, **45**, 271, 1932; Newcomb, *loc. cit.*

satisfactory criterion for the retaining or rejection of apparently bad observations—unless, of course, the observer has noted at the time that the observation is not expected to be as good as the others. In what follows we shall assume that we are dealing with a set of observations which, *as far as the observer knows*, are all of equal weight. Several criteria have been suggested, but they have been criticised severely by many authors. Their derivation depends on the assumption that the normal law holds at least as far as the error of the observation under consideration. It is, however, exactly here, in the region of large errors, that the Gaussian error law no longer represents the observed distribution in many cases. It is also clear that any rule is unsatisfactory which retains with full weight an observation whose error, for example, is $4{\cdot}9r$, and rejects completely one whose error is $5{\cdot}0r$, where r is the probable error.

The problem we shall attack is therefore twofold: firstly, we must find the actual error law which best fits the residuals, and then obtain the system of weighting corresponding to this law—for the arithmetic mean is the best value only if the errors follow the normal law. Newcomb (*loc. cit.*) and Jeffreys (*loc. cit.*) have solved the problem by rather different methods, and one object of this paper is to show that these two methods both lead to the same result in practice. The best system of weighting can be achieved much more directly by the method given in the next paragraph, which is simpler than the Newcomb-Jeffreys method.

2. *Method of Weighting*

Suppose that from the examination of a very large number of observations of a certain quantity we have found the probability that an observation is in error by an amount between x and $x+dx$. Let this be $\phi(x)dx$. Now suppose that we wish to find the best value which can be deduced from a considerably smaller number of observations of the same quantity. We shall assume, as mentioned, that all observations are *a priori* of equal weight. Let the observed values be $x_1, x_2, \ldots x_n$, then if the true value of the quantity is η, the probability of making these errors is proportional to

$$\psi(\eta) = \phi(\eta - x_1)\phi(\eta - x_2) \ldots \phi(\eta - x_n).$$

Newcomb (*loc. cit.*) defines the "evil" (e) associated with any particular result (η_0) by

$$e(\eta_0) = \int_{-\infty}^{+\infty} (\eta - \eta_0)^2 \psi(\eta) d\eta,$$

and takes the value for which the evil is least as the best value, *i.e.* that which should be adopted. This is then η_0 where

$$\int_{-\infty}^{+\infty} (\eta - \eta_0)\psi(\eta) d\eta = 0. \qquad \text{(A)}$$

Jeffreys (*loc. cit.*), on the other hand, takes for the best value that given by making $\psi(\eta)$ a maximum

$$\psi'(\eta_0) = 0. \qquad \text{(B)}$$

For a symmetrical $\psi(\eta)$ these are identical, and in any case there would be very little difference in practice. The most important consideration is that the definition (B) is very much easier to work with. The rigorous use of definition (A) is not practicable when dealing with more than three or four observations. In his paper Newcomb assumes $\phi(x)$ to be of the form given in equation (1) and works out an approximate method for evaluating η_0 when there are many observations. It is easily verified that in this case the value obtained (Newcomb, equation (14)) is exactly that given by the definition (B). In other words, the approximations which one has to make to evaluate η_0 from the definition (A) are such as to destroy any lack of symmetry in the curve $\psi(\eta)$. We shall therefore take the equation (B) as giving the best value, or the value with the maximum likelihood *, without placing any restriction on the form of $\phi(x)$, except that it shall not lead to negative values for the weights derived from equation (B).

Equation (B) now gives

$$\Sigma_r \frac{\phi'(\eta_0 - x_r)}{\phi(\eta_0 - x_r)} = 0, \tag{2}$$

which may be written

$$\Sigma_r(\eta_0 - x_r)\omega_r = 0, \tag{3}$$

where $\omega_r = \dfrac{\phi'(\eta_0 - x_r)}{\phi(\eta_0 - x_r)(\eta_0 - x_r)}$. The interpretation of (3) is now clear. We must attach weights to our observations proportional to the expression ω_r. When $\phi(\eta_0 - x_r) = e^{-h^2(\eta_0 - x_r)^2}$ we find $\omega_r = \text{const.}$, the normal error law leading to the arithmetic mean as the best value. It is interesting to consider the interpretation of the weighting factors in the case taken by Newcomb. Suppose, for simplicity, that $\phi(x)$ is given by

$$\phi(x) = p_1 h_1 e^{-h_1^2 x^2} + p_2 h_2 e^{-h_2^2 x^2},$$

where $h_1 > h_2$. A large residual will now have a greater likelihood of belonging to the second group with parameter h_2 than will a small residual. It is therefore more likely to have a small weight. Only if the observations satisfy a normal error law are we justified in attaching equal weight to them.

3. *Results*

The residuals chosen for analysis are those obtained from the measurements of the variation of latitude made at Greenwich with the Cookson floating zenith telescope during the years 1927–36. The actual quantities measured are the mean zenith distances of a large number of pairs of stars. From these we subtract the tabular mean place and the variation of latitude, both of which are known fairly accurately, and also a small diurnal term and a wind-effect term. (For full details see the Greenwich publication: *Zenith Telescope Observations, 1911–36.*) It is assumed that each result now represents a random error of observation, and we shall refer to them as "residuals."

For the years 1927–36 there are 9319 residuals available, but this material

* We avoid the term "most probable value" as there are difficulties in its use.

cannot be considered all together, because there is evidence that the probable error of an observation is increasing during the years in question. We have therefore first divided the residuals in two separate groups, containing the years 1927–31 and 1932–36. The justification for the analysis of the data in two large groups without further subdivision will be given later.

In Table I we give the residuals in full for the two periods, as we believe that this is the largest series of residuals yet examined. r denotes the value of the residual in units of 0″·01 and n the number of such residuals, n_1 for the period 1927–31, and n_2 for 1932–36. The asymmetry is not great, and is assumed to be accidental. The figures for positive and negative residuals have therefore been combined and smoothed by using Spencer's Formula.* These values have then been plotted and a smooth curve (A in fig. 1) drawn through them, neglecting the small waves which usually arise when data are smoothed in this way. We have also drawn the error curve (B in fig. 1), which has the same area and P.E. The general features referred to in § 1 are very clearly shown. In fig. 1 the curves are drawn for the period 1927–31. The other period, 1932–36, gives a somewhat more pronounced excess of large and small residuals.

Points are now chosen on the curve A, and the values of $\omega(x) = \phi'(x)/x \,.\, \phi(x)$ are found by measuring the slope of the tangent. These values of $\omega(x)$ have been plotted in fig. 2 (for the period 1927–31), and the full line represents the value of $\omega(x)$ adopted. The dotted line gives the corresponding value of $\omega(x)$ for the period 1932–36, but the plotted points all refer to the first period. The spread of the points is due to the inaccuracy of determining the gradient, but as a large number of points may be taken, a good curve can be drawn, except in the region $x < 0''{\cdot}15$ and $x > 0''{\cdot}70$. In the former region the weight does not vary much, and in any case a small change in weight produces only a second-order change in the value of the weighted mean residual. A more accurate method of determining the weights in the region $x > 0''{\cdot}70$ would be to draw parabolas through about 15 consecutive points and use the slope of the parabola at the middle ordinate. This, however, is a refinement which has a completely negligible effect on the result.

Strictly speaking, the weights found in fig. 2 are a first approximation. They should be used to find a better value for the variation of latitude, and then the new set of residuals (*i.e.* using the new value for the latitude) should be analysed to yield a second approximation to the best weights. Actually the first approximation is entirely adequate for our purposes.

To test the change made by reweighting the residuals, we have recomputed the individual points on the curve of latitude variation for the years 1927–29 inclusive. This is shown in fig. 3. The full circles are the original values and the open ones the revised values, the size of the circle being indicative of the weight to be attached to the result. The curve represents the latitude variation adopted in the Greenwich publication quoted. No open circles have been drawn when the point has been unchanged. It will be seen that the divergence of the observed points from

* See Whittaker and Robinson, *Calculus of Observations*, 290.

TABLE I

r	n_1	n_2	r	n_1	n_2	r	n_1	n_2	r	n_1	n_2
< −100	6	15	−50	7	6	+ 1	95	101	+ 52	5	6
−100	0	0	−49	7	5	+ 2	87	90	+ 53	8	8
− 99	0	1	−48	4	5	+ 3	90	112	+ 54	4	5
− 98	0	0	−47	1	7	+ 4	90	99	+ 55	1	6
− 97	1	0	−46	6	11	+ 5	93	109	+ 56	1	6
− 96	2	1	−45	5	14	+ 6	91	98	+ 57	3	5
− 95	0	0	−44	7	15	+ 7	95	94	+ 58	5	1
− 94	0	1	−43	10	10	+ 8	80	84	+ 59	4	4
− 93	0	0	−42	7	12	+ 9	90	100	+ 60	4	5
− 92	0	0	−41	11	8	+10	83	86	+ 61	1	4
− 91	0	0	−40	10	12	+11	75	82	+ 62	0	9
− 90	1	1	−39	7	23	+12	77	89	+ 63	3	2
− 89	0	1	−38	11	20	+13	78	90	+ 64	2	4
− 88	3	2	−37	14	23	+14	65	67	+ 65	2	3
− 87	2	1	−36	15	17	+15	79	76	+ 66	1	3
− 86	1	0	−35	18	19	+16	62	51	+ 67	4	3
− 85	0	1	−34	19	22	+17	68	86	+ 68	3	1
− 84	0	0	−33	12	22	+18	55	63	+ 69	3	0
− 83	1	0	−32	21	13	+19	60	56	+ 70	1	3
− 82	2	2	−31	20	24	+20	55	46	+ 71	1	2
− 81	3	0	−30	24	29	+21	49	58	+ 72	1	1
− 80	1	2	−29	27	23	+22	39	56	+ 73	1	4
− 79	1	0	−28	26	31	+23	36	44	+ 74	0	3
− 78	1	1	−27	34	29	+24	38	43	+ 75	2	4
− 77	1	1	−26	26	39	+25	26	30	+ 76	1	2
− 76	0	1	−25	37	37	+26	22	42	+ 77	1	1
− 75	2	2	−24	36	33	+27	28	31	+ 78	0	3
− 74	1	1	−23	38	54	+28	33	42	+ 79	0	1
− 73	1	2	−22	46	41	+29	33	19	+ 80	1	4
− 72	0	1	−21	48	33	+30	29	36	+ 81	1	3
− 71	1	3	−20	49	45	+31	15	21	+ 82	1	3
− 70	0	2	−19	39	62	+32	24	26	+ 83	1	2
− 69	2	9	−18	42	62	+33	9	15	+ 84	2	3
− 68	1	3	−17	64	66	+34	17	15	+ 85	0	2
− 67	1	4	−16	57	71	+35	21	10	+ 86	0	1
− 66	0	1	−15	77	54	+36	15	11	+ 87	0	3
− 65	1	2	−14	65	88	+37	13	23	+ 88	0	2
− 64	3	3	−13	71	81	+38	12	12	+ 89	0	1
− 63	2	2	−12	76	60	+39	15	6	+ 90	3	1
− 62	0	4	−11	82	93	+40	6	12	+ 91	0	2
− 61	0	4	−10	95	76	+41	8	14	+ 92	0	4
− 60	1	0	− 9	88	98	+42	11	11	+ 93	0	1
− 59	3	2	− 8	86	102	+43	10	6	+ 94	1	2
− 58	6	6	− 7	98	90	+44	4	8	+ 95	0	0
− 57	1	2	− 6	83	93	+45	8	12	+ 96	0	1
− 56	0	2	− 5	111	97	+46	5	8	+ 97	1	2
− 55	4	5	− 4	104	99	+47	10	9	+ 98	0	0
− 54	2	5	− 3	114	108	+48	5	8	+ 99	1	0
− 53	8	5	− 2	109	114	+49	5	10	+100	1	1
− 52	3	3	− 1	107	113	+50	4	11	> +100	7	15
− 51	3	8	0	90	107	+51	7	5			

n_1 = Period 1927–1931 ; n_2 = Period 1932–1936.

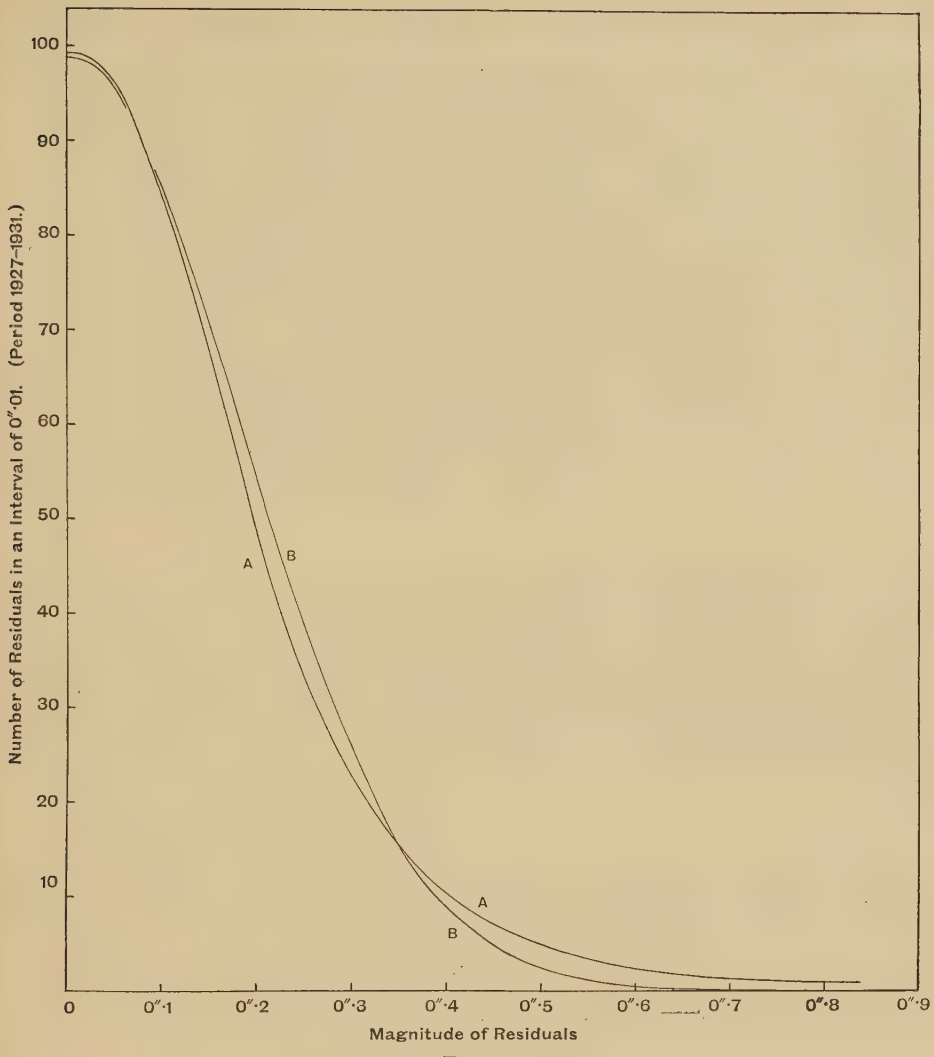
Number of Residuals in an Interval of 0″·01. (Period 1927–1931.)
100
90
80
70
60
50
40
30
20
10
A
B
A
B
0
0″·1
0″·2
0″·3
0″·4
0″·5
0″·6
0″·7
0″·8
0″·9
Magnitude of Residuals

FIG. 1.

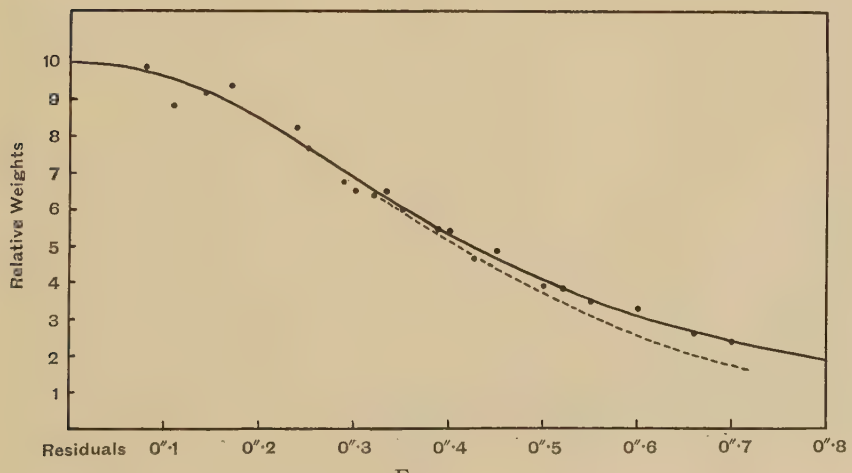
Relative Weights
10
9
8
7
6
5
4
3
2
1
Residuals
0″·1
0″·2
0″·3
0″·4
0″·5
0″·6
0″·7
0″·8

FIG. 2.

the curve is decreased in those cases when it is possible to say that the observed value is definitely too high or too low. The method of weighting therefore improves the results, and is at the same time more satisfactory than a simple rejection of those observations yielding a residual greater than a more or less arbitrary multiple of the probable error.

It is still necessary to justify the analysis of the data in two large groups, despite the fact that the probable error of an observation is increasing with time. As we have seen in the first paragraph, any distribution of the type given by equation (1) yields a curve of the type A (fig. 1). Hence a normal distribution whose parameter is a function of the time is of this type when the residuals over a long period are considered together. On the other

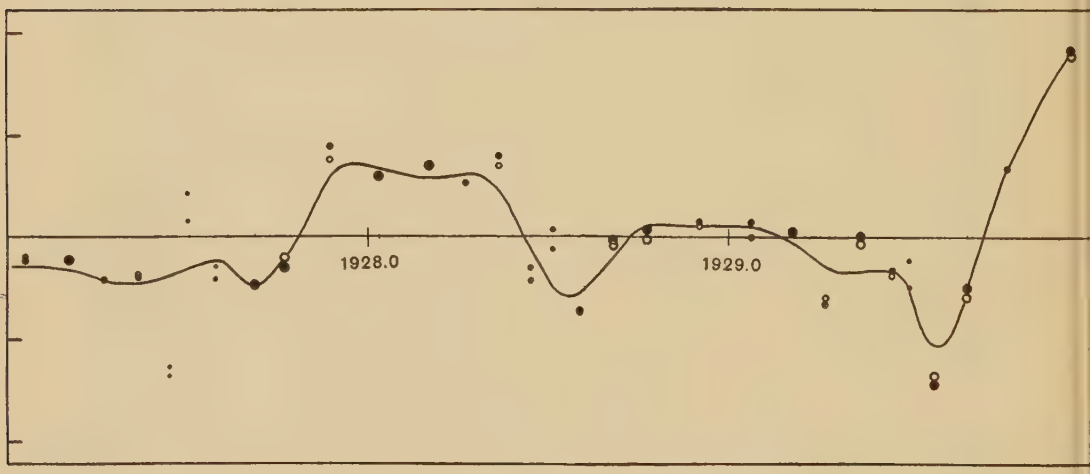

Latitude Variation 1927–1930. (Mean minus observed latitudes.)

FIG. 3.

(The divisions of the ordinate scale represent 0″·1.)

hand, for a group of observations made at the same time the distribution would be approximately normal, and the arithmetic mean would be the best result. It is easy to see, however, that only a very small part of the excess of large residuals can be due to the time variation of the probable error. The probable errors for single observations in the two groups 1927–31 and 1932–36 are 0″·124 and 0″·131, and a count of the number of residuals over 0″·60 for each year suggests that the increase is a steady one. On this assumption a simple calculation shows that the actual (steady) increase in probable error would only produce an excess of about 1 per cent. of residuals at about four times the P.E., whereas in this region the actual excess is about 100 per cent. It is clear, therefore, that each of the two groups can be treated as a whole, and that there is every reason to expect that the distribution of residuals shown in the curve of fig. 1 would apply to a small group taken during a small interval of time.

Accompanying the change in probable error there is a small change in

the weights as shown by the two curves of fig. 2. It is, however, not worth while interpolating to find appropriate weights for each year.

The method of weighting described has also been applied to the results of the measurement of parallax. The residuals taken from the Greenwich publication, *Observations of Stellar Parallax*, vol. ii, have been analysed as described. Only those were included to which the observer gave full weight after examining the plate. The set comprises 5753 observations. The curve of residuals shows the same general features as the curve A of fig. 1, though not to such a marked degree, presumably because of the careful selection of the plates to which full weight is given. The probable error of these is 0″·025, and the weight $\omega(x)$, as determined by the method described, drops from unity to 0·6 for an observation with an error of 0″·10.

The authors' thanks are due to Prof. R. A. Fisher and Dr. H. Jeffreys for opportunities of discussing the subject-matter.

Summary

The normal law of errors is not well founded, either experimentally or theoretically, and does not offer any really satisfactory criterion for the rejection of large observations. Following Newcomb and Jeffreys, a method is developed which allows a system of continuous weighting to be found for a series of observations. This is applied to the results of the latitude observations at Greenwich with a small but definite improvement of the results.

Royal Observatory,
Greenwich.

ON THE INTERPRETATION OF THE SPECTROSCOPICALLY OBSERVED ROTATIONS OF GALAXIES

Erik Holmberg

(Communicated by the Astronomer Royal)

I.—*Observations of Spectroscopic Rotation*

1. A great deal of observational work has been done on the spectroscopic rotation of extragalactic objects. During the last ten years the rotational effects to be found within our own galactic system have been very much discussed. However, the first definite evidence of rotation was found, not in our own system, but in external galaxies. The first spectroscopic observations of the rotation of a spiral object were performed by V. M. Slipher * in 1914. Later on evidence has been obtained by Slipher, F. G. Pease †, M. Wolf ‡ and H. W. Babcock §, for the rotations of several galaxies.

According to Slipher, rotations have been definitely established for six objects. These are N.G.C. 221, 224, 1068, 2683, 3623 and 4594. Measurements of the rotations represent extremely difficult work. In general Slipher gives no numerical values of the rotational change of radial velocity. The present paper is intended as a contribution to the interpretation of the observed spectroscopic rotations. When numerical values become accessible for the above six objects it will be possible to enlarge considerably the material of the present investigation.

Very detailed informations about spectroscopic rotation are given by Pease for the two objects N.G.C. 224 and N.G.C. 4594. The rotational change of radial velocity is measured along the major axis at different distances from the centre of the object. For the Andromeda spiral the rotation is determined along the minor axis, too. For both objects the measurements extend over an interval of about $2'{\cdot}5$ on each side of the centre.

The measurements of Babcock refer to the Andromeda spiral. They extend over the very large interval of $30'$ on each side of the centre of the system. Within the central core the observed rotation agrees with that found by Pease.

2. In this connection the largest interest lies in the relation found between radial velocity and distance from the centre of the object. The above measurements by Pease result in a *linear* relation. This means that the observed angular velocity of rotation is about the same at different distances from the centre. For N.G.C. 224 the rotational change of radial velocity amounts to about 29 km./sec. per $1'$, whereas a value of 167 km./sec. per $1'$ is found for N.G.C. 4594.

It is true that the measurements by Babcock show that the above linear

* *Lowell Bull. II*, 65, 1914.
† Cf. *Handb. d. Astroph.*, V, **2**, 851, 1933.
‡ See *Upsala Medd.*, **40**, 1928.
§ *P.A.S.P.*, **50**, 174, 1938.

relation does not hold at greater distances from the centre of the system N.G.C. 224. The velocity seems to fall off outside 4′ from the centre, reaching zero at a distance of 10′. Then the velocity increases again and maintains a constant value from 22′ to 30′.

However, the central part of N.G.C. 224 and the whole system N.G.C. 4594 seem to rotate with a constant angular velocity. At first thought this may seem somewhat surprising since a rotation of this kind apparently does not agree with the classical theory of gravitation. There have been several attempts to find a solution of this problem. First, it has been suggested * that, in this case, the law of Newton should be replaced by some other law of attraction. Secondly, it has been pointed out that it is possible to explain the constancy of the angular velocity by the assumption of a constant mass density. However, the large increase of surface brightness that is generally found towards the centre of a spiral object must indicate a correspondingly large increase of mass density. Finally a third explanation has been put forward. According to F. Zwicky †, the internal gravitational viscosity of the system must be taken into consideration. It may be possible to assume such a high value for this viscosity that the system, as regards rotation, will behave like a solid body.

In the present paper it will be shown that it is possible to explain (wholly or partially) the linear increase of the observed radial velocity in a fourth way. It seems as if, in previous discussions of this subject, too little attention has been paid to the relation between observed radial velocity and corresponding orbital velocity. In general, the latter velocity has, without any comments, been put equal to the former one. This is not always correct. By studying the problem more closely we will find that the two velocities are not always the same and that the relation between them is of a rather complicated nature. The relation will be dependent on the distributions of light and absorption within the system (or the nucleus).

The present paper is not intended to give a complete discussion of the dynamics of a spiral object. In order to try to find the above relation between orbital and radial velocity it seems sufficient to start from a simplified model of a spiral. Thus we will start from the assumption that all parts of the object move, in the same direction, in circular orbits according to Newton's law of attraction. Further, we will assume that the internal gravitational viscosity can be neglected. The latter assumption is made since we want to prove that it is possible to explain a linear increase of the observed radial velocity without the help of any viscosity.

II.—*Relation between Orbital Velocity and Observed Spectroscopic Rotation*

3. In the following pages we will try to find the relation between observed spectroscopic rotation and corresponding orbital velocity, *i.e.* the velocity of the orbital motion of a component element around the centre of the galaxy.

* *Cf.* H. D. Curtis, *Handb. d. Astroph.*, V, 2, 852, 1933.
† *Ap. J.*, 86, 217, 1937.

We will start from the simplified model described above, and Newton's law will be accepted to represent the gravitation.

In order to be able to find the radial component of the orbital motion we first have to make some assumption regarding the general form of the

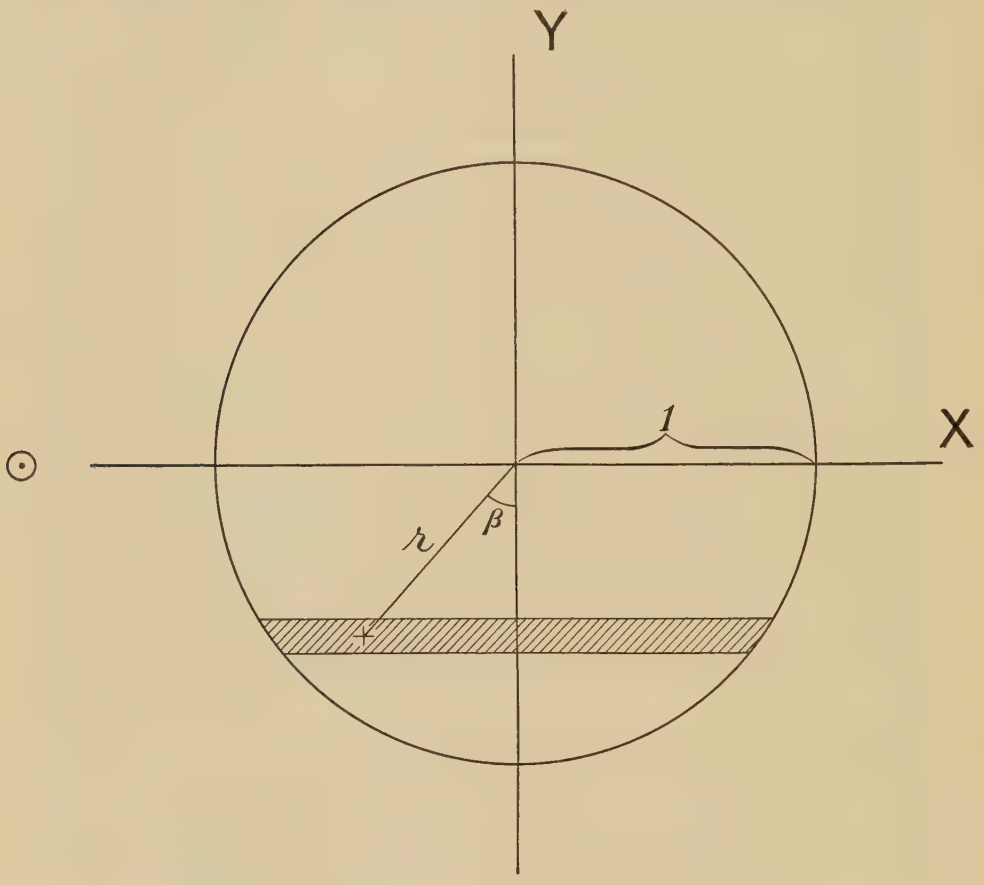

FIG. 1.—*Schematic representation of the nucleus of a spiral.*

nucleus of a spiral. The measurements of spectroscopic rotation generally refer to the condensed nuclear regions. It seems, in general, very reasonable to compare the nucleus of a spiral to an oblate spheroid. Thus two of the axes, which are situated in the principal plane of the galaxy, will be of the same size. As regards the relative size of the third axis we will refer to some investigations by C. G. Danver * concerning the forms of arms and nuclei of spiral objects. It appears that the ratio of minor and major axis is, on an average, equal to 0·5. Thus the oblateness of the nuclei is, in general, not very large. In the following discussion we will, for the sake of simplicity, start from the assumption of spherical nuclei. However, possible errors introduced by this assumption will be considered later.

In fig. 1 the circle represents the nucleus of a spiral. The plane of the

* *V.J.S.*, **72**, Heft 4 ; *Lund Medd.*, I, No. 147, 1937, and unpublished papers.

figure is assumed to coincide with the principal plane of the object. The radius of the circle is put equal to unity. We have introduced a system of co-ordinates, x and y. The x-axis is assumed to coincide with the line of sight. In reality, the inclinations of the objects towards the line of sight are never exactly zero. However, small deviations of this kind are of little importance for the following discussion.

Now we are able to find the radial velocity, v_y, corresponding to a certain distance y from the centre of the nucleus. Evidently we have to make an integration over all values x of the radial components of the orbital motions. The interval of integration is represented by the dark area in fig. 1. According to Newton's law the circular orbital velocity of a component element is proportional to $\sqrt{\mu_r}/\sqrt{r}$. Here μ_r means the total mass within a distance r from the centre of the object. Consequently the observed radial velocity can be schematically expressed as follows :—

$$v_y = \int_{-x'}^{+x'} dx \frac{\sqrt{\mu_r}}{\sqrt{r}} \cos\beta. \qquad (1)$$

The projection angle β is defined in fig. 1. For the sake of convenience the integration limit $\sqrt{1-y^2}$ is denoted by x'.

4. Before proceeding further we have to introduce some denotations for the distributions of mass, light and absorption within the nucleus. By performing the integration of formula (1) we should evidently give every volume element a weight proportional to the amount of light emitted from it. On the other hand, we have also to consider the absorption effects to be found within the nucleus. The final weight should be proportional to the amount of light that really reaches the instrument of the observer. The following denotations will be introduced :—

distribution of mass $= f(x, y, z)$,
,, ,, light $= \phi(x, y, z)$,
,, ,, absorption $= \psi(x, y, z)$.

The function $\psi(x, y, z)$ represents the optical density at the point x, y, z, *i.e.* the relative loss of light per unit of length for light passing this point.

Formula (1) will now have the following appearance :—

$$v_y = C \cdot \int_{-x'}^{+x'} dx \cdot \frac{y}{(x^2+y^2)^{3/4}} \cdot \left[\int_{S_r} f(x, y, z)\,dx\,dy\,dz\right]^{1/2} \cdot \phi(x, y, 0) \cdot e^{-\int_{-x'}^{x} dx \,.\, \psi(x, y, 0)}. \qquad (2)$$

The first factor within the integration sign represents the quantity $\cos\beta/\sqrt{r}$ given in formula (1). The second factor represents the square root of the mass μ_r. The denotation S_r implies that the integration should be performed within a sphere of radius r. The last factor within the integration sign, or the absorption factor, gives the relative size of the part of the light $\phi(x, y, 0)$ that really reaches the observer. For the derivation of this factor we beg to refer to a previous paper * by the present writer. Finally we will

* *Lund Ann.*, **6**, 73, 1937.

consider the factor C. In fact this factor should be expressed as follows :—

$$1/C = C' \cdot \int_{-x'}^{+x'} dx \cdot \phi(x, y, 0) \cdot e^{-\int_{-x'}^{x} dx \cdot \psi(x, y, 0)}.$$

The value of the constant C' depends on the units used for mass, distance and time.

In order to be able to solve the above integral we have to make some assumptions regarding the three distribution functions $f(x, y, z)$, $\phi(x, y, z)$ and $\psi(x, y, z)$. It seems very reasonable to start from the supposition that the three functions have the same form. The simplest assumption to be made is that every function can be replaced by a constant. However, this assumption does not agree with observational facts. Within the nucleus of a spiral there is always a very large concentration of light towards the centre. Thus, three normal functions may represent a better approximation. In the following discussion two different assumptions will be made. For the sake of completeness we will first assume the three distribution functions to be constants, secondly we will start from normal functions. By comparing the final results we will be able to decide in how far the derived radial velocities are dependent on the forms of the three distributions. Sometimes the concentration of mass towards the centre of the nucleus may be larger than that corresponding to a normal distribution. However, it will be possible to take this into account by combining the results corresponding to normal, or constant, distribution with the results corresponding to the assumption of a constant central mass to be discussed below.

Before proceeding further we will mention the possibility of a *constant central mass*. This means that the mass μ_r is independent of the radius r. This possibility may occur if the spectroscopic rotation is determined for the outer parts of a spiral having a large and bright nucleus. Thus the mass factor contained in the integral expression of formula (2) should be replaced by a constant. Since the case of a constant central mass seems to be of a certain interest it will be included in the following solutions.

5. According to the above discussion we will start from the following assumptions :—

$$\left.\begin{aligned} f(x, y, z) &= f, \\ \phi(x, y, z) &= 1, \\ \psi(x, y, z) &= a. \end{aligned}\right\} \qquad (3)$$

The mass factor of formula (2) will have the following appearance :—

$$\int_{S_r} f(x, y, z)\, dxdydz = f \cdot 4/3\pi(x^2+y^2)^{3/2}.$$

The absorption factor can be expressed in the following simple way :—

$$e^{-\int_{-x'}^{x} dx \cdot \psi(x, y, 0)} = e^{-a(x+x')}.$$

At this point we will try to find the meaning of the absorption constant a.

Let us introduce the total absorption Δm from the centre of the nucleus to the edge. The latter absorption can be expressed as follows :—

$$\Delta m = 1{\cdot}09 \int_{-1}^{0} dx \,.\, \psi(x, 0, 0) = 1{\cdot}09a.$$

Thus it is possible to express the quantity a by means of the total absorption Δm.

Now we will return to formula (2). By means of the above assumptions it is possible to perform a solution of the integral expression of this formula. If the mass factor is included, a theoretical solution is possible. If we assume a constant central mass, a mechanical integration must be performed.

Let us first consider the assumption of a constant central mass. The solution is given in fig. 2. Here the distance, y, from the centre of the nucleus is introduced as abscissa, whereas the velocity quotient v_y/v_1 is given as ordinate. The velocity v_1 means the value of v_y for $y = 1$, *i.e.* the observed spectroscopic rotation for the edge of the nucleus. The different curves of the figure correspond to different values of the absorption Δm, *i.e.* the total absorption from the centre of the nucleus to the edge. The values of Δm range from 0^m to ∞. For Δm equal to 0^m the value of v_y increases very rapidly when the abscissa value changes from 0·0 to 0·1 or 0·2, whereas it is comparatively constant for larger values of y. As the absorption assumes larger values the curves approach more and more to a straight line. For $\Delta m = \infty$ the relation is represented by the straight line.

If the mass factor is included in the integral of formula (2) a theoretical solution is possible, as was pointed out above. The solution is, in this case, independent of the absorption within the nucleus. For all values of Δm the relation between v_y/v_1 and y is represented by the straight line of fig. 2. Thus the radial velocity v_y is always strictly proportional to the distance from the centre of the nucleus.

6. Now we will pass on to the other assumption to be made regarding the distributions of mass, light and absorption within the nucleus. Let us start from the following normal functions :—

$$\left.\begin{aligned} f(x, y, z) &= f \,.\, D(x, y, z), \\ \phi(x, y, z) &= D(x, y, z), \\ \psi(x, y, z) &= a \,.\, D(x, y, z), \\ D(x, y, z) &= \frac{1}{\sigma_1\sigma_2\sigma_3 \,.\, (2\pi)^{3/2}} e^{-\frac{x^2}{2\sigma_1^2} - \frac{y^2}{2\sigma_2^2} - \frac{z^2}{2\sigma_3^2}}. \end{aligned}\right\} \qquad (4)$$

Here σ_1, σ_2 and σ_3 mean the dispersions of x, y and z respectively. Theoretically the value of the function $D(x, y, z)$ is zero only for infinite values of x, y or z. In this case it is, for practical reasons, necessary to cut off the distribution somewhere. In the following derivations we will put the dispersions equal to 0·5. Since the semi-major axis of the nucleus is, according to fig. 1, equal to 1·0, this means that the value of $D(x, y, z)$ should be equal to zero for all values of the variables larger than twice the corresponding dispersion.

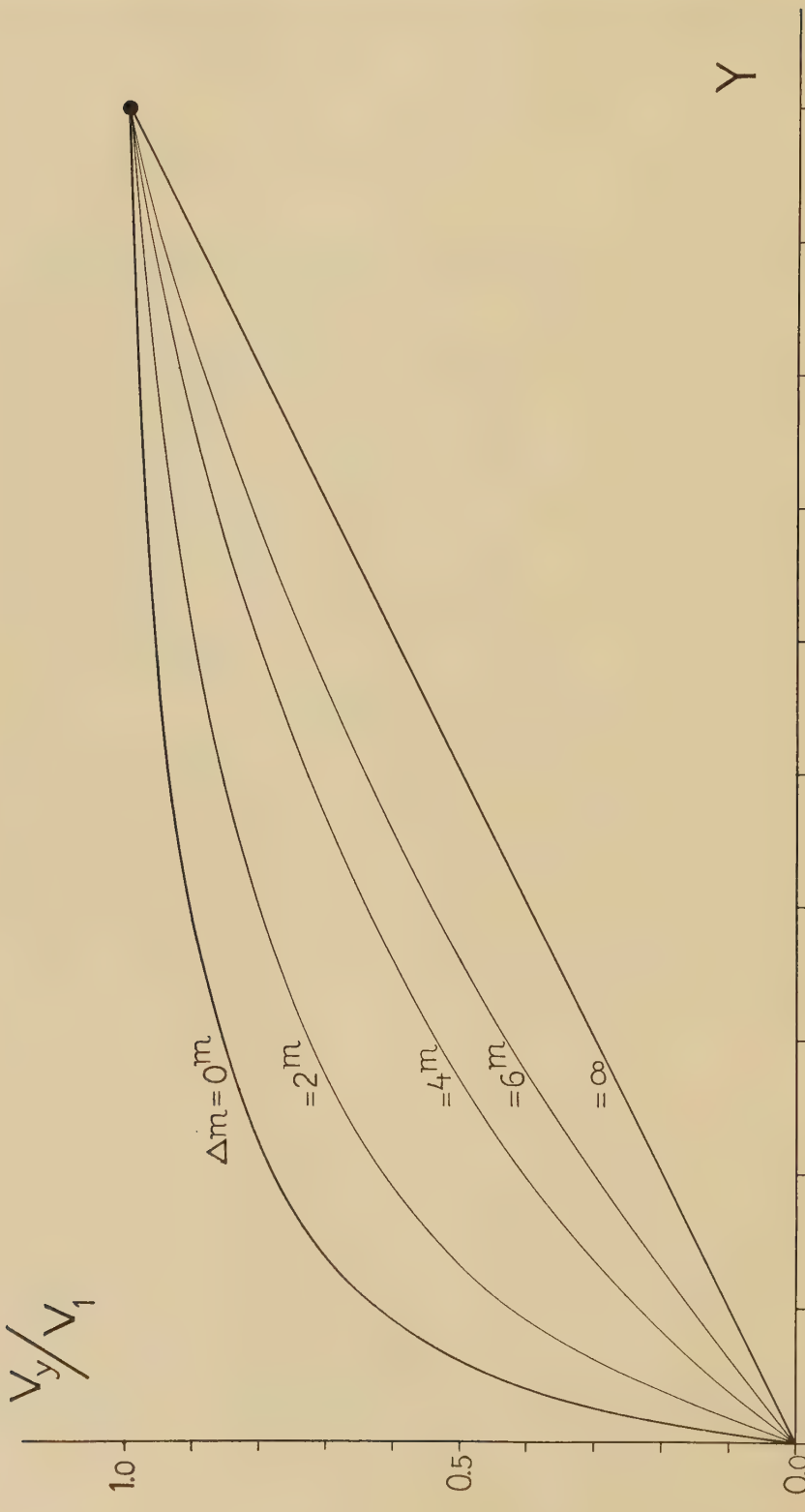

FIG. 2.—*Rotational change of radial velocity corresponding to constant central mass and to constant distributions of light and absorption.*

The mass factor of formula (2) will have the following appearance :—

$$\int_{S_r} f(x, y, z)\, dxdydz = 2{\cdot}70f\left[P(r) - \frac{2r}{\sqrt{2\pi}} e^{-2r^2}\right]$$

$$P(r) = \int_0^r \frac{2dr}{\sqrt{2\pi}} e^{-2r^2}.$$

The absorption factor can be expressed in the following way :—

$$e^{-\int_{-x'}^{x} dx\,.\,\psi(x, y, 0)} = e^{-\frac{4a}{2\pi}\,.\,Q(x)\,.\,e^{-2y^2}}$$

$$Q(x) = \int_{-x'}^{x} \frac{2dx}{\sqrt{2\pi}} e^{-2x^2}.$$

The total absorption Δm from the centre of the nucleus to the edge will have the following value :—

$$\Delta m = 1{\cdot}09 \int_{-1}^{0} dx\,.\,\psi(x, 0, 0) = 0{\cdot}33a.$$

Having derived the above expressions for mass and absorption factors we now go back to our primary formula (2). In this case it is, of course, not possible to get any theoretical solutions of the integral expression. We have to perform mechanical integrations and this involves a great deal of computation. As before, the integrations will be performed first with the mass factor included and secondly without this factor. The latter case corresponds to the assumption of a constant central mass.

Let us begin with the assumption of a constant central mass. The solutions are given in fig. 3. The different curves correspond to different values of the absorption Δm, this absorption ranging from 0^m to ∞. As the absorption gets larger the curves approach more and more to the straight line corresponding to infinite values of the absorption.

If the mass factor is included in formula (2) the solutions will be different. They are given in fig. 4. When the absorption Δm is equal to zero the solution is represented by a slightly curved line. For larger values of the absorption the curves gradually approach a straight line.

7. Before entering into a discussion of the solutions given of the integral equation (2) we will go back to the assumption made above about the outer form of the nuclei of spiral objects. It was assumed, for the sake of simplicity that the nucleus of a spiral could be represented by a sphere. At the same time it was pointed out that a nucleus is, in general, to be compared with an oblate spheroid, the oblateness having a value of about 0·5. If the sphere used in the above derivations is replaced by this oblate spheroid, how large an effect will this have on the solutions of the integral equation (2)?

It may be remarked at once that the exchange of an oblate nucleus for a spherical one will have no effect on those solutions corresponding to the assumption of a constant central mass. If there is no constant central mass the effect will be small if a normal distribution of mass is assumed, whereas it will be somewhat larger if the mass density is assumed to have a constant

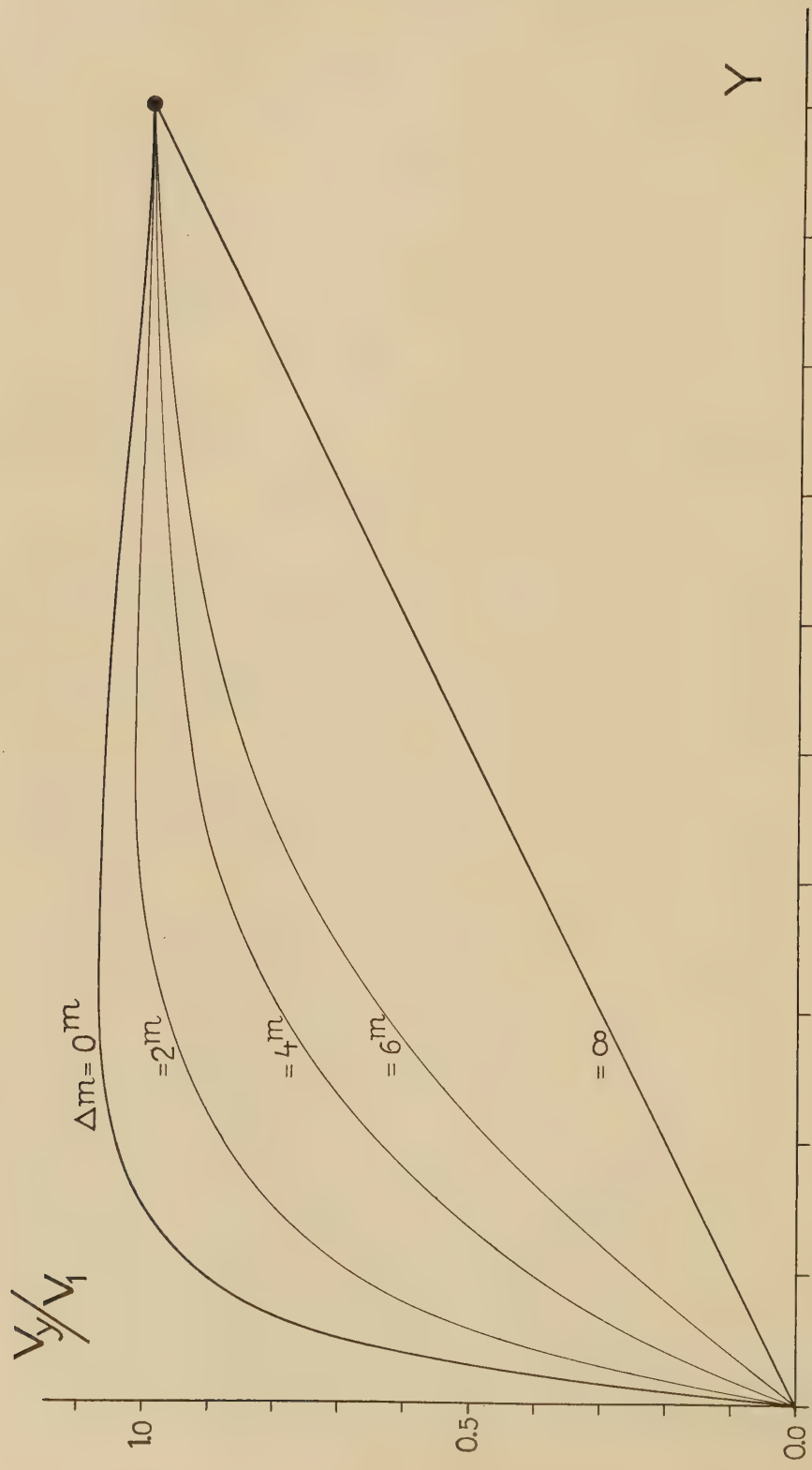

FIG. 3.—*Rotational change of radial velocity corresponding to constant central mass and to normal distributions of light and absorption.*

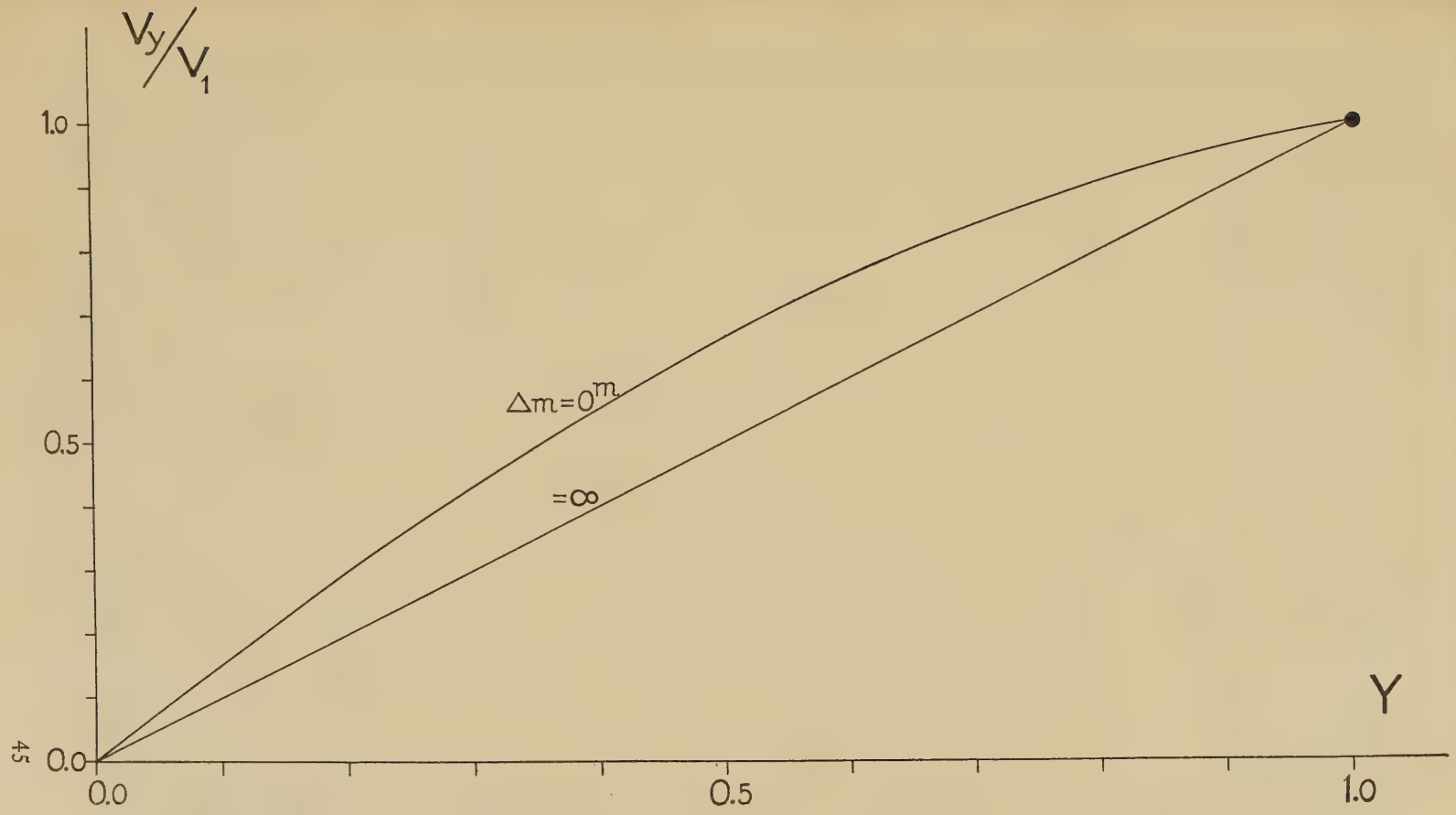

FIG. 4.—*Rotational change of radial velocity corresponding to normal distributions of mass, light and absorption.*

value. The largest deviations in the radial velocity defined in equation (2) will be found if we consider a particle situated at the edge of the nucleus.

Let us denote the mass of a spherical nucleus having constant mass density by M. The mass of a corresponding spheroid (semi-major axis = sphere's radius) with an oblateness of 0·5 will then be equal to $M/2$. The gravitational force acting upon a particle at the edge of the sphere is proportional to the mass M. If we consider a particle at the edge of the spheroid the force will be proportional to the following expression :—

$$\frac{M}{2} \cdot \frac{3}{2e^3}(\text{arc sin } e - e\sqrt{1-e^2}).$$

Here e means the eccentricity of the meridian section of the spheroid. If the oblateness is equal to 0·5, the eccentricity will have a value of 0·87. Consequently the above expression will be equal to about $3/4\ M$. The radial velocity, which in this case is equal to the corresponding orbital velocity, is proportional to the square root of this quantity. Thus the exchange of the spheroid for a sphere will result in a change of the theoretically derived radial velocity amounting to about 10 per cent.

The above value of 10 per cent. represents a maximum deviation. If we consider a volume element situated nearer the centre of the nucleus the deviation will be very small or zero. The same is the case if the assumption of a constant mass density is exchanged for the assumption of a normal mass distribution. Thus the errors introduced in the above solutions of the integral equation (2) are sure to be small, and it does not seem necessary to pay any attention to them in this connection.

8. Above, two different assumptions have been made regarding the distributions of mass, light and absorption within the nucleus of a spiral object. First the distributions were replaced by constants, secondly they were represented by normal functions. Assuming a constant value of the central mass we arrived at the solutions of formula (2) that are given in fig. 2 and fig. 3. It appears that the differences between these two solutions are comparatively small. Including the mass factor we obtained two other solutions. If the above distributions are represented by normal functions, the curves corresponding to different absorptions are situated within the area limited by the two curves of fig. 4. If the distributions are represented by constants, all curves coincide with the straight line. In this case, too, we thus find a comparatively small difference between the solutions corresponding to different distribution functions.

Thus we find that the radial velocity defined by the integral expression of formula (2) is to a certain extent independent of the form assumed for the distributions of mass, light and absorption. This is of some importance. Surely the nuclei of spiral objects cannot always be represented by simple statistical models. In the present case deviations from the adopted statistical distribution functions will correspond to comparatively small changes of the theoretically derived spectroscopic rotations.

The principal purpose of the above discussion has been to find a theoretical relation between radial velocity and distance from the centre of the object.

Let us first consider the case of a constant central mass. According to fig. 2 and fig. 3 the radial velocity should continuously *increase* from the centre outwards. Those curves of fig. 3 that correspond to small absorption values represent the only exception to this rule. As the absorption has larger values the curves approach more and more the straight line corresponding to an infinite absorption.

However, the largest interest lies in those solutions of equation (2) that include the mass factor. According to fig. 4 the relation between radial velocity and distance from the centre of the nucleus can, with very good approximation, be represented by a straight line. As the absorption has larger values the relation curve approaches more and more closely the straight line. We do not know very much about the absorption within the nucleus of a spiral. However, the total absorption from the centre to the edge probably amounts to several magnitudes. Consequently the curvature of the relation line will be very small.

It appears from the above discussion that the assumption of a normal (or constant) mass distribution gives a smaller curvature of the relation line than the assumption of a constant central mass. The real mass distribution within the nucleus of a spiral object probably corresponds to a combination of these two assumptions. If the absorption has a large value the curvature of the relation line will still be comparatively small. In this connection we beg to refer to a recently published paper by B. Lindblad *, which may give some idea of the distribution of light and mass within the nucleus of a spiral. By means of photometric measurements the apparent distribution of light was determined for the central part of the Andromeda spiral. It was found that this apparent distribution could be effectively dissected into two parts, one corresponding to a homogeneous spheroid and the other to a small central sphere. If proportionality is assumed between light intensity and mass the above distribution will refer to the mass, too. However, in the above paper no attention is paid to the absorption within the nucleus. Probably this absorption is so large that photometric observations will refer only to the outer layers of the nucleus. In conclusion it seems justified to say that, for the present, it is difficult to obtain any accurate values for the *real* distributions of mass, light and absorption within the central parts of a spiral object.

Summary

Rotations have been established for several extragalactic objects by means of spectroscopic observations. The *linear* increase of observed radial velocity found for N.G.C. 4594 and the central part of N.G.C. 224 is a matter of great theoretical interest. Several attempts to explain this have been put forth, such as the assumptions of a linear law of attraction, a constant mass density, or a large internal viscosity. The present paper gives a fourth explanation. By paying due attention to the absorption within a galaxy and to the relation between observed radial velocity and corresponding orbital velocity, we find that Newton's law of attraction will result in more or less linear relations of the above kind.

* *Stockholm Medd.*, 45, 1939.

APSIDAL MOTION IN BINARY STARS (II) DISTRIBUTIONS OF DENSITY

T. E. Sterne

Introduction.—In an earlier paper * expressions were obtained for the secular motion of the apse, in the orbits of binary stars whose components were assumed to be composed of compressible fluids, for the limiting case in which the orbital period was long compared with the free harmonic periods of the components. Account was taken of the deformations due to axial rotations with angular velocities ω_1 and ω_2, and of the variations of the tidal deformations with time. Terms of an order up to but not including the tenth power of (a_i/A), where the mean radii are a_1 and a_2 and the semi-major axis of the relative orbit is A, were retained in the final results. The orbital eccentricity e entered the analysis exactly through closed expressions valid for all values of e less than unity. The motion was found to be a precession, and the results were the same as Cowling's † to his order of accuracy, which included terms of the fifth order in (a_i/A). The results were obtained in a form applicable to any stellar model, and the superficial tidal and rotational distortions were found incidentally.

It is desirable to apply the theory of the apsidal motions to eclipsing binary stars for which the motions are determinable. In this note the theory will be applied to the five eclipsing binaries Y Cygni, GL Carinæ, H.V. 7498, YY Sagittarii, and V 523 Sagittarii. For these it is believed not only that apsidal motion has been demonstrated, but also that the motions and light elements are determinable with an accuracy sufficient for quantitative applications of the theory. It is of course possible that not all of these stars are really binary systems, and that some of them contain three, or perhaps even more, components. To complex systems of this sort the simple theory already developed should not necessarily be applicable. Yet the observations themselves, of these eclipsing stars, leave little room for third bodies of appreciable mass. If the mass-luminosity relation is to be relied upon, companion bodies of appreciable mass could hardly fail to be observed. There is some evidence, based upon radial-velocity measures, for the existence of a third body in Y Cygni; the third body cannot be very massive, however, and the discussions of Redman ‡ and of Russell and Dugan § show that it would be only under rather special circumstances, involving a period of less than three months for the third body, that a third body could produce an apsidal motion, in the close pair, comparable to the motion that is actually observed. If the apsidal motion caused by the third body is small enough, the simple theory already developed

* T. E. Sterne, *M.N.*, **99**, 451, 1939, hereafter to be called "Paper I."
† *M.N.*, **98**, 734, 1938. ‡ *M.N.*, **90**, 754, 1930. § *M.N.*, **91**, 212, 1930.

should be approximately applicable. I am aware of no observational evidence tending to indicate the existence, in the other stars to be studied here, of third bodies; and certainly no assumption of their existence is required, in order to understand the observed apsidal motions. The dynamical nature of a simple binary system will, it is hoped, be shown to provide, by itself and without recourse to improbable distributions of density, an adequate explanation of the observed apsidal motions of all these stars, Y Cygni included. In this note distributions of density will be sought which could give rise to the observed apsidal motions, in the mentioned systems when they are regarded as simple binaries.

The less well-determined apsidal motions of other systems, including some to which as yet only upper limits can be assigned, will be discussed in another note; I shall postpone also, for the present, a discussion of the ellipticities.

Y Cygni.—Russell and Dugan * give for Y Cygni $(a_1/A) = (a_2/A) = 0{\cdot}20$; $P'/P = 5700$, a precession. Redman † (orbit "D") gives $e = 0{\cdot}15$, and masses $17{\cdot}4\ \odot$ and $17{\cdot}6\ \odot$ which are essentially equal. We take the rotations ω_1 and ω_2 to equal the mean orbital motion ν, and thus use equations (14*a*), (15) and (16) of Paper I; in these equations we set $m_1/m_2 = 1$. The predicted apsidal motion is not sensitive to small changes in this adopted ratio of masses. Larger values of the ω's would lead to the inference of greater degrees of concentration than we shall find, smaller values of the ω's to somewhat smaller ‡ degrees of concentration. We take the two components to have similar distributions of density, so as to make corresponding k's, for the two components, equal. By the use of equations (18), one finds that $g_2(e) = 1{\cdot}047$, $f_2(e) = 1{\cdot}158$, $f_3(e) = 1{\cdot}273$, $f_4(e) = 1{\cdot}426$. Hence by equation (17)

$$P/P' = 0{\cdot}01246k_2 + 0{\cdot}00091k_3 + 0{\cdot}00007k_4. \qquad (19)$$

Now for any stellar model at all, we can always integrate equation (5) of Paper I and find the k's; these k's inserted in equation (19) will furnish the corresponding expected rate of apsidal precession. If one considers any one-parametered family of models (for example, the family of polytropes of index n, the parameter being n), one can thus compute the rate of apsidal motion to be expected for each of several values of the parameter, and by inverse interpolation one can find what value of the parameter would correspond to the observed rate of apsidal motion. If one considers two families, A and B, it is in general true that if k_2, computed for a certain member of family A, equals k_2 for a certain member of family B, the k_3's and k_4's will nevertheless differ for the two members. It is therefore not possible to compute k_2, k_3 or k_4 (any one of which could be used to describe

* *Loc. cit.* † *Loc. cit.*

‡ Were the ω's to be zero, equation (14) shows that the expected $\dot{\varpi}_2/\nu$ would be diminished by about two parts in seventeen, while $\dot{\varpi}_3/\nu$ and $\dot{\varpi}_4/\nu$ would not be changed; the polytropic index would then have to be diminished from 3·02 to about 2·96 in order still to lead to an agreement between the expected and observed apsidal motions. The results are therefore not very sensitive to the ω's.

the degree of concentration) from the observed rate of apsidal motion, without selecting some definite family of stellar models.* The simplest procedure would appear in general to be to select some definite one-parametered family of models, and to find what value the parameter must have in order to make the predicted rate of apsidal precession (given in general by an equation of the form (19)) agree with that observed.

The family of polytropes is a suitable family, and the k's for five different values of the parameter are listed in Paper I. In the following table, the first column contains the polytropic index; the second contains the corresponding ratio of central to mean density; the third, fourth and fifth columns contain the contributions, given by the three terms in (19), to P/P' made by the spherical harmonic deformations of the second, third and fourth orders; the seventh column contains the expected ratio P'/P of the apsidal to the orbital period.

Polytropic Index	$\rho_c/\bar{\rho}$	$\dot{\varpi}_2/\nu$	$\dot{\varpi}_3/\nu$	$\dot{\varpi}_4/\nu$	P/P'	P'/P	$\log_{10}\left(\frac{P'}{P}\right)$
1	3·29	$3{\cdot}24 \times 10^{-3}$	$0{\cdot}10 \times 10^{-3}$	$0{\cdot}00 \times 10^{-3}$	$3{\cdot}34 \times 10^{-3}$	299	2·476
3/2	5·99	$1{\cdot}80 \times 10^{-3}$	$0{\cdot}05 \times 10^{-3}$	$0{\cdot}00 \times 10^{-3}$	$1{\cdot}85 \times 10^{-3}$	541	2·733
2	11·4	$9{\cdot}23 \times 10^{-4}$	$0{\cdot}22 \times 10^{-4}$	$0{\cdot}01 \times 10^{-4}$	$9{\cdot}46 \times 10^{-4}$	1057	3·024
3	54·2	$17{\cdot}94 \times 10^{-5}$	$0{\cdot}33 \times 10^{-5}$	$0{\cdot}01 \times 10^{-5}$	$18{\cdot}28 \times 10^{-5}$	5470	3·738
4	623	$16{\cdot}70 \times 10^{-6}$	$0{\cdot}22 \times 10^{-6}$	$4{\cdot}9 \times 10^{-9}$	$16{\cdot}92 \times 10^{-6}$	59100	4·772

It appears that the ratio of apsidal to orbital period is approximately proportional, in Y Cygni, to the ratio of central to mean densities. Since this approximate proportionality arises principally from the form of the dependence of k_2 upon the polytropic index, it should hold for the family of polytropes, and for all stars, whenever the (a_i/A)'s are not much larger than one-fifth and when, therefore, the first term is the most important term in the right-hand member of the appropriate equation of the form (19).

The observed value of $\log_{10}(P'/P)$ for Y Cygni is 3·756. It is found, by interpolating the last three values in the last column to differences of the second order, that Y Cygni should be expected to show the observed apsidal motion if its components are polytropes with indices of 3·02.

It is necessary to make sure that the equilibrium theory of the tides, employed in the development of Paper I, is applicable to Y Cygni; it will be applicable if the free period, T_f, corresponding to a second-order spherical harmonic deformation, is short compared to the orbital period. Emden † gives for the T_f of a polytrope in convective equilibrium

$$T_f^2 = 3\pi/2G\bar{\rho}$$

---

* On the other hand, it is highly probable, since k_3 and k_4 are if anything generally smaller than k_2, and since the successive coefficients in the right-hand members of equations of the form (19) diminish rapidly for stars showing determinable apsidal motions, that values of k_2 would not differ very much when found from different families of models applied to the same binary star.

† *Gaskugeln*, p. 451, 1907, Teubner.

in C.G.S. units. G is the constant of gravitation, and $\bar{\rho}$ is the mean density. By Kepler's third law, the orbital period is given by

$$T_0^2 = 3\pi/G[\bar{\rho}_1(a_1/A)^3 + \bar{\rho}_2(a_2/A)^3]$$

in the same units; the subscripts refer to stars 1 and 2. Hence the ratio T_f/T_0 for star 1 is given by

$$\frac{T_f^2}{T_0^2} = \frac{1}{2}\left[\left(\frac{a_1}{A}\right)^3 + \frac{\bar{\rho}_2}{\bar{\rho}_1}\left(\frac{a_2}{A}\right)^3\right], \tag{20}$$

while the ratio for star 2 is given by the same expression with the subscripts interchanged. Generally, if the right-hand member of (20) is, for both stars, small compared to unity, then one should feel considerable confidence that the theory of Paper I is applicable.* In a polytrope of index n in convective equilibrium, the effective "ratio of specific heats", γ, of the mixture of matter and radiation equals $1 + 1/n$. It is unlikely, if n equals three or more, that γ can be as small as $1 + 1/n$; and if it is greater, so that the polytrope of index n is not in convective equilibrium, the free second-order spherical harmonic period will be shorter than the value given by Emden. Emden has, moreover, ignored perturbations in gravity, and this also tends to cause his formula to overestimate the free period. Equation (20) should therefore be, if anything, on the safe side. In Y Cygni the ratio of mean densities is nearly unity, and with the values given, the right-hand member of (20) is 0·008—small enough for the theory we have used to be applicable.

Our analysis does not, of course, have anything to say as to whether or not the components of Y Cygni are polytropes; it merely shows that if the components are polytropes with the same index for each, then the observed rate of apsidal motion requires the index to be very nearly 3·02. The numerical uncertainty in this value arises chiefly from the uncertainty in the adopted value 0·20 for the relative radii of the components, which occurs to the fifth power in the most important term in P/P'; an uncertainty of one part in twenty in the adopted value 0·20 would make the index uncertain by approximately 0·12. The result, $n = 3{\cdot}02$, is not sensitive to the adopted value of the orbital eccentricity e, or to the observed ratio P'/P. A change of 10 per cent. in the observed P'/P would require a change, in the index, of only 0·05. A rough estimate of the total probable error of the index is thus $\pm$ 0·12.

GL Carinæ.—Shapley and Miss Swope † state the accurately determinable period of the apsidal precession to be 25·2 years. Since $P = 2^d{\cdot}4222$, the ratio P'/P is thus 3800. The eccentricity e is given as 0·157, and from a "uniform" solution $a_1/A = a_2/A = 0{\cdot}215$. Dr. Shapley has kindly estimated the probable error of the last value as $\pm$ 0·015. The ratio of masses should

* If the ratio of T_f/T_0 is comparable to unity, the dynamical theory of the tides would have to be used instead of the equilibrium theory of Paper I; the effect would be a rate of apsidal motion different from that given by the treatment of Paper I, and usually larger; while for values of the ratio lying between certain critical limits the apsidal motion would be a regression.

† *H.B.*, 909, 1938.

be nearly unity since the luminosities are very nearly equal. From these data it is found, by the same method as for Y Cygni, that if the components of GL Carinæ are polytropes with a common index, then the observed rate of apsidal motion demands that the index be 3·01. The probable error of this index, arising almost entirely from the uncertainty in the relative radii, is only $\pm$ 0·15. The ratio P'/P is so well determined observationally that its uncertainty does not contribute appreciably to the resultant probable error of the index, nor does the uncertainty in e. Criterion (20) shows the theory of Paper I to be applicable.

H.V. 7498.—This star is stated by Shapley and Miss Swope * to show apsidal motion. They state P to be $3^{d}\cdot471$, and assign lower limits to P' and to e of 400 years and 0·4, respectively. Mrs. Shapley has carried through a preliminary solution of the unpublished observational material for the light elements on the uniform hypothesis, and she has very kindly communicated her results to me. She finds an inclination of about 89°; that $L_1 = 0\cdot45$ and $L_2 = 0\cdot55$; and, by considering the primary eclipse as though the orbit were circular, that the relative radii $r_1' = 0\cdot136$ and $r_2' = 0\cdot113$. Since the observations cover merely a small fraction of the apsidal period P', the latter is not well determined. To determine P' as well as possible, I have made a least squares solution.

Miss Swope has very kindly supplied me, from the unpublished material, with observational values of the quantity $t_s - t_p$ at nine separate dates over a thirty-eight year interval, during which the difference has increased from 0·731 to 0·788 periods. Here t_s and t_p are the times of secondary and primary mid-eclipses. For an inclination $i = 90°$, the time interval $t_s - t_p$ can be shown to obey the exact † equation, obtained from the theory of motion in an ellipse,

$$\left.\begin{aligned}\frac{t_s - t_p}{p} - \frac{1}{2} &= \frac{1}{\pi}\left[\tan^{-1}\left(\frac{e}{(1-e^2)^{1/2}}\cos\varpi\right) + \frac{e\cos\varpi}{1 - e^2\sin^2\varpi}(1-e^2)^{1/2}\right] \\ &= f(\varpi, e),\end{aligned}\right\} \qquad (21)$$

where ϖ is the longitude of periastron, measured from the node in the direction of motion. From three of the observed time differences, at known dates, I obtained preliminary values of e, of the value ϖ_0 of ϖ at an arbitrary epoch, and of the constant time derivative $\dot{\varpi}$ of ϖ.

Differential corrections were obtained to these preliminary values e, ϖ_0 and $\dot{\varpi}$ as follows. From equation (21), and the preliminary values, values f_0 were computed for all of the dates at which f was observed. Now

$$f - f_0 = \Delta e\frac{\partial f_0}{\partial e} + \Delta\varpi\frac{\partial f_0}{\partial \varpi},$$

where Δe and $\Delta\varpi$ are the corrections to e and ϖ. Let ϖ_1 and ϖ_2 be the preliminary values of ϖ at the times t_1 and t_2 of the first and last observations of f; and let $\Delta\varpi_1$ and $\Delta\varpi_2$ be their corrections. Then at any time t the

* *H.B.*, 909, 1938.

† The equation is correct to a high accuracy for inclinations close to 90°.

correction $\Delta\varpi$ to the preliminary value of ϖ is $(1-x)\Delta\varpi_1+x\Delta\varpi_2$, where $x=(t-t_1)/(t_2-t_1)$. Thus

$$\frac{\partial f_0}{\partial e}\Delta e+(1-x)\frac{\partial f_0}{\partial \varpi}\Delta\varpi_1+x\frac{\partial f_0}{\partial \varpi}\Delta\varpi_2=f-f_0. \qquad (22)$$

The partial derivatives are best computed from the expansion, equivalent to the exact equation (21),

$$f(\varpi, e)=\frac{1}{2\pi}[4e\cos\varpi-(\tfrac{2}{3}e^3+\tfrac{1}{4}e^5)\cos 3\varpi+\tfrac{3}{20}e^5\cos 5\varpi+\ldots] \quad (21a)$$

given correctly up to terms of order e^5. Besides nine observational equations of the form (22) there was a tenth observational equation in Δe, $\Delta\varpi_1$ and $\Delta\varpi_2$ involving the observed ratio of widths of the two minima at a mean epoch. Before the tenth equation was used, its weight was carefully taken into account. A least squares solution of the ten observational equations yielded the values of the auxiliary unknowns Δe, $\Delta\varpi_1$ and $\Delta\varpi_2$; residuals were computed with the improved elements by the exact equation (21); a recomputation based on these residuals showed the first differential corrections to have been sufficient. The final values were $e=0{\cdot}506\pm 0{\cdot}018$ (p.e.), $P'=566\pm 124$ (p.e.) years; while ϖ, at the mean date of the primary light-curve from which Mrs. Shapley found the light-elements, was close to 330°. The direction of the motion is definitely a precession. It will be noticed that in the determination of the apsidal elements by least squares, no use was made of the observed deviations of the actual times of minimum from the times predicted by a uniform ephemeris; only the observed time intervals between secondary and primary minimum were employed. The latter procedure is simpler than the former, and should probably be more accurate as well.

Mrs. Shapley's values of r_1' and r_2', obtained on the circular hypothesis from the light-curve of primary eclipse, must be corrected for the effect of the large orbital eccentricity. A consideration of the nature of motion in an ellipse shows that

$$(a_i/A)=r_i'(1+e\sin\varpi)/(1-e^2)^{1/2}$$

very nearly when the (a_i/A)'s are small, and thus $a_1/A=0{\cdot}118$ and $a_2/A=0{\cdot}098$. The ratio of the L's implies a ratio $m_2/m_1=1{\cdot}08$ nearly; $P'/P=59600\pm 13100$ (p.e.). It is found from the preceding data that if $\omega_1=\omega_2=\nu$, the observed apsidal motion is that which would be caused by polytropic indices of 3·46 in the components. The probable error of this value arising from the uncertainty of P'/P is $\pm 0{\cdot}10$; that arising from the uncertainty in e is about $\pm 0{\cdot}04$; that arising from the observational uncertainty in the relative radii—for which the value $\pm 0{\cdot}02$ would be perhaps on the large side—is very approximately $\pm 0{\cdot}43$. The small uncertainty in the mass-ratio, probably close to unity, does not contribute appreciably, and thus a very rough estimate of the total probable error of the index 3·46 is about $\pm 0{\cdot}44$. The right-hand member of equation (20) is small, and our analysis should be applicable.

YY Sagittarii.—This star, of period $2^d.628$, is stated by Shapley and Miss Swope * to show apsidal motion, with a period probably greater than 300 years and an eccentricity probably larger than 0·15. It is also stated that the sense of the rotation of the apse is indeterminate, although it is later said, " . . . the rather fragmentary data of the first decade of our observations suggest that the principal minimum may then have been the wider, a result that would require a regressing line of apsides." The observational evidence for regression being very weak, and theory predicting a precession, I assume that the motion is actually a precession. The inclination of the orbit is stated to be nearly ninety degrees. Mrs. Shapley has communicated to me the results of a preliminary solution, based on the combined minima of the unpublished material, for the light elements on the uniform hypothesis. A range of solutions is possible, the extremes being $a_1/A = a_2/A = 0.127$, and $a_1/A = 0.137$, $a_2/A = 0.117$. I adopt here the former limiting solution. Then, the ratio of brightnesses being nearly unity, the ratio of masses may be taken to be unity.

Miss Swope has supplied me with observational values of the quantity f, of equations (21) and (21*a*), at nine different dates covering a forty-six year interval. The first and last values of f were -0.015 and -0.083. Preliminary values of e, ϖ_1, and ϖ_2 were corrected differentially by a least squares solution based upon nine observational equations of the form (22). The final values were $e = 0.140 \pm 0.010$ (p.e.), $P' = 282 \pm 49$ (p.e.) years. Thus $P'/P = 39200 \pm 6800$ (p.e.).

It is found from the preceding values that if $\omega_1 = \omega_2 = \nu$, the observed apsidal motion is that which would be caused by polytropic indices of 2·83 in the components. The probable error of this value is about ± 0.20. The right-hand member of (20) is small, and the analysis should be applicable. If the latter of the limiting solutions is adopted, the mass ratio becomes $m_1/m_2 = 1.14$ and the index becomes 2.84 ± 0.20 (p.e.). Thus the polytropic index is almost completely independent of the indeterminacy found by Mrs. Shapley.

V 523 Sagittarii.—This star, of period $2^d.3238$, is stated by Miss Edith Jones † to show apsidal motion, with a period greater than 120 years and an e greater than 0·15. The sense of the rotation does not appear to be determinate, although such evidence as there is tends to show that the primary minimum is narrower than the secondary, and this in turn would indicate a precession. The evidence for precession is weak, and I assume that the motion is a precession since theory predicts a precession.

In Miss Jones's paper, the phases of mid-primary and mid-secondary eclipse are given for thirteen dates covering a forty-two year interval; these yield thirteen values of the quantity f of equations (21) and (21*a*). The inclination is appreciably less than ninety degrees, rendering both (21) and (21*a*) slightly inaccurate; e, however, is not very large and one may employ the formula given by Russell ‡ which ignores terms in e^3 :

---

* *H.B.*, 909, 1938. † *H.B.*, 909, 1938. ‡ *Ap. J.*, 36, 57, 1912.

$$f(\varpi, e) = \frac{1}{\pi} e(1 + \operatorname{cosec}^2 i) \cos \varpi. \qquad (21b)$$

By the use of this equation, preliminary values of $\frac{1}{2}e(1 + \operatorname{cosec}^2 i)$, ϖ_1 and ϖ_2 were corrected differentially. Thirteen observational equations of the form (22) were solved by least squares, and furnished the values $\frac{1}{2}e(1 + \operatorname{cosec}^2 i) = 0{\cdot}179 \pm 0{\cdot}020$ (p.e.), $P' = 209 \pm 24$ (p.e.) years. Thus $P'/P = 32900 \pm 3800$ (p.e.).

Mrs. Shapley has kindly provided me with the results of a "uniform" solution, based on a combination of the light-curves of the two minima published by Miss Jones, for the light elements. The eclipses are partial, and the solution is indeterminate. One extreme limit is $i = 81°{\cdot}5$, $a_1/A = a_2/A = 0{\cdot}20$, $L_1 = L_2 = 0{\cdot}5$; the other is $i = 85°$, $a_1/A = 0{\cdot}24$, $a_2/A = 0{\cdot}15$, $L_1 = 0{\cdot}7$, $L_2 = 0{\cdot}3$. For the former limiting solution, $e = 0{\cdot}177 \pm 0{\cdot}020$ (p.e.), and the ratio of masses is unity ; if $\omega_1 = \omega_2 = \nu$, then the observed apsidal motion is that which would be caused by polytropic indices of 3·80 in the components. The probable error of this value is about $\pm 0{\cdot}23$. The right-hand member of (20) is small and the analysis should be applicable.

For the latter limiting solution, $e = 0{\cdot}178 \pm 0{\cdot}020$ (p.e.), and the ratio of masses is $m_1/m_2 = 1{\cdot}40$ nearly ; the observed apsidal motion is that which would be caused by polytropic indices of $3{\cdot}83 \pm 0{\cdot}23$ (p.e.) in the components.

I wish again to record my indebtedness to Mrs. Shapley, to Miss Swope and to Dr. Shapley.

Summary.—The theory of the apsidal motion developed in *M.N.*, **99**, 451, 1939, has been applied to the eclipsing stars Y Cygni, GL Carinæ, H.V. 7498, YY Sagittarii and V 523 Sagittarii. If these stars are binary systems, then they should be expected to show the observed apsidal motions if their components are polytropes with indices of $3{\cdot}02 \pm 0{\cdot}12$, $3{\cdot}01 \pm 0{\cdot}15$, $3{\cdot}46 \pm 0{\cdot}44$, $2{\cdot}83 \pm 0{\cdot}20$ and $3{\cdot}80 \pm 0{\cdot}23$ respectively. The probable errors that are assigned to these indices are rough values, based upon the estimated accuracies of the quantities from which the indices have been determined.

Harvard College Observatory :
1939 May 22.

APSIDAL MOTION IN BINARY STARS
(III) LIMITING RATIOS OF CENTRAL TO MEAN DENSITY

T. E. Sterne

Introduction.—It is apparent from the discussions of Papers I and II * that one cannot, from a knowledge of the orbital and light elements, and of the apsidal motion, infer uniquely the value of the ratio of central to mean density of an eclipsing binary star. It is necessary to select some definite family of stellar models (in Paper II the family of polytropes was chosen); if one supposes that the components are constructed according to some member of this family, it is then possible, from the known data, to find which member of the family it must be. Corresponding to that member, there is always a certain ratio C of central to mean density, but in general the value of C, found for a given eclipsing star, depends upon what family was chosen.

In this note we shall show that it is possible to determine observationally a lower limit to the ratio of central to mean density, in the more concentrated component of an eclipsing binary star. No appeal is necessary to the theory of the internal constitution; nor is any assumption made, concerning the nature of the stellar model, other than that the density is not to increase outwards. Lower limits of the ratio will be found for Y Cygni, GL Carinæ, H.V. 7498, YY Sagittarii and V 523 Sagittarii.

The Generalized Roche Model.—Consider either component of a binary star, and let its mass, its radius, and therefore its mean density, be fixed. Let one further specify that the central density is to have some definite value, greater than or equal to the mean density, and that the density is not to increase outwards. Consider all possible distributions of the matter, within the volume of the star, consistent with these conditions. Now any transfer of matter inwards must decrease the rate of apsidal motion, for the transferred matter moves into a region of smaller oblateness, and its approach (even at constant oblateness) to the centre would be enough by itself to diminish the apsidal motion. Since the density is not to increase outwards, the slowest apsidal motion is obtained when all the matter is collected into a sphere † of uniform density, equal to the central density, about the centre; with an infinitesimal density extending from the surface of this sphere to that of the star. This distribution of matter may be called ‡ the "generalized Roche model", and leads one to consider the family of generalized Roche models. The members of the family may be specified by the value of the

* *M.N.*, **99**, 451, 1939; **99**, 662, 1939.

† . . . in the undisturbed state; in the disturbed state it would not of course be spherical.

‡ See Jeans, *Astronomy and Cosmogony*, 255, 1929. Jeans specifies that the nucleus is to be incompressible; we of course do not need to.

parameter x, the radius of the nucleus divided by that of the star, or alternatively by C, evidently equal to $1/x^3$. Members of the family have the property that with the sizes, masses, axial rotations and orbital elements of the components of any particular eclipsing star, they yield slower apsidal motions than do all other models, having the same C's, in which the density does not increase outwards.

If, using the family of generalized Roche models, one repeats the analyses of Paper II, one obtains values of C that are lower limits to the actual values. Any other models, with densities not increasing outwards, must lead with the same C's to apsidal motions more rapid than those observed; and hence, to secure agreement, their C's must be made larger than the C's computed from the generalized Roche model. In carrying out the analyses, one supposes that the two components correspond to the same model; if one is in fact more highly concentrated than the other, its C must be larger than the C computed for both on the assumption of equality; hence the C computed by the methods of Paper II, but on the basis of the generalized Roche model, is a lower limit to the C of the more highly concentrated component.

We compute the k's of the generalized Roche model.

The k's of the Generalized Roche Model.—It is seen that in equation (5) of Paper I, the distance, r, from the centre may be measured in any units whatever; for convenience, therefore, one may take the radius to be unity. The quantity ρ/ρ_m is evidently unity when $r < x$, and zero when $r > x$. When $n=2$, equation (5) thus becomes

$$r\frac{d\eta_2}{dr}+\eta_2^2+5\eta_2=0, \qquad r<x;$$

$$r\frac{d\eta_2}{dr}+\eta_2^2-\eta_2-6=0, \qquad x<r<1;$$

subject to the boundary conditions that $\eta_2=0$ at $r=0$, and that η_2 is continuous * at the interface. The solution is

$$\eta_2=0, \qquad r<x;$$
$$\eta_2=6(r^5-x^5)/(2+3x^5), \qquad x<r<1.$$

At the surface, therefore, η_2 has the value $6(1-x^5)/(2+3x^5)$, and thus $k_2=3x^5/4$. One can solve (5) similarly when $n=3$ and $n=4$, and one finds, in terms of the parameter C,

$$\left.\begin{aligned} k_2&=(3/4)C^{-5/3},\\ k_3&=(3/8)C^{-7/3},\\ \text{and}\qquad k_4&=(1/4)C^{-3}. \end{aligned}\right\} \tag{23}$$

As a check, one notices that when $C=1$, the k's are obtained for the homogeneous model, as given in Paper I.

* Y, of Paper I, is continuous; hence η_2, by its definition, is finite, and hence, by (5), continuous.

Results.—When one repeats the analyses of Paper II, using the same data but on the basis of the generalized Roche model, one finds for Y Cygni that $C = 10{\cdot}9 \pm 1{\cdot}6$; for GL Carinæ that $C = 10{\cdot}7 \pm 2{\cdot}2$; for H.V. 7498 that $C = 20 \pm 12$; for YY Sagittarii that $C = 8{\cdot}8 \pm 2{\cdot}3$ with the first limiting set of light elements and $C = 8{\cdot}9 \pm 2{\cdot}3$ with the second; for V 523 Sagittarii that $C = 32 \pm 10$ with the first limiting solution and $C = 34 \pm 10$ with the second. The probable errors that are assigned to the C's are rough values, based upon the estimated accuracies of the quantities from which the C's have been determined.

It is likely that these C's are not only lower limits to the actual ratios of central to mean density, but are in fact very much smaller. The generalized Roche model, if composed of compressible fluid, is convectively unstable and should not be able to exist. It is nevertheless of interest to observe what lower limits to the ratios of central to mean density may be inferred from the observed apsidal motions, without either any appeal to the theory of the internal constitution, or any assumption, concerning the nature of the stellar models, other than that the densities are not to increase outwards.

It is a pleasure to acknowledge the opportunity that I have had for discussing this problem with Professor Russell.

Summary.—A lower limit to the ratio of central to mean density, in the more concentrated component of an eclipsing binary star, may be inferred from the observed apsidal motion. This lower limit may be observationally determined, without any appeal to the theory of the internal constitution, and without making any assumption, concerning the nature of the stellar model, other than that the density is not to increase outwards. The lower limits thus found have for Y Cygni, GL Carinæ, H.V. 7498, YY Sagittarii and V 523 Sagittarii the values $10{\cdot}9 \pm 1{\cdot}6$, $10{\cdot}7 \pm 2{\cdot}2$, 20 ± 12, $8{\cdot}8 \pm 2{\cdot}3$ and 32 ± 10 respectively. The probable errors are rough values, based upon the estimated accuracies of the quantities from which the lower limits have been determined. It is probable that the lower limits are considerably smaller than the actual ratios.

Harvard College Observatory:
1939 *June* 2.

THE MINIMUM CENTRAL TEMPERATURE OF A GASEOUS STAR

S. Chandrasekhar

1. This paper is devoted to the consideration of the following problem :—

What is the minimum central temperature T_c for a gaseous star of a given mass M and radius R in which the density ρ and the temperature T are both assumed not to increase outward?

In solving this problem we shall further assume that the mean molecular weight μ is a constant throughout the entire configuration. It is clear from dimensional considerations that we should have a relation of the form

$$(T_c)_{\min} = \tfrac{1}{2} Q(M\mu^2) \frac{\mu H}{k} \frac{GM}{R}, \tag{1}$$

where Q is a dimensionless quantity depending on $M\mu^2$ only. The problem we are to consider is essentially one of specifying the function $Q(M\mu^2)$.

2. The mathematical problem that is presented can be formulated as follows :—

Since the configuration is one of equilibrium we have, in a standard notation,

$$\frac{dP}{dr} = -\frac{GM(r)}{r^2}\rho, \tag{2}$$

and

$$\frac{dM(r)}{dr} = 4\pi r^2 \rho. \tag{3}$$

For a gaseous star, which is the case under consideration,

$$P = \frac{k}{\mu H}\rho T + \tfrac{1}{3} a T^4, \tag{4}$$

where H is the mass of the proton and the other symbols have their usual meanings. We regard equation (4) as giving T implicitly as a function of P and ρ :

$$T \equiv T(P, \rho). \tag{5}$$

According to our assumption, $T(P, \rho)$ and ρ both do not increase outward. The problem is to find the minimum value of $T_c \equiv T(P_c, \rho_c)$ for an equilibrium configuration of assigned mass and radius. The problem, when formulated in this manner is seen to be a special case of the following more general problem :—

Consider an arbitrary continuous function $K(P, \rho)$, $(P, \rho \geqslant 0)$. Let us assume that K and ρ both do not increase outward. What is the minimum

value of $K_c \equiv K(P_c, \rho_c)$ for an equilibrium configuration of a given mass M and radius R? With suitable restrictions on $K(P, \rho)$ we can solve this problem. We shall prove :

Theorem.—If $K(P, \rho)$ be an arbitrary continuous function in the variables P and ρ such that

$$2P\frac{\partial K}{\partial P} + \rho\frac{\partial K}{\partial \rho} > 0, \tag{6}$$

and

$$\frac{\partial K}{\partial P} > 0, \tag{7}$$

then in any equilibrium configuration in which both $K(P, \rho)$ and ρ do not increase outward, the minimum value of $K_c \equiv K(P_c, \rho_c)$ is attained in the sequence of equilibrium configurations which consist of cores of constant K and homogeneous envelopes.

It will be noticed that the special case of the above theorem which arises when K has the form

$$K = P/\rho^{(n+1)/n} \tag{8}$$

has already been proved by the author.* The condition (6) on K is now readily seen to be equivalent to the restriction $n > 1$ which was imposed in proving the special case (cf., *loc. cit.*). We shall verify in paragraph 3 that the function $T(P, \rho)$ [implicitly defined by equation (4)] satisfies the conditions of the theorem.

The proof of the theorem depends on the following lemma :—

Lemma.—In the configuration in which K_c attains the minimum, either $d\rho/dr = 0$ or $dK/dr = 0$ for all r, $0 \leqslant r \leqslant R$.

For, if not, in the configuration in which K_c attains its minimum there must exist a finite interval

$$0 < r_1 \leqslant r \leqslant r_2 < R, \tag{9}$$

in which

$$\frac{d\rho}{dr} < 0\,; \qquad \frac{dK}{dr} < 0. \tag{10}$$

Let P and ρ refer to the configuration we are considering, namely, the one in which K_c attains its minimum.

By means of the following transformation we construct the pressure and density distributions defined by

$$0 \leqslant r \leqslant r_1 \qquad P^* = (1-\epsilon)^2 P\,; \qquad \rho^* = (1-\epsilon)\rho, \tag{11}$$

$$r_1 < r \leqslant r_2 \qquad P^* = P + \epsilon P_1\,; \qquad \rho^* = \rho + \epsilon\rho_1, \tag{12}$$

$$r_2 < r \leqslant R \qquad P^* = P\,; \qquad \rho^* = \rho, \tag{13}$$

where P^* and ρ^* refer to the new distributions of pressure and density,

* S. Chandrasekhar, *Ap. J.*, **87**, 535, 1938. This paper will be referred to as *loc. cit.*

ϵ is a small *positive* constant, and P_1 and ρ_1 (which are functions of r in the interval $r_1 \leqslant r \leqslant r_2$) are for the present unspecified.

If P^* and ρ^* should refer to an equilibrium configuration of the same mass M as the original configuration the following conditions have to be fulfilled :—

(i) *Continuity of P^* and ρ^*.* From (11), (12) and (13) we see that to ensure the continuity at $r=r_1$ and $r=r_2$ we should require

$$\rho_1 = -\rho, \quad (r=r_1); \quad \rho_1 = 0, \quad (r=r_2); \tag{14}$$

$$P_1 = -2P, \quad (r=r_1); \quad P_1 = 0, \quad (r=r_2). \tag{15}$$

Equation (15) is correct to the first order in ϵ.

(ii) *Constancy of Mass.*—This requires

$$4\pi\int_0^R \rho^* r^2 dr = 4\pi\int_0^R \rho r^2 dr. \tag{16}$$

By (11), (12) and (13) we find that (16) reduces to

$$M(r_1) = 4\pi\int_{r_1}^{r_2} \rho_1 r^2 dr. \tag{17}$$

The left-hand side of (17) is a known quantity. We can clearly choose a function ρ_1 in the interval $r_1 \leqslant r \leqslant r_2$ such that equation (17) and the boundary conditions (14) at r_1 and r_2 are all satisfied. We shall assume that ρ_1 has been chosen to satisfy these conditions.

(iii) *The distributions P^* and ρ^* satisfy the equation of hydrostatic equilibrium.*—The pressure density distributions in any configuration of equilibrium must satisfy the equation

$$\frac{1}{r^2}\frac{d}{dr}\left(\frac{r^2}{\rho}\frac{dP}{dr}\right) = -4\pi G\rho. \tag{18}$$

Given that P and ρ satisfy (18), we have to show that P^* and ρ^* distributions (with a suitable choice of P_1) satisfy (18).

It is immediately obvious that in the interval $0 \leqslant r \leqslant r_1$ and $r_2 < r \leqslant R$ equation (18) is satisfied. For $r_1 < r \leqslant r_2$ we have according to (12) and (18)

$$\frac{1}{r^2}\frac{d}{dr}\left(\frac{r^2}{\rho}\frac{dP_1}{dr} - \frac{r^2}{\rho^2}\rho_1\frac{dP}{dr}\right) = -4\pi G\rho_1. \tag{19}$$

From (19) we derive

$$\frac{1}{r^2}\frac{d}{dr}\left(\frac{r^2}{\rho}\frac{dP_1}{dr}\right) = F(r), \tag{20}$$

where

$$F(r) = -4\pi G\rho_1 + \frac{1}{r^2}\frac{d}{dr}\left(\frac{r^2}{\rho^2}\rho_1\frac{dP}{dr}\right). \tag{21}$$

Since P and ρ are assumed to be known functions of r and ρ_1 has been

chosen according to (ii) above, we can regard $F(r)$ as a known function of r. From (20) we easily derive

$$P_1 = \int_{r_2}^{r} \frac{\rho}{r^2}\left\{\int_{r_1}^{r} \xi^2 F(\xi)d\xi + c_1\right\}dr + c_2, \tag{22}$$

where c_1 and c_2 are two constants of integration. We now choose c_1 and c_2 such that P_1 defined by (22) satisfies the boundary conditions (15).

We thus see that with P_1 and ρ_1 chosen as specified in (ii) and (iii) above, P^* and ρ^* refer to an equilibrium configuration of the same mass and radius as the original configuration.

Finally, since in the interval $r_1 \leqslant r \leqslant r_2$, ρ and K are strictly decreasing [inequality (10)] we can choose a positive (*non zero*) ϵ sufficiently small that ρ^* and K^* (defined with respect to P^* and ρ^*) are decreasing functions of r.

We have thus shown that from the given equilibrium configuration we can construct another satisfying the restrictions on ρ and K. But the configuration specified by the functions P^* and ρ^* defines

$$K_c^* = K(P_c - 2\epsilon P_c,\ \rho_c - \epsilon\rho_c), \tag{23}$$

or, to the first order in ϵ,

$$K_c^* = K(P_c,\ \rho_c) - \epsilon\left(2P\frac{\partial K}{\partial P} + \rho\frac{\partial K}{\partial \rho}\right)_{P=P_c;\ \rho=\rho_c}. \tag{24}$$

From (6) and (24) it now follows that

$$K_c^* < K_c, \tag{25}$$

which contradicts our hypothesis that in the configuration in which K_c attains its minimum there exists an interval (9) in which (10) holds. This proves the lemma.

The theorem now follows almost immediately. The argument proceeds as in *loc. cit.* (p. 539), appeal now being made to our second restriction (7) on K.

3. The theorem that we have proved in paragraph 2 enables us to solve the problem of the minimum central temperatures of gaseous stars. For, according to equation (4),

$$\delta P = \frac{k}{\mu H}(\rho\delta T + T\delta\rho) + \tfrac{4}{3}aT^3\delta T \tag{26}$$

or

$$\frac{\delta T}{T} = \frac{1}{\dfrac{k}{\mu H}\rho T + \tfrac{4}{3}aT^4}\left(\delta P - \frac{k}{\mu H}T\delta\rho\right). \tag{27}$$

Hence

$$\frac{P}{T}\frac{\partial T}{\partial P} = \frac{\dfrac{k}{\mu H}\rho T + \tfrac{1}{3}aT^4}{\dfrac{k}{\mu H}\rho T + \tfrac{4}{3}aT^4} > 0, \tag{28}$$

and

$$\frac{\rho}{T}\frac{\partial T}{\partial \rho} = -\frac{\frac{k}{\mu H}\rho T}{\frac{k}{\mu H}\rho T + \frac{4}{3}aT^4}. \tag{29}$$

Hence

$$2\frac{P}{T}\frac{\partial T}{\partial P} + \frac{\rho}{T}\frac{\partial \rho}{\partial T} = \frac{\frac{k}{\mu H}\rho T + \frac{2}{3}aT^4}{\frac{k}{\mu H}\rho T + \frac{4}{3}aT^4} > 0. \tag{30}$$

Hence $T(P, \rho)$ satisfies the restrictions required for the validity of the theorem proved in paragraph 2. As stated for this special case the theorem will read:

In any gaseous equilibrium configuration of prescribed mass and radius and of constant mean molecular weight μ in which both ρ and T do not increase outward, the minimum value of T_c is attained in the sequence of equilibrium configurations which consist of isothermal cores and homogeneous envelopes.

It has to be noticed that we have only proved that the minimum value of T_c along the sequence of composite configurations (consisting of isothermal cores and homogeneous envelopes) is the absolute minimum of T_c under the restrictions $d\rho/dr \leqslant 0$, $dT/dr \leqslant 0$. But we have not yet specified the *particular* composite configuration in which the minimum value of T_c is attained; to be able to do so, we shall have to study the function $T_c(A)$, where A is the fraction of the radius occupied by the isothermal core. We now proceed to study this function.

4. We consider a composite configuration in which the isothermal core extends to a fraction A of the radius R. Hence if $r = r_1$ defines the place at which we have the interface between the isothermal and the homogeneous regions we have

$$r_1 = AR. \tag{31}$$

Let $\bar{\rho}_1$ be the mean density of the isothermal core and ρ_1 the constant density in the homogeneous part. Let B denote the ratio

$$B = \frac{\bar{\rho}_1 - \rho_1}{\rho_1}. \tag{32}$$

Finally, let P_1 be the pressure at the interface.

By considering the equilibrium of the homogeneous envelope we obtain [cf., *loc. cit.*, equations (23) and (27)]

$$M = \tfrac{4}{3}\pi R^3 \rho_1 (1 + A^3 B), \tag{33}$$

$$P_1 = \tfrac{2}{3}\pi G \rho_1^2 R^2 [1 - A^2 + 2A^2 B(1 - A)]. \tag{34}$$

Consider next the equilibrium of the isothermal core: in the core we can write

$$P = K\rho + D, \tag{35}$$

where

$$K=\frac{k}{\mu H}T_c\,; \qquad D=\tfrac{1}{3}aT_c^4, \tag{35'}$$

where K and D are constants. The reduction to the Emden isothermal equation is made by the substitutions *

$$\rho=\lambda e^{-\psi}\,; \qquad P=K\lambda e^{-\psi}+D, \tag{36}$$

$$r=\left(\frac{K}{4\pi G\lambda}\right)^{1/2}\xi. \tag{37}$$

Let ψ and ξ refer to the interface. Then P_1, ρ_1 and r_1 are given by the above formulæ. Further, let the radiation pressure be a fraction $(1-\beta_1)$ of the total pressure P_1 at the interface, so that

$$\beta_1 P_1=\frac{k}{\mu H}\rho_1 T_c\,; \qquad (1-\beta_1)P_1=\tfrac{1}{3}aT_c^4. \tag{38}$$

From (36) and (38) we have

$$P_1=\frac{1}{\beta_1}\frac{k}{\mu H}\rho_1 T_c=\frac{K}{\beta_1}\lambda e^{-\psi}. \tag{39}$$

Equating (34) and (39) and using equations (36) and (37) we have

$$\frac{K}{\beta_1}\lambda e^{-\psi}=\tfrac{2}{3}\pi G(\lambda e^{-\psi})^2\left(\frac{K}{4\pi G\lambda}\right)\xi^2\frac{1-A^2+2A^2B(1-A)}{A^2}. \tag{40}$$

After some reductions the above equation simplifies to

$$\frac{6}{\beta_1}=\xi^2 e^{-\psi}\cdot\frac{1-A^2+2A^2B(1-A)}{A^2}. \tag{41}$$

Introduce the homology-invariant functions u and v defined by

$$u=\frac{\xi e^{-\psi}}{\psi'}\,; \qquad v=\xi\psi', \tag{42}$$

where ψ' refers to the derivative of ψ with respect to ξ. In terms of u and v equation (41) can be rewritten as

$$\tfrac{1}{6}\beta_1 uv=\frac{A^2}{1-A^2+2A^2B(1-A)}. \tag{43}$$

Further,

$$B=\frac{\bar{\rho}_1}{\rho_1}-1, \tag{44}$$

or, using the relation between the mean and the central densities for isothermal configurations, we have

$$B=3\frac{\psi'}{\xi e^{-\psi}}-1, \tag{45}$$

* See S. Chandrasekhar, *An Introduction to the Study of Stellar Structure* (Chicago), p. 155.

or, according to (42),

$$B=\frac{3}{u}-1. \tag{46}$$

Equations (43) and (46) are our equations of fit. If the isothermal function $\psi(\xi)$ is known, then for a given ξ, u and v are known, and (43) and (46) determine A as the solution of a cubic equation.

We have next to determine T_c in terms of A, R, M and β_1. In terms of β_1 we can write for the interfacial pressure P_1, the expression

$$P_1=\left[\left(\frac{k}{\mu H}\right)^4\frac{3}{a}\frac{1-\beta_1}{\beta_1^4}\right]^{1/3}\rho_1^{4/3}. \tag{47}$$

Hence, according to equations (34) and (47),

$$\left[\left(\frac{k}{\mu H}\right)^4\frac{3}{a}\frac{1-\beta_1}{\beta_1^4}\right]^{1/3}=\tfrac{2}{3}\pi G\rho_1^{2/3}R^2[1-A^2+2A^2B(1-A)]. \tag{48}$$

From (33) we have, on the other hand,

$$\rho_1^{2/3}=\frac{M^{2/3}}{(\frac{4}{3}\pi)^{2/3}}\frac{1}{R^2}\frac{1}{(1+A^3B)^{2/3}}. \tag{49}$$

Eliminating $\rho_1^{2/3}$ between the equations (48) and (49) we obtain

$$\left[\left(\frac{k}{\mu H}\right)^4\frac{3}{a}\frac{1-\beta_1}{\beta_1^4}\right]^{1/3}=\tfrac{1}{2}(\tfrac{4}{3}\pi)^{1/3}GM^{2/3}\frac{1-A^2+2A^2B(1-A)}{(1+A^3B)^{2/3}}, \tag{50}$$

or alternatively

$$M=\frac{1+A^3B}{[1-A^2+2A^2B(1-A)]^{3/2}}M^*(\beta_1), \tag{51}$$

where

$$M^*(\beta_1)=\left(\frac{6}{\pi}\right)^{1/2}\left[\left(\frac{k}{\mu H}\right)^4\frac{3}{a}\frac{1-\beta_1}{\beta_1^4}\right]^{1/2}\frac{1}{G^{3/2}}. \tag{52}$$

Again, from equations (34) and (38) we have

$$\frac{k}{\beta_1\mu H}\rho_1T_c=\tfrac{2}{3}\pi G\rho_1^2R^2[1-A^2+2A^2B(1-A)], \tag{53}$$

or

$$\frac{k}{\mu H}T_c=\beta_1\,.\,\tfrac{2}{3}\pi G\,.\,\rho_1R^2[1-A^2+2A^2B(1-A)]. \tag{54}$$

Eliminating ρ_1 between the equations (33) and (54) we have

$$\frac{k}{\mu H}T_c=\tfrac{1}{2}\beta_1\frac{1-A^2+2A^2B(1-A)}{1+A^3B}\frac{GM}{R}. \tag{55}$$

We can therefore write

$$T_c=\tfrac{1}{2}Q\frac{\mu H}{k}\frac{GM}{R}, \tag{56}$$

where

$$Q=\beta_1\frac{1-A^2+2A^2B(1-A)}{1+A^3B}. \tag{57}$$

Using (43) we can rewrite equation (57) as

$$Q=\frac{6}{uv}\frac{A^2}{1+A^3B}. \tag{58}$$

This solves the equilibrium problem of the composite configurations. For an assumed value for ξ and β_1, determine A and B according to equations (43) and (46); equations (51) and (52), and (56) and (58) determine the mass of the configuration and the temperature of the isothermal core respectively.

Equation (43) is a cubic equation for A. Eliminating B between (43) and (46) we find that the equation for A can be written more conveniently as

$$2v(3-u)A^3+3\left[v(u-2)+\frac{2}{\beta_1}\right]A^2-uv=0. \tag{59}$$

Also, collecting our other results,

$$B=\frac{3}{u}-1, \tag{60}$$

$$M=\frac{1+A^3B}{[1-A^2+2A^2B(1-A)]^{3/2}}M^*(\beta_1), \tag{61}$$

$$T_c=\tfrac{1}{2}Q\frac{\mu H}{k}\frac{GM}{R}, \tag{62}$$

where

$$M^*(\beta_1)=\left(\frac{6}{\pi}\right)^{1/2}\left[\left(\frac{k}{\mu H}\right)^4\frac{3}{a}\frac{1-\beta_1}{\beta_1^4}\right]^{1/2}\frac{1}{G^{3/2}}, \tag{63}$$

and

$$Q=\frac{6}{uv}\frac{A^2}{1+A^3B}. \tag{64}$$

5. Our next problem is to determine the minimum value of T_c as given by equations (59)–(64) for prescribed values of M and R; in other words, we need the minimum value of Q for an assigned value of M. According to the equations (59), (60) and (61)

$$M=M(\xi,\beta_1); \tag{65}$$

while according to (59), (60) and (64)

$$Q=Q(\xi,\beta_1). \tag{66}$$

For a given M and an assumed value of ξ, equation (65) determines β_1. Equation (66) then specifies the appropriate value of Q. In this manner, we can effect the elimination of β_1 between the relations (65) and (66). We then repeat this calculation for a series of values of ξ and then determine the

minimum value of the derived $Q(\xi)$'s. This is the procedure that should be adopted to determine the minimum central temperature for a gaseous star of a *given* mass. The actual labour that will be involved in effecting the elimination of β_1 between the equations (65) and (66) for different values of ξ and for different initially prescribed values of M will be enormous. There is, however, an indirect but a more convenient method which can be adopted in practice. In this indirect method we first prescribe a certain value for β_1. We then determine M and Q according to equations (59)–(64) for various values of ξ. The calculations are then repeated for a series of initially assigned values of β_1. We obtain in this way a family of $(M\mu^2, Q)$ curves. We next draw the envelope to these curves. It is clear that this envelope to the $(M\mu^2, Q)$ curves will give the relation between $M\mu^2$ and the corresponding minimum value of Q, which we shall denote by $Q_{\min}$.

Table I summarizes the results of the calculations that were undertaken for determining the minimum central temperatures for gaseous stars. Only such parts of the calculations as are relevant to the drawing of the envelope of the $(M\mu^2, Q)$ curves are reproduced. Further, in this table the unit of mass used is M_3 defined by

$$M_3 = -4\pi\left(\frac{K_2}{\pi G}\right)^{3/2}\left(\xi^2\frac{d\theta_3}{d\xi}\right)_{\xi=\xi_1}, \tag{67}*$$

where K_2 is the relativistic-degenerate constant and θ_3 is the Lane-Emden function of index 3. Numerically, we have

$$M_3 = 5{\cdot}75\odot\mu^{-2}. \tag{68}$$

In terms of (67) we can rewrite equation (63) as

$$M^*(\beta_1) = 0{\cdot}3034 M_3\left(\frac{960}{\pi^4}\frac{1-\beta_1}{\beta_1{}^4}\right)^{1/2}. \tag{69}$$

It will be noticed that equation (63) is identical with the quartic equation † which determines the maximum value $(1-\beta^*)$ of the radiation pressure $(1-\beta_c)$, at the centre of a gaseous configuration of mass M^*.

The computations summarized in Table I were made possible through the courtesy of Mr. Gordon Wares who kindly provided the writer with a table of the isothermal function more accurate and more extensive than any that has been published so far.

The $(M/M_3, Q)$ curves for the different values of β_1 given in Table I were plotted and the envelope to these curves was drawn. From this envelope the values of $Q_{\min}$ for different values of M/M_3 were directly read off. The results are given in Table II. For any given value of the mass (expressed in units of M_3) we can now obtain by interpolation the

* See S. Chandrasekhar, *An Introduction to the Study of Stellar Structure* (Chicago), p. 422.

† S. Chandrasekhar, *Observatory*, 59, 47, 1936. Also *M.N.*, 96, 644, 1936. An alternative form for (69) is

$$M^*(\beta_1)/M_3 = 0{\cdot}9525(1-\beta_1)^{1/2}\beta_1{}^{-2}. \tag{69'}$$

TABLE I

β_1	ξ	A	M	Q
	4·6	0·6745	0	0·6407
	4·8	·6773	0	·64014
1·00	5·0	·6798	0	·64010
	5·2	·6817	0	·64044
	3·2	0·6244	0·3946	0·6465
	3·6	·6402	·3971	·6363
	4·0	·6516	·3958	·6302
	4·4	·6601	·3920	·6272
	4·6	·6634	·3894	·6267
0·95	4·8	·6662	·3863	·6266
	5·0	·6685	·3831	·6268
	5·2	·6704	·3796	·6275
	5·6	·6734	·3722	·6298
	6·0	·6754	·3646	·6331
	3·6	0·6285	0·6047	0·6183
	4·0	·6400	·6017	·6137
	4·4	·6482	·5947	·6116
0·90	4·6	·6515	·5905	·6115
	4·8	·6542	·5854	·6119
	5·2	·6584	·5746	·6134
	5·6	·6613	·5630	·6163
	6·0	·6631	·5509	·6200
	3·2	0·6006	0·8012	0·6062
	3·6	·6162	·8023	·5991
	4·0	·6274	·7966	·5955
	4·2	·6318	·7919	·5949
0·85	4·4	·6356	·7862	·5947
	4·6	·6388	·7798	·5950
	4·8	·6414	·7728	·5956
	5·2	·6455	·7575	·5980
	5·6	·6482	·7415	·6014
	3·2	0·5876	1·0112	0·5842
	3·6	·6030	1·0106	·5787
	4·0	·6140	1·0011	·5764
	4·2	·6184	0·9947	·5761
0·80	4·4	·6220	·9867	·5763
	4·6	·6252	·9778	·5771
	4·8	·6277	·9682	·5781
	5·2	·6317	·9482	·5812
	5·6	·6343	·9272	·5852
	3·2	0·5738	1·246	0·5608
	3·6	·5889	1·242	·5569
	3·8	·5948	1·236	·5559
	4·0	·5998	1·228	·5557
0·75	4·2	·6040	1·218	·5559
	4·4	·6075	1·207	·5566
	4·8	·6130	1·184	·5591
	5·2	·6168	1·158	·5627

β_1	ξ	A	M	Q
	2·8	0·5386	1·510	0·5423
	3·2	·5590	1·517	·5362
	3·6	·5738	1·508	·5336
0·70	3·8	·5795	1·499	·5331
	4·0	·5844	1·488	·5334
	4·2	·5885	1·476	·5340
	4·4	·5920	1·462	·5352
	4·8	·5972	1·431	·5383
	2·8	0·5232	1·836	0·5144
	3·2	·5432	1·839	·5100
	3·4	·5510	1·834	·5089
0·65	3·6	·5576	1·825	·5085
	3·8	·5632	1·812	·5087
	4·0	·5679	1·798	·5094
	4·4	·5752	1·763	·5121
	2·8	0·5068	2·237	0·4853
	3·2	·5262	2·234	·4822
	3·4	·5338	2·226	·4816
0·60	3·6	·5402	2·212	·4818
	3·8	·5456	2·195	·4825
	4·0	·5501	2·175	·4835
	2·8	0·4890	2·742	0·4544
	3·0	·4992	2·741	·4532
	3·2	·5079	2·732	·4526
0·55	3·4	·5152	2·718	·4527
	3·6	·5214	2·699	·4532
	4·0	·5309	2·650	·4557
	2·8	0·4700	3·397	0·4221
	3·0	·4798	3·391	·4213
	3·2	·4882	3·377	·4213
0·50	3·4	·4952	3·356	·4217
	3·6	·5010	3·330	·4226
	4·0	·5100	3·265	·4256
	2·8	0·4493	4·274	0·3880
	3·0	·4588	4·262	·3877
	3·2	·4667	4·239	·3880
0·45	3·4	·4734	4·209	·3888
	3·6	·4790	4·173	·3900
	4·0	·4874	4·086	·3935
	2·4	0·4036	5·494	0·3533
	2·6	·4162	5·500	·3524
	2·8	·4268	5·492	·3520
0·40	3·0	·4358	5·471	·3521
	3·2	·4434	5·437	·3529
	3·6	·4548	5·345	·3553
	4·0	·4626	5·229	·3587

β_1	ξ	A	M	Q
	2·4	0·3802	7·281	0·3148
	2·6	·3922	7·282	·3143
	2·8	·4022	7·262	·3143
0·35	3·0	·4106	7·227	·3147
	3·2	·4177	7·179	·3156
	3·6	·4284	7·051	·3182
	2·2	0·3413	10·020	0·2752
	2·4	·3545	10·034	·2747
	2·6	·3657	10·024	·2744
0·30	2·8	·3750	9·988	·2748
	3·2	·3894	9·863	·2762
	3·6	·3990	9·686	·2786
	2·2	0·3137	14·60	0·2331
	2·4	·3259	14·60	·2328
0·25	2·6	·3362	14·57	·2329
	2·8	·3448	14·51	·2333
	3·2	·3577	14·32	·2348

β_1	ξ	A	M	Q
	2·2	0·2824	23·03	0·1894
	2·4	·2934	23·02	·1894
0·20	2·6	·3027	22·95	·1896
	2·8	·3104	22·85	·1900
	3·2	·3218	22·56	·1914
	2·0	0·2348	41·28	0·1443
	2·2	·2462	41·29	·1443
0·15	2·4	·2558	41·25	·1443
	2·6	·2638	41·13	·1445
	2·8	·2704	40·95	·1449
	3·2	·2801	40·47	·1459
	2·0	0·1930	93·66	0·0976
	2·2	·2023	93·66	·0976
0·10	2·4	·2102	93·51	·0976
	2·8	·2220	92·92	·0980
	3·2	·2296	92·06	·0986

TABLE II

M/M_3	$Q_{\min}$	$1-\beta^*$	M/M_3	$Q_{\min}$	$1-\beta^*$
0	0·640	0	4·0	0·396	0·575
0·4	·624	0·110	5·0	·364	·614
0·6	·610	·180	6·0	·337	·643
0·8	·592	·238	7·0	·318	·667
1·0	·574	·286	8·0	·300	·686
1·2	·557	·326	9·0	·287	·702
1·4	·541	·361	10·0	·273	·717
1·6	·524	·390	12·5	·246	·744
1·8	·508	·416	15·0	·230	·764
2·0	·494	·440	23·0	·189	·807
2·5	·463	·485	41·2	·144	·854
3·0	·438	·521	93·7	·0976	0·902
3·5	0·414	·551	∞	0	1·000

appropriate value of $Q_{\min}$. The minimum central temperature for a gaseous star having the prescribed mass is then given by

$$(T_c)_{\min} = \tfrac{1}{2} Q_{\min} \frac{\mu H}{k} \frac{GM}{R}, \tag{70}$$

or numerically

$$(T_c)_{\min} = 11{\cdot}54 Q_{\min} \mu \left(\frac{M}{\odot}\right)\left(\frac{R_\odot}{R}\right) \times 10^6 \text{ degrees.} \tag{71}$$

Before we proceed to numerical applications of Table II to practical cases, we shall first consider the limiting forms for $Q_{\min}$ for the cases $M \to 0$ and $M \to \infty$.

For $M \to 0$, it is clear that the minimum central temperature can be

obtained by neglecting the radiation pressure in the equation of hydrostatic equilibrium. In that case, the problem effectively reduces to to determining the minimum value of P/ρ. The solution to this problem is contained in the author's earlier paper (*loc. cit.*, § VI). We therefore have

$$Q_{\min} \to 0{\cdot}640, \qquad M \to 0. \tag{72}$$

On the other hand, as $M \to \infty$, it is readily verified that

$$\beta_1 \to 0, \qquad A \to 0, \tag{73}$$

and that

$$Q_{\min} \to \beta^*, \tag{74}$$

where

$$M = \left(\frac{6}{\pi}\right)^{\frac{1}{2}} \left[\left(\frac{k}{\mu H}\right)^4 \frac{3}{a} \frac{1-\beta^*}{\beta^{*4}}\right]^{\frac{1}{2}} \frac{1}{G^{3/2}}. \tag{75}$$

Fig. 1 illustrates the general $(1-\beta^*, Q_{\min})$ relation. We notice that this curve intersects the $(1-\beta^*)$ axis at an angle of 45°; this is of course in agreement with (74).

6. Finally, Table III illustrates the method of using the results of § 5 to practical cases. In this table we have given the minimum central temperatures for a few typical cases.

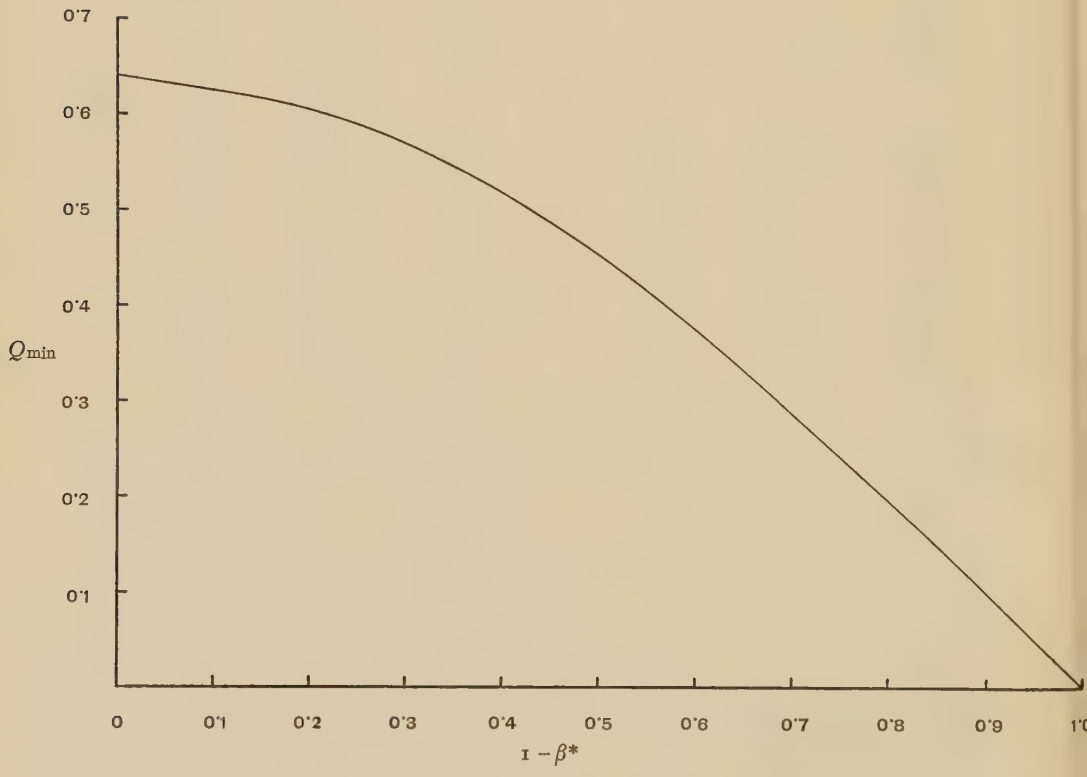

FIG. 1.—*The* $[(1-\beta^*), Q_{\min}]$ *Curve.*

TABLE III

Star	$M/\odot$	$R/R_\odot$	μ	M/M_3	$1-\beta^*$	$Q_{\min}$	T_c min millions of degrees
Sun	1·00	1·00	1·00	0·174	0·030	0·636	7·3
Sirius A	2·34	1·78	1·00	0·41	·114	·622	9·4
Capella A	4·18	15·9	1·00	0·73	·22	·60	1·82
ζ Aur (K star)	14·8	200	1·00	2·57	·49	·46	0·39
Trumpler's Stars T_2	100	7·2	0·50	4·3	·59	·38	30
Trumpler's Stars T_3	140	6·6	0·50	6·1	·645	·34	42
Trumpler's Stars T_6	400	17	0·50	17	0·78	0·21	29

Summary

In this paper the problem of determining the minimum central temperatures of gaseous stars is solved. It is shown that in any equilibrium configuration in which the temperature and the density do not increase outward the minimum central temperature is attained in the sequence of equilibrium configurations consisting of isothermal cores and homogeneous envelopes. By a study of the appropriate sequence of composite configurations it is found that we can write

$$(T_c)_{\min} = \tfrac{1}{2} Q_{\min} \frac{\mu H}{k} \frac{GM}{R},$$

where $Q_{\min}$ is a dimensionless quantity depending on $M\mu^2$ only. In Table II, $Q_{\min}$ is tabulated as a function of the mass of the star expressed in a suitable unit (M_3). Numerical applications (Table III) are also given.

In conclusion I wish to express my indebtedness to Mrs. T. Belland who undertook the rather tiring numerical work connected with the preparation of Table I; but for Mrs. Belland's assistance this paper would not have been written. My thanks are also due to Mr. G. W. Wares who generously placed at my disposal his unpublished integration of the isothermal function.

Yerkes Observatory :
1939 *March* 24.

A NEW PROJECTION MICROMETER MACHINE FOR STELLAR SPECTROGRAMS

R. O. Redman

(Communicated by the Director of the Radcliffe Observatory, Pretoria)

Self-recording and almost entirely automatic instruments are being introduced into scientific work in increasing numbers and have even invaded the field of wave-length measurement in laboratory spectroscopy, impossible although this appeared to be ten years ago. Whether the more difficult problem of devising apparatus for measuring star spectra automatically is likely to be solved in the immediate future remains doubtful, however, except possibly in the simplest cases, and there is likely to remain an almost indefinite amount of work to be done by older and more conventional methods. It appears profitable, therefore, to seek to improve the ordinary measuring machine, with the double aim of reducing fatigue and speeding up the measures.

In the usual type of micrometer machine for measuring spectra, the plate is viewed through a microscope and the screw is operated with a handle at the right. For each reading the observer has to set a crosswire on a certain part of the spectrum, looking in the microscope (which often has only a monocular eyepiece); he then moves his head, taking care not to upset his measures by touching the eyepiece with his nose, refocuses his eyes, and makes a reading on the drum at the end of the screw. The reading is given by a vernier, or involves estimating a tenth of a division by eye only. He then returns to the microscope, again refocusing his eyes and being careful not to touch the eyepiece, makes another setting and then another reading. After perhaps four readings, he lets go the handle of the drum, picks up a pencil and writes a mean value on a pad near by, his eyes having a third distance to which to adjust themselves. If he measures for only half an hour, all this is done without undue fatigue, but in a spell of continuous measuring, perhaps filling every day for weeks, any reduction of the number of movements necessary for hand and eyes is a very appreciable gain.

It has been realized for some years that a less tiring sequence of operations than the above can be devised for the type of measurement work under consideration. For example, in the measurement of photographic plates for positional astronomy, Schlesinger and Bennett * found it useful and convenient to project the image of the plate on a screen, instead of viewing it through a microscope, a principle which can be made to reduce eye fatigue very materially and which has lately been adopted at a number of

* *M.N.*, 93, 382, 1933.

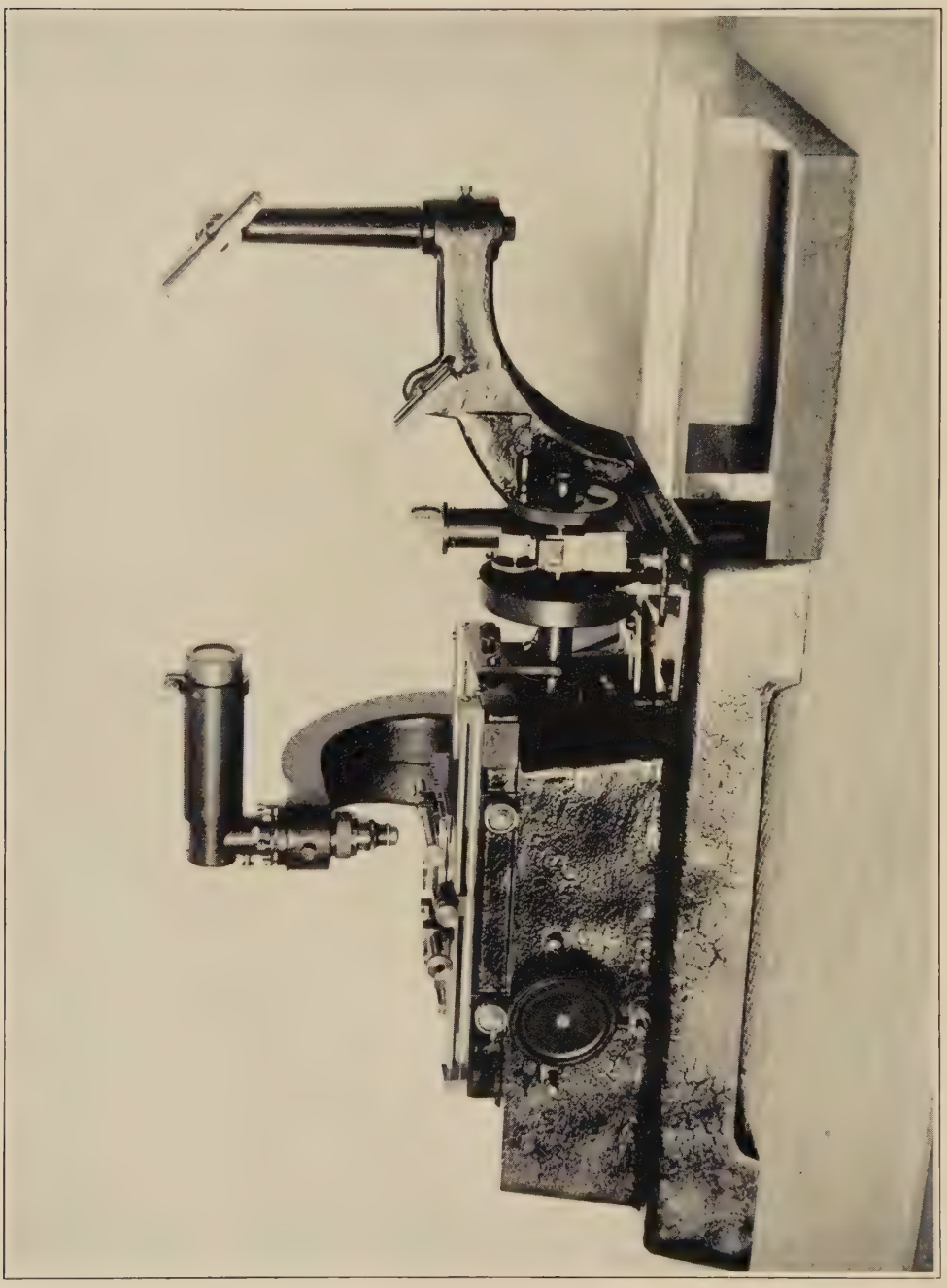

R. O. Redman, A New Projection Micrometer Machine for Stellar Spectrograms.

observatories. The same idea has recently been applied successfully to the measurement of stellar spectrograms, for instance by Petrie.*

One other improvement over conventional practice may also be made. Most astronomers write with the right hand and find it difficult to use the left for this purpose. But most of them can easily grow accustomed to making accurate adjustments to the position of a drum with the left hand, and it seems therefore desirable to design a machine so that this is done, the right hand being kept free for writing. It is believed that measuring machines at the Mt. Wilson Observatory use such an arrangement, although there appear to be very few examples elsewhere.

The present machine has been made with these ideas in view, and embodies the following features: (*a*) the photographic image is projected on to a screen, which lies very nearly in the same plane as the paper on which readings are written down, (*b*) the drum readings are also projected on to the same screen, (*c*) readings can be made to 0·001 mm. without interpolation or the use of a vernier, (*d*) the screw can be operated with the left hand.

Optical Arrangement.—The general appearance of the machine may be seen in Plate 22. Light from a 30-watt projection lamp, held at the back of the main casting, is fed in through a condensing lens, coming under the carriage and then being turned up through a 90° reflecting prism, so as to give a small bright illuminated patch on the plate. Above the latter is a 25-mm. microscope objective, which focuses an image of the spectrum on to a crosswire, immediately above which there is another 90° prism, turning the light into a horizontal direction through a lens of 7·5 cm. focal length, the latter producing an enlarged image of plate and crosswire on a screen of matt celluloid, lying on the table to the right of the machine. For this, one more reflection is necessary, namely, in a plane aluminized mirror situated about 40 cm. above the screen. It is rather important that the crosswire should not be situated on the screen itself, as any disturbance of the mirror would immediately affect the measures. In the present arrangement this disadvantage is avoided.

The whole optical train is provided with full collimation adjustments. The total magnification between plate and screen is about 40 diameters, which has been found convenient for spectra with sharp lines. The field covers about 2·5 mm. of plate and the illumination is sufficiently bright for work in a partially darkened room.

An alternative magnification is also provided, about 20 diameters from plate to screen. The optical arrangement used for this is of rather better design than that just described, being more efficient and cheaper. The problem of projecting the plate image and crosswire on to the screen is from an optical point of view very nearly the same as is encountered in making a telescope eyepiece, in that one has to take light from a real image which may cover an appreciable field, but each point of which is formed by a fairly narrow cone of light, while on emerging from the optical system the light from any given point of the image is nearly parallel. It was found, in fact, that two simple plano-convex lenses, arranged as in a normal Ramsden

* *Journal R.A.S. Canada*, **31**, 289, 1937.

eyepiece, gave very satisfactory results for the lower magnification, better indeed than the single compound lens used for the greater magnification.

The drum readings are projected so as to appear also on the screen. It is essential that the observer should not be able to distinguish the reading when he is making a setting, with his centre of vision fixed on the plate image. But apart from this, the nearer readings and spectrum are to each other the better, and matters have been arranged with this end in view. The drum is a glass disc, with 1000 divisions engraved near its periphery, every 10th division being numbered. A fiducial mark is mounted almost in contact with the disc, so that its image is also thrown on the screen, and, as with the spectrum, disturbances of the optical train have little or no effect on the readings. The 1 μ divisions are about 2 mm. apart in the projected image, over 20 being included in the field at once. Thus the observer can make his readings very quickly, without the use of any vernier, and without having to subdivide the drum by eye (see Plate 23). A small lamp, consuming about 3 watts, is sufficient to give ample illumination.

The drum gives only fractions of a revolution of the screw. Whole millimetres are read on a counter, situated close to the drum itself, and immediately to the left of the screen. Since these readings are needed less frequently than the others, and in routine work are often entirely neglected, it has been considered unnecessary to project them.

Mechanical Parts.—The plate is held on a stage, with longitudinal adjustment independent of the screw. For the size most often used (2″ by 4″) the holder has tilt and cross adjustments ; for other sizes a table with adjustable clips is provided. The present instrument is intended mainly for small plates, but it can measure to the edge of plates 18 cm. long and 15 cm. wide, and a second model shortly to be made will be able to take the longest plate ever used in a normal laboratory spectrograph.

The plate stage in its turn is mounted on a carriage, running on rollers which bear on carefully machined surfaces, allowing almost frictionless movement. The whole machine is used in a tilted position, primarily so that the screen and writing table are at as convenient an angle as possible, and this fact is utilized to hold the plate carriage on its bearing surfaces by the force of gravity. To avoid any slight mechanical strain which might affect the readings, the carriage is not linked mechanically with the nut on the measuring screw, but is merely held against it by the constant pull of a cord which runs over a pulley and is held in tension by a small weight. The screw is of very substantial proportions, of 1 mm. pitch and 25 mm. diameter, with a working length of just over 120 mm. It is held at one end in a conical thrust bearing, the thrust being provided by a spring which affects only that end of the screw shaft. At the other end is a plain bearing, so that the only end thrust operating along the screw itself is that due to the constant pull of the carriage. The nut is prevented from rotating by a tailpiece, furnished at its end with a hardened cylinder which is held firmly against an adjustable bar. If desired, residual errors of the screw could be compensated by cutting a suitable profile in the bar, but this degree of refinement is in general unnecessary.

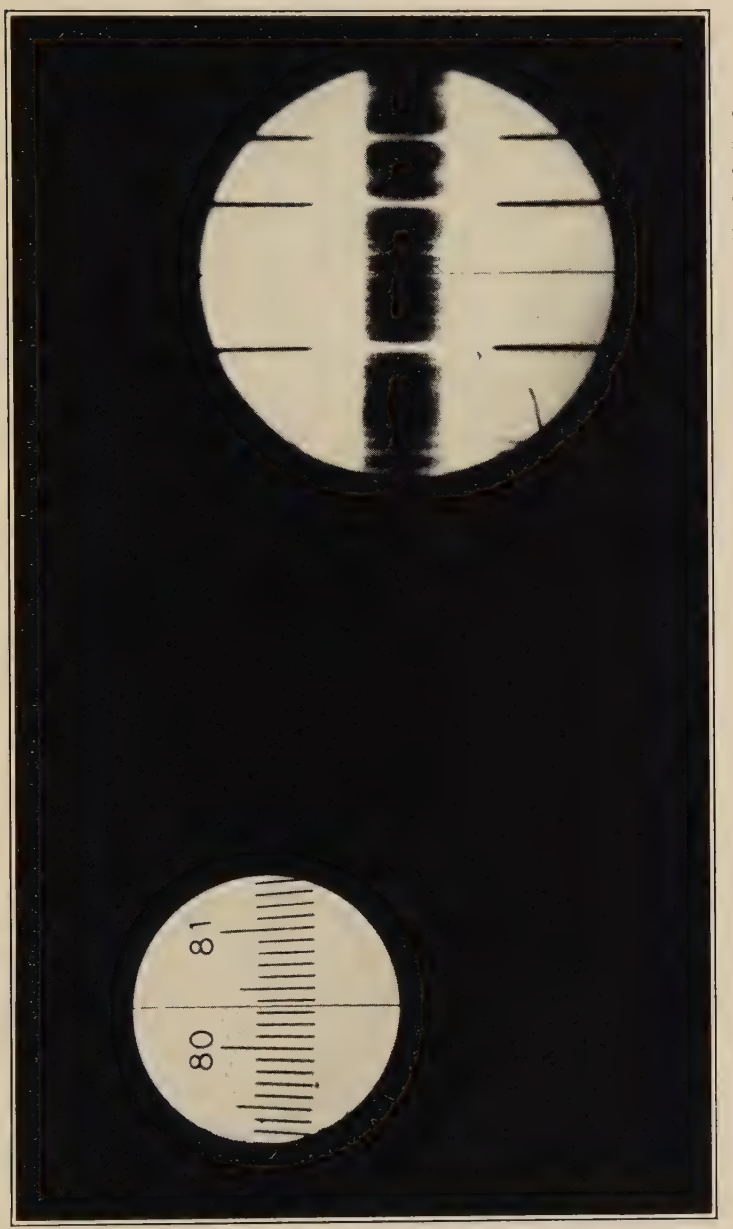

R. O. Redman, A New Projection Micrometer Machine for Stellar Spectrograms.

The screw can be rotated by a handle at the right-hand end, in the conventional position. This is intended only for moving the carriage to and fro quickly. Normally, setting is made by a hand-wheel brought out at right angles to the screw, at the front of the instrument and in a convenient position for the left hand. This makes four revolutions for one of the screw shaft, the connecting gear being of such a form as not to transmit any harmful stresses to the latter.

Accuracy of the Screw.—In the case of a machine intended for measuring photographic plates, there is a very definite limit to the standard of accuracy which need be attained. It is generally understood that a photographic emulsion shows average irregular displacement errors of about 0·5 μ, quite apart from plate grain. We also recall that the average error of good values of stellar velocity in the line of sight, derived from the Doppler effect measured along one spectrogram with sharp lines, corresponds generally to a shift on the plate of about 0·5 μ. Similarly, the wave-length differences between individual observers of spectrum lines obtained in the laboratory, when translated into linear displacements on the plate, are also of about this size. (This last does not refer to interferometer work.) Everything points to a practical working limit about 0·5 μ, and it appears unprofitable to aim at making any machine for measuring photographic plates much more accurate than this.

One other point has to be borne in mind. Owing to the method by which spectra are generally measured, involving the use of a standard spectrum with known lines spaced at intervals rarely exceeding a few millimetres on the plate, and often much less, the instrumental errors most to be feared are those of short period.

Errors due to the machine may be separated into (*a*) periodic errors due to inaccurate centring of the screw in its bearings, of the drum on the screw, etc., and (*b*) errors due to changes of pitch of the screw thread. Errors (*a*) are usually to be found as a regular wave, with period 1 or $\frac{1}{2}$ revolution of the screw. These were tested by repeated measures of seven intervals, each of about 0·1 mm., defined by diamond scratches on a glass plate. Each interval was measured twenty times at as many different parts of the drum, and the residuals from the average for each interval were plotted against the drum reading. Results obtained after the final polishing of the screw are shown in fig. 1 (p. 690) and indicate an irregular double wave in the readings over 1 revolution, of amplitude about 0·5 μ. The greatest error resulting from this wave, necessitating the measurement of one particular interval of about 0·6 mm., on one particular part of the revolution, is 1 μ, but the average error for intervals of any size is well under half this quantity. A short series of measures, made later at another part of the screw, after the instrument had been dismantled and reassembled, showed a slightly greater error, unrelated in phase to the wave of fig. 1, so that it is supposed that what is found is mostly due to irregularity in the screw thread itself.

Variations in pitch along the length of the screw were found by measuring repeatedly an interval of about 0·5 mm. between two diamond scratches on glass, the settings being made at as nearly as possible the same drum

readings throughout, so as to eliminate any periodic error of type (*a*). The results are shown in fig. 2. The average residual between the individual measured intervals and the mean of all 115 readings was 0·67 μ, this falling to 0·60 μ if the first and last 10 mm. of screw were not used. The internal consistency of individual readings showed that the greater part of this error lay in the machine and was not due to the observer. There was a systematic variation of pitch from one end to the other, amounting to 0·14 per cent.

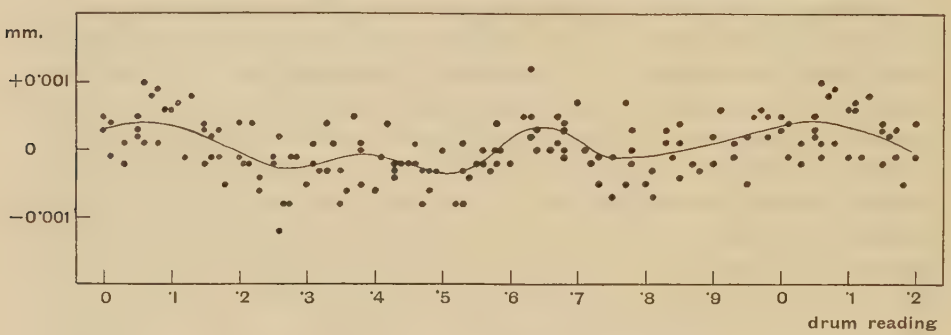

FIG. 1.—*Errors of machine on one particular revolution of the screw.*

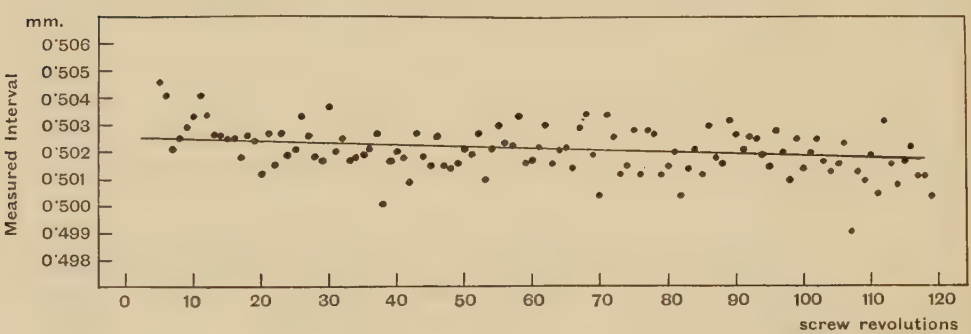

FIG. 2.—*Results of measuring a constant interval on each separate turn of the screw.*

over 100 mm. This is of no practical importance because (i) spectrum lines are always measured relative to near-by comparison lines, so that slow variation in the screw would be incorporated into the correction curve normally used in reducing the measures, (ii) a plate is generally measured in two ways, direct and reversed, and the mean value would then be relatively free from this error, and (iii) the bar against which the tail of the nut bears is adjustable and the pitch can be made effectively constant.

No attempt has been made to evaluate the errors of the machine in absolute units, since all that is required for the measurement of stellar spectra is that it should be self-consistent.

It will be obvious that in normal work no attempt would be made to take readings any closer than the nearest 1 μ, or possibly $\frac{1}{2}$ μ, but in the tests just described the open scale in the projected drum image was read easily to the nearest 0·1 μ, which was a great help in evaluating the errors under investigation, as well as a tribute to the clarity of the scale. The

results of the tests, in view of the limitations of photographic emulsions, are very satisfactory, the instrument proving to be as accurate as required for normal stellar spectroscopy, as well as being convenient and easy to operate.

The machine was made by Messrs. C. F. Casella and designed by them jointly with members of the staff of the Radcliffe Observatory, Pretoria.

Summary.—A new machine for measuring stellar spectrograms is described. It has been designed especially to minimize the fatigue experienced by the observer when measuring large numbers of plates. The image of the spectrum to be measured is projected on to a screen, lying in nearly the same plane as the writing paper on which results are recorded. Drum readings, also projected on the same screen, may be made to 1 μ without interpolation or the use of a vernier. The screw is operated by the left hand, the right being kept free for writing. The accuracy of the machine has been tested and its errors are shown to be negligible for all normal stellar spectroscopy.

ON THE ORIGIN OF THE SOLAR SYSTEM

W. J. Luyten

A few years ago Lyttleton advanced a theory for the origin of the solar system, starting from the hypothesis that the Sun has once been a component of a binary system whose companion has been removed by collision with a third star. E. L. Hill and myself have indicated that it is highly improbable that the formation of our planets could have taken place in this way, since (*a*) Lyttleton's vector diagram was in error, (*b*) he had neglected to make allowance for the considerable amount of kinetic energy required to liberate the planets, and (*c*) he had assumed the whole planetary filament to be available for capture, whereas we show that only a very small portion—6 per cent. linearly—is thus available. We had considered in detail Lyttleton's own case, viz. that where the masses of all three stars were the same, and likewise that where the intruding star is less massive.

In a recent paper Lyttleton has replied to our arguments, and while he accepts our calculation in the matter of the kinetic energy required, he claims that the theory may still be allowed to stand because of two other important factors, viz. the fact that the escaping material has a velocity nearer to that of the less massive of the stars involved, and the fact that the velocity of the Sun must have changed because of the presence of the third star. The former of these can hardly be considered as new since our vector diagram and calculation of the planetary point show clearly that we made use of the very fact that the "planetary" velocity must be closer to that of the less massive of the stars. The latter point had also been considered by us, but could not be taken into account since one of Lyttleton's original postulates was that the Sun could be ignored during the collision.

Lyttleton now considers specifically the case of a much more massive intruder. This had not been mentioned by us because it had appeared obvious to us that such would constitute a very unfavourable case for his theory. It may seem surprising, therefore, that Lyttleton now claims to have established a good case for the larger mass, but further consideration of the following three points shows our original viewpoint to have been correct, and Lyttleton's arguments to be in error.

1. The theory stands or falls with the possibility of getting the final points M_0' and P within the escape limit of each other (of the order of 10 km./sec.). Accepting for the moment Lyttleton's calculation on the change in the velocity of M_0, we find that the locus of GM_0' is a cone with axis GM_0; if the end point M_0' is to lie within a specified distance of P the vector GM_0' must be virtually coincident with the plane $M_1M_1'GM_2M_2'$, or, in other words, the intruder must have moved virtually in the orbital

plane of M_0M_1. This not only further reduces the already slender probability of the occurrence but also leads to other objections, as will be shown later. Also, as I pointed out at the R.A.S. meeting, if indeed M_0' should fall within 10 km./sec. of P, it is likely also to fall within 17 km./sec. of M_1', in which case M_0 and M_1 will not separate.

Furthermore, Lyttleton's calculation on the change of velocity of M_0 seems too simple and too favourable. Since all three bodies are assumed to be at the same mutual distance at the beginning and at the end of the encounter, the motion of M_0 will not be described as if the combined mass M_1+M_2 were stationary at G. As another extreme we may assume the motion to have been under the influence of M_2-M_1 at G. The eccentricity of the relative hyperbolic orbit is then 1·84 and the maximum change in angle only about 65°. The actual situation may lie between these two extremes, but it may be very different in view of the near-coplanarity of all three orbits, and it may certainly not be assumed without a more detailed numerical investigation of this three-body problem that M_0' and P can come within the required distance of each other. It may be possible, but it is evident from the above that it is exceedingly improbable in any event.

2. In his fig. 2 Lyttleton gives a rough diagram of the paths of the three bodies during the hyperbolic encounter and collision of M_1 and M_2. Unfortunately, as it appears, this diagram is in error both qualitatively and quantitatively. Lyttleton assumes that "the hyperbolic approach of M_1 and M_2 may be regarded as beginning and ending when their distance apart attains successively some value comparable to the original extension of the binary star" and, following the estimate made by Hill and myself, assumes the duration of the collision to be of the order of 10 years. Our estimate was based on Lyttleton's previous assumptions, *i.e.* with all three masses equal; now, however, the masses of M_1 and M_2 are 2 and 8, respectively, hence a hyperbolic encounter beginning and ending at a distance of 18 a.u. will take only 3·5 years. On the other hand, Lyttleton now agrees with us that the encounter cannot be considered as "over" until the attraction of the Sun on the planets is at least comparable to that of the other stars. Now dynamical reasons demand that capture shall take place at a distance from the Sun of the order of 18 a.u., and with a mass of 8 for the intruder; this latter star would have to be at least 50 a.u. away, which in turn implies that the collision and encounter will last of the order of 30 years. Accepting our calculation that only 6 per cent. of the filament is available for capture, and also Lyttleton's assumption of velocities linearly distributed until the moment of capture, it follows that the planetary filament at that time should be of the order of 4 a.u. long. The velocities of the different parts of the filament will lie mainly *in* the plane of the orbit of M_1M_2, and again we see that the velocity of the Sun must also have been nearly parallel to these and hence the Sun's orbit coplanar with that of M_1 around M_2.

Under these circumstances it is seen from Lyttleton's fig. 2 that the Sun must have passed very close to M_2 some time during the encounter, which violates his postulate that the Sun shall *not* suffer a close approach.

Capture is not an instantaneous occurrence, and since the portions of the filament amenable to capture are balanced precariously around the point of equality of attraction of M_1 and M_2, it would seem that capture cannot take place until the attraction of the Sun on the filament—always at a distance of 18 a.u.—is considerably greater than that of either of the parent stars; that is to say, more than a century after the collision. It would seem that this in turn necessitates that the Sun has been running roughly parallel to the planetary portion for some considerable time or that the velocity point of the Sun must be virtually coincident with *P*. This appears to be wellnigh out of the question.

3. Lyttleton accepts the value calculated by Hill and myself for the energy required to liberate the planetary material, but in his calculations uses only half the amount and later on claims that the actual amount may well have been smaller still, and no more than one-eighth of the amount given by us. In his own words: "Since the total mass of the planets is less than 0·0015 an amount of 0·003 might suffice for an estimate of the original material." By this is meant, I believe, the material originally disturbed by the collision, including everything that does not escape. Now Hill and I have shown that the part of the filament available for capture amounts to, at most, 6 per cent. linearly and that, furthermore, the present planets constitute at most 50 per cent. of the mass originally available, owing to the dissipation of hydrogen, helium and other volatile materials. The combined mass of the eight large planets is now 0·00134, hence that of their original matrix at least 0·0027, and if this is 6 per cent. of the filament then the total mass originally disturbed by the collision must have been of the order of 0·045 (assuming a uniform distribution along the planetary filament, which seems the only fair thing to do in the absence of any definite information to the contrary), which is 5 times as much as that considered by Lyttleton. The energy required to impart to this amount of matter velocities ranging uniformly from 0 to 620 km./sec.—the escape limit at the surface of the Sun—is then found to be 3200 units (Sun's mass, km./sec.). This seems entirely reasonable, and the value of 1900 units Hill and I adopted before should be considered as an absolute minimum.

Lyttleton further reduces this required energy by suggesting M_2 to have been a star similar to Capella A, whose value M/R is only one third of that of the Sun. Firstly, stars of this kind appear to be excessively rare in space, and thus the invoking of one would still further diminish the probability of the collision; and secondly, the density of these stars is so extremely low that there would seem to exist grave doubt as to whether it is possible to shear off as much matter as 0·045 by a collision. The same would hold, *a fortiori*, for stars such as Betelgeuse which, though perhaps more frequent in space, are of still lower density. In fact, with any red or yellow giant participating, one could hardly speak of a grazing collision, since the average star of mass 2 would have to pass right through the larger and less dense star in order to reach a region of any appreciable density at all.

If a star of mass 8 is required for the collision, it would seem far more probable for it to have been a normal B star of this mass, viz. a star with

a radius of about 4 times that of the Sun, or $M/R=2$. This would *increase* the amount calculated above for liberating the planets to 6400 units, or more than 6 times the amount used by Lyttleton, and 25 times his later value. This in turn would necessitate a relative velocity at infinity of at least 90 km./sec., even with masses of 8 and 2, and capture seems out of the question.

Finally there remains the question of probabilities. While I agree with Lyttleton that the single fact of an improbable collision does not, alone, supply an argument against the theory, the situation is altered if many other improbabilities enter as well. It would seem to the writer that in order to retain the double star theory we must be prepared to accept the following series of occurrences :—

The Sun revolves about another star of somewhat greater mass, at a distance of about 18 astr. units, thus forming a system entirely normal in space. A third star, belonging to that very small minority of stars which have high mass but low density, approaches the system with a velocity, normal in amount, but so accurately directed, not only virtually in the orbital plane of the other two but also so that the intruder collides with the Sun's companion, passes close to the Sun, all in such a way as to divorce the Sun from its companion and to deliver the Sun in such a position and with such a velocity that for many years it runs virtually parallel to the planets which have presumably been formed in the part of the ribbon which escapes the participating stars. The collision must take place in such a way as to shear off an amount of the order of $0{\cdot}05\odot$ from the two stars, despite the very low density of the intruder; furthermore, the portion of this filament which can escape both stars must condense quickly, despite the enormously high temperature to which it was raised.

It is true that none of these highly improbable events have been proved impossible as yet, and perhaps the problem is too vague and too complicated for such a general proof to be given. The dynamical restrictions alone appear to be severe enough, however, to narrow down the dynamical possibilities to cases which are physically impossible. Furthermore, I believe that in order to consider the theory as tenable at least one specific case should be calculated through by numerical quadratures, and shown to be dynamically possible.

In dealing with a theory as important as that concerning the origin of our planetary system it is my conviction that one cannot accept anything as possible merely because it has not yet been proved impossible.

Summary.—Lyttleton's reply to the criticisms advanced by Hill and Luyten against his theory for the origin of the solar system are reconsidered. It is shown that Lyttleton's arguments, claiming to establish a favourable case for an intruding star much more massive than the Sun, are in error both qualitatively and quantitatively. In particular it is here shown that (1) it is exceedingly improbable that the Sun could capture any part of the filament, without itself becoming captured by the intruder; (2) even in the situation most favourable to capture the Sun must have been running

roughly parallel to the filament for some time, and must itself have suffered a close approach or collision with the intruder—which possibility was distinctly ruled out by Lyttleton's postulates; and (3) Lyttleton's invoking of a special star such as a yellow giant to engender the planetary system is shown to be not only physically inadequate because of the low density of such stars, but further to increase the already enormous odds against the occurrence of such a collision.

OBSERVATIONS OF NOVÆ, 1938–1939

W. H. Steavenson

The observations here recorded were, unless otherwise stated, made with the 20½-inch Hindle reflector. References to the comparison stars used will be found in earlier papers, and particularly in *M.N.*, **92**, 720, 1932.

Nova Aquilæ (1918)

Observed on twelve nights. This nova appears to be very slightly variable, but there has been no appreciable change in its mean brightness for several years.

Date	Mag.	Date	Mag.	Date	Mag.
1938 June 5	11·3	1938 June 27	11·2	1938 July 26	11·1
20	11·2	30	11·2	Aug. 23	11·1
21	11·2	July 13	11·1	Sept. 16	11·1
25	11·2	19	11·1	25	11·1

Nova Aquilæ (1936, *No.* 1)

Observed on fifteen nights. The slow and regular fading, noted in the last report, has been continued.

Date	Mag.	Date	Mag.	Date	Mag.
1938 June 5	13·3	1938 July 26	13·6	1938 Sept. 25	13·9
21	13·3	Aug. 23	13·5	29	13·9
25	13·3	Sept. 16	13·7	30	13·9
27	13·3	21	13·8	Oct. 16	14·0
July 19	13·5	22	13·9	Nov. 8	14·1

Nova Aquilæ (1936, *No.* 2)

Observed on six nights. There has been considerable fading since the date of the last report. The present short series of observations shows little change and no signs of the violent fluctuations recorded in 1937.

Date	Mag.	Date	Mag.
1938 June 5	15·0	1938 June 27	15·1
21	15·2	July 19	15·0
25	15·2	26	15·2

Nova (*T*) *Coronæ* (1866)

Observed on one night, 1938 May 23, when the magnitude was estimated to be 9·71. This value confirms the impression, recorded in the last report, that this nova is slightly brighter now than in recent years. The probability that the tenth magnitude object commonly observed is not the true nova is discussed by Humason in *Ap. J.*, **88**, 228.

Nova Cygni (1876)

Observed on eight nights. Slight variability is again indicated by the observations, and the mean brightness is somewhat greater than that observed in 1937.

Date	Mag.	Date	Mag.
1938 June 5	14·61	1938 July 19	14·65
21	14·65	26	14·71
25	14·71	Aug. 20	14·91
27	14·66	Sept. 22	14·66

Nova Cygni (1920)

Observed on two nights. The general fading of this nova appears now to have ceased. Indeed it has shown little change in brightness for some years past.

Date	Mag.
1938 June 5	15·5
25	15·4

Nova Herculis (1934)

Observed on twenty-seven nights. The slow fading from the secondary maximum of 1935 September is still proceeding. The strong blue-green colour, developed by the nova about the time of the above-mentioned secondary maximum, persists ; but the telescopic appearance of the image has undergone a marked change in the course of the past year. On 1938 June 5 it was noted as being sensibly stellar, but on 1939 May 28 it was observed to have expanded into a fairly well-defined disc, about 2″ in diameter. The disc was uniformly bright, except for a slight fading at its extreme edge, and had exactly the appearance of a small planetary nebula. It resembled very closely the two bright objects of this type in Hercules and Ophiuchus (Σ5 and Σ6, N.G.C. 6210 and 6572), though considerably smaller than either. There was no sign of anything stellar in the image, which was in marked contrast to those of neighbouring stars in the field. The estimates of magnitude were made with the 3-inch finder.

Date	Mag.	Date	Mag.	Date	Mag.
1938 May 6	8·5	1938 June 25	8·6	1938 Sept. 30	8·9
7	8·6	27	8·6	Oct. 7	8·9
8	8·6	30	8·6	21	9·0
15	8·6	July 4	8·6	Nov. 1	8·9
20	8·6	Aug. 18	8·6	8	9·1
22	8·6	Sept. 16	8·7	Dec. 3	9·1
23	8·6	21	8·9	5	9·1
June 5	8·6	22	8·9	1939 May 23	9·3
21	8·5	25	8·9	28	9·5

Nova Lacertæ (1910)

Observed on one night, 1938 June 5, when the magnitude was estimated to be 14·4. There has been no sensible change in the light of this nova for many years.

Nova Lacertæ (1936)

Observed on thirty-two nights. The steady fall in brightness, noted in the last report, has continued. In the present series of observations the values adopted for the magnitudes of the comparison stars are those of Mitchell and Wirtanen (*M.N.*, **99**, 40, 1938). At the date of the first observation given below there was a difference of $0^m.7$ between the scale of this sequence and that of the B.A.A. sequence hitherto used, the nova being rated at 13·1 on the older scale.

Date	Mag.	Date	Mag.	Date	Mag.
1938 June 5	12·4	1938 Aug. 20	12·7	1938 Oct. 21	12·8
18	12·4	23	12·7	Nov. 1	12·8
20	12·5	Sept. 16	12·7	10	13·0
21	12·5	21	12·9	19	12·9
25	12·5	22	12·8	26	13·0
27	12·5	25	12·8	28	13·0
30	12·5	29	12·8	30	13·0
July 4	12·5	30	12·7	Dec. 5	12·9
13	12·6	Oct. 7	12·8	1939 Jan. 12	13·0
19	12·5	11	12·7	May 28	13·4
26	12·6	16	12·7		

Nova Ophiuchi (1848)

Observed on nine nights. The observations are perhaps hardly sufficient to establish any real variability, such as has been observed in past years.

Date	Mag.	Date	Mag.
1938 June 5	12·7	1938 July 13	12·6
21	12·8	19	12·7
25	12·8	26	12·7
27	12·8	1939 May 28	12·6
30	12·7		

Nova Persei (1901)

Observed on thirty-five nights. The observed range of variability was rather small, amounting to only $0^m.72$, and the nova was unusually quiescent up to the end of 1938 November.

Date	Mag.	Date	Mag.	Date	Mag.
1938 Aug. 18	12·79	1938 Oct. 16	12·74	1938 Dec. 12	12·43
Sept. 16	12·79	20	12·74	17	12·37
19	12·69	21	12·74	1939 Jan. 1	12·37
21	12·74	Nov. 1	12·74	12	12·69
22	12·53	8	12·74	15	12·69
25	12·69	14	12·69	Feb. 20	12·48
29	12·74	19	12·69	23	12·32
30	12·64	26	12·32	28	12·69
Oct. 1	12·74	28	12·22	Mar. 2	12·64
2	12·64	30	12·53	4	12·64
7	12·74	Dec. 5	12·43	Apr. 22	12·94
11	12·69	6	12·27		

A NEW MEMBER OF THE URSA MAJOR CLUSTER

W. M. Smart, M.A., D.Sc.

Professor Hertzsprung has drawn my attention to the star Gr. 1970 (G.C. 17919), apparent magnitude 6·74, spectral type Go, in connection with my recent paper * on the Ursa Major Cluster. Some years ago he had suggested † its probable connection with the cluster and the results of the present calculations appear to substantiate this suggestion fully.

The co-ordinates of the star for 1950·0 are: $13^h\ 11^m\ 34^s$, $+56°\ 58'$; the proper motion components, μ_α and μ_δ, are $+0^s·0135$ and $-0''·035$ respectively; the total proper motion is $0''·115$ in position angle $107°·6$, the probable error of the latter being $\pm 1°·6$ (derived from the probable errors of the proper motion components).

With my values of the co-ordinates of the convergent point, the angular distance of the star from the convergent point is $132°·3$; the calculated position angle is $99°·9$, the difference between observed and calculated being $+7°·7$, which is just a little higher than the largest difference (for No. 11 in my list) found for stars belonging to the cluster.

The calculated radial velocity is $-12·8$ km./sec. According to Moore's Catalogue ‡, the observed radial velocity is $-7·9 \pm 0·9$ km./sec., while Hertzsprung quotes § the value $-11·1$ km./sec. determined by J. S. Plaskett at Victoria.

The parallax calculated on the supposition that the star belongs to the cluster is $0''·039$, as against the observed value (Schlesinger's Catalogue of Parallaxes) of $0''·045 \pm 0''·009$. The calculated absolute magnitude is 4·70—the normal value for a Go dwarf.

According to the criteria depending on the position angle of the proper motion, radial velocity, parallax and absolute magnitude we conclude that Gr. 1970 is a member of the Ursa Major Cluster.

University Observatory,
Glasgow, W. 2:
1939 *May* 15.

* *M.N.*, 99, 441, 1939.
† *B.A.N.*, I, 86, 1920; VI, 60, 1930.
‡ *Lick Publ.*, XVIII, 1932.
§ *B.A.N.*, VI, 60, 1930.

OCCULTATIONS OBSERVED AT TEDDINGTON DURING 1938

John L. Haughton, D.Sc., F.Inst.P.

The occultations were observed as last year. The clock was checked against the B.B.C. time signals through the intermediary of the chronograph instead of using a stop-watch as on previous occasions. This should mean that the corrected clock reading is more accurate than in other years. As in previous reports, a correction for estimated lag has been applied to the time given in column 6 of Table I. The amounts subtracted are: 4 seconds for No. 129 (see note at foot of Table I); 0·8 seconds for No. 135; 0·5 seconds for Nos. 142 and 146; 0·3 seconds for Nos. 134, 136, 138 and 139; and 0·2 seconds for the rest.

The meaning of column 7 Table I has been questioned in connection with previous reports. It represents the root mean square of the maximum errors considered likely to have occurred in the corrected clock time and in the observation of the occultation.

The author is again indebted to Messrs. Scientific Computing Service, Ltd., for the reduction of the occultations, in which the correction of $+3''\cdot0$ has been applied to the Moon's mean longitude as given in the *Nautical Almanac*. The results of the reductions are given in Table II.

TABLE I

1 No.	2 Date	3 Star	4 Mag.	5 Phase	6 U.T. h m s	7 P.E. s
125	Jan. 14	ζ Tauri	3·0	D	4 29 04·5	0·3
127	Mar. 8	B.D. +20° 785	5·7	D	18 50 55·6	0·3
128	10	B.D. +19° 1430	7·4	D	18 45 42·5	0·5
129*	11	B.D. +16° 1551	7·4	D	22 07 38·0	?
130	12	A^1 Cancri	5·7	D	21 52 37·4	0·4
131	13	A^2 Cancri	5·7	D	0 10 13·5	0·3
132	Apr. 5	B.D. +20° 969	6·8	D	21 33 45·6	0·3
133	5	B.D. +20° 989	6·1	D	22 57 14·4	0·3
134	10	19 Sextantis	5·9	D	20 39 48·8	0·4
135*	11	62 Leonis	6·2	D	19 51 56·7	0·6
136	May 5	B.D. +15° 1775	6·1	D	20 16 53·9	0·3
137*	5	B.D. +14° 1850	6·4	D	21 30 09·4	0·3
138	8	B.D. +1° 2495	6·3	D	20 55 40·8	0·4
139	8	B.D. +1° 2502	6·9	D	23 25 51·5	0·4
140	June 5	87 Leonis	5·1	D	21 32 43·2	0·4
141	9	B.D. −17° 4200	6·8	D	22 59 01·8	0·2
142*	Aug. 3	B.D. −18° 3997	6·8	D	20 56 54·5	0·5
143	Oct. 7	λ Piscium	4·6	D	21 09 07·4	0·5
145	Nov. 12	B.D. +17° 1479	6·2	R	0 57 00·5	0·3
146*	29	B.D. −7° 5727	7·4	D	17 18 01·2	0·3
147	Dec. 3	B.D. +9° 167	7·2	D	17 47 09·9	0·2

Remarks.—No. 129. A haze rendered seeing very difficult. The star kept disappearing and reappearing and it was estimated that key was tapped 4 seconds after final disappearance. Note that $\Delta\sigma = 0\cdot0$!
No. 135, Uncertain. No. 137, Graze. No. 142, Difficult. No. 146, Uncertain.

TABLE II

No.	p	q	p^2	pq	q^2	$\Delta\sigma$	$p\Delta\sigma$	$q\Delta\sigma$
125	+ 45	+89	20	+40	80	−1·0	−0·4	−0·9
127	+100	− 1	100	− 1	0	−0·8	−0·8	−0·0
128	+ 58	+83	31	+46	69	−0·5	−0·3	−0·4
129	+ 96	+27	93	+26	7	0·0	0·0	0·0
130	+ 99	+14	98	+14	2	+0·6	+0·6	+0·1
131	+ 91	−42	82	−38	18	−0·4	−0·4	+0·2
132	+ 89	+46	79	+41	21	−0·8	−0·7	−0·4
133	+ 82	+57	68	+47	32	−0·9	−0·7	−0·5
134	+ 49	−87	24	−43	76	+0·4	+0·2	−0·3
135	+ 97	−24	94	−23	6	−0·4	−0·4	+0·1
136	+ 73	+68	53	+50	47	+0·3	+0·2	+0·2
137	+ 22	−98	5	−21	95	+0·9	+0·2	−0·9
138	+ 91	+42	82	+38	18	−1·8	−1·6	−0·8
139	+ 99	+11	99	+11	1	−1·7	−1·7	−0·2
140	+ 87	−50	75	−43	25	+0·6	+0·5	−0·3
141	+ 84	+55	70	+46	30	−2·8	−2·4	−1·5
142	+100	+ 9	99	+ 9	1	−2·3	−2·3	−0·2
143	+ 98	+21	96	+21	4	−1·1	−1·1	−0·2
145	− 99	+15	98	−15	2	+0·6	−0·6	+0·1
146	+ 98	−19	96	−19	4	−0·9	−0·9	+0·2
147	+ 74	−67	55	−50	45	−2·2	−1·6	+1·5